THE ROLE OF CDK5 IN THE REGULATION OF DOPAMINE NEUROTRANSMISSION,

NEURONAL EXCITABILITY,

AND REWARD-RELATED BEHAVIOR

APPROVED BY SUPERVISORY COMMITTEE

James A. Bibb, Ph.D.

Robert W. Greene, M.D., Ph.D.

Eric J. Nestler, M.D., Ph.D.

Ege T. Kavalali, Ph.D.

DEDICATION

I would like to thank my family, friends, and Jenn for their love and encouragement.

THE ROLE OF CDK5 IN THE REGULATION OF DOPAMINE NEUROTRANSMISSION, NEURONAL EXCITABILITY, AND REWARD-RELATED BEHAVIOR

by

DAVID ROGER BENAVIDES

DISSERTATION

Presented to the Faculty of the Graduate School of Biomedical Sciences

The University of Texas Southwestern Medical Center at Dallas

In Partial Fulfillment of the Requirements

For the Degree of

DOCTOR OF PHILOSOPHY

The University of Texas Southwestern Medical Center at Dallas

Dallas, Texas

May, 2010

THE ROLE OF CDK5 IN THE REGULATION OF DOPAMINE NEUROTRANSMISSION, NEURONAL EXCITABILITY, AND REWARD-RELATED BEHAVIOR

David Roger Benavides, Ph.D.

The University of Texas Southwestern Medical Center at Dallas, 2010

James A. Bibb, Ph.D.

Cyclin-dependent kinase 5 (Cdk5) regulates dopamine neurotransmission and synaptic plasticity and has been implicated as a homeostatic target of chronic psychostimulant exposure. In order to investigate the role of Cdk5 in the modulation of signal transduction pathways that regulate motivation and reward-related behavior, we developed several Cre/loxP conditional knock-out systems that allow temporal and spatial control of Cdk5 expression in the adult brain. Loss of Cdk5 in the adult brain increased the psychomotor-activating properties of cocaine and enhanced incentive motivation for food. Behavioral changes were accompanied by increased excitability of medium spiny neurons in the nucleus accumbens (NAc) in conditional Cdk5 knock-out mice. Targeted deletion of Cdk5 in the NAc facilitated cocaine-induced locomotor sensitization and conditioned place preference for cocaine. These results suggest that Cdk5 acts as

a negative regulator of neuronal excitability in the NAc and that Cdk5 may govern the behavioral effects of cocaine and motivation for reinforcement.

In a candidate search for putative Cdk5 substrates that may regulate dopamine-cAMP dependent kinase (PKA) signaling, we identified, confirmed, and characterized Cdk5-dependent phosphorylation of Thr69 RIIβ. We generated novel phosphorylation state-specific antisera to pThr69 RIIβ and found that pThr69 RIIβ levels were reduced in conditional Cdk5 knock-out mice. Functionally, phosphorylation of Thr69 dramatically enhanced calpain-mediated cleavage of RIIβ *in vitro*, but did not alter inhibition of PKA_{cat} or cAMP binding. Phosphorylation of Thr69 also increased the interaction of RIIβ with an A-kinase anchoring protein (AKAP) docking motif *in vitro*. In addition, we generated novel phosphorylation state specific antibodies to regulatory phosphorylation sites on cAMP-specific phosphodiesterase 4 (PDE4), an important modulator of PKA signaling. These antibodies to Ser53 PDE4D3 (PKA site) and pSer573 PDE4D3 (ERK site) provide insight into the crosstalk between PKA and ERK pathways in the regulation of cAMP. Finally, we identified and confirmed Thr292 as the site of Cdk5-dependent phosphorylation of MEK1. In conclusion, Cdk5 likely regulates PKA signaling through numerous pathways, including but not limited to DARPP-32, RIIβ, PDE, and MEK1. In summary, these studies identify novel regulatory mechanisms through which Cdk5 controls PKA signaling as well as the interplay between PKA and ERK signaling pathways that regulate motivation and reward-related behavior.

TABLE OF CONTENTS

PRIOR PUBLICATIONS

Hayashi K*****, **Benavides DR***, Nishi A, Kouser M, Fina MW, Dietz D, Nairn AC, Greengard P, Nestler EJ, Houslay MD, Taussig R, Bibb JA (2010) Cdk5 regulates cAMP phosphodiesterase 4 and serves as a potential target for the treatment of depression. *****_Equal contribution. Manuscript in submission._

Lagace DC, **Benavides DR**, Kansy JW, Mapelli M, Greengard P, Bibb JA, Eisch AJ (2008) Cdk5 is essential for adult hippocampal neurogenesis. *Proc Natl Acad Sci USA* 105(47):18567-18571.

Benavides DR, Quinn JJ, Zhong P, Hawasli AH, DiLeone RJ, Kansy JW, Olausson P, Yan Z, Taylor JR, Bibb JA (2007) Cdk5 modulates cocaine reward, motivation and striatal neuron excitability. *J Neurosci* 27(47):12967-12976.

Hawasli AH*****, **Benavides DR***, Nguyen C, Kansy JW, Hayashi K, Chambon P, Greengard P, Powell CM, Cooper DC, Bibb JA (2007) Cyclin-dependent kinase 5 governs learning and synaptic plasticity via control of NMDAR degradation. *Nat Neurosci* 10(7):880-886. *****_Equal contribution._

Benavides DR and Bibb JA (2004) Role of Cdk5 in drug abuse and plasticity. *Ann NY Acad Sci* 1025:335-344.

LIST OF FIGURES

LIST OF ABBREVIATIONS

AC, adenylyl cyclase

aCSF, artificial cerebrospinal fluid

AKAP, cAMP-dependent protein kinase anchoring protein

Ala, alanine

AMPA, α-amino-3-hydroxy-5-methyl-4-isoxazolepropionic acid

ANOVA, analysis of variance

ATP, adenosine 5'-triphosphate

BAPTA, 1,2-bis(o-aminophenoxy)ethane-N,N,N',N'-tetraacetic acid

BSA, bovine serum albumin

cAMP, cyclic adenosine monophosphate

CaMKII, Ca^{2+}/calmodulin-dependent protein kinase II

CCD, charge-coupled device

Cdk, cyclin-dependent kinase

cKO or CKO, conditional knock-out

CMV, cytomegalovirus

CNS, central nervous system

Con, control

Cer, cerebellum

Cor, cortex

CPu, caudatoputamen

Cre, Cre recombinase

DA, dopamine

D1, dopamine D1-like receptor

D2, dopamine D2-like receptor

DAPI, 4'-6-diamidino-2-phenylindole

DARPP-32 or D32, dopamine- and cAMP-regulated phosphoprotein, M_r 32,000

D/L, dark-light habituation

DMSO, dimethyl sulfoxide

DTT, dithiothreitol

EDTA, ethylene diamine tetraacetic acid

EGTA, glycol-bis(2-aminoethylether)-N,N,N',N'-tetraacetic acid

EPM, elevated plus maze

EPSC, excitatory postsynaptic current

EGFP, enhanced green fluorescence protein

EGFPCre, enhanced green fluorescence protein—Cre recombinase fusion protein

ERK, extracellular signal-regulated kinase

EYFP, enhanced yellow fluorescence protein

GABA, gamma amino butyric acid

GFP, green fluorescence protein

GPCR, G-protein coupled receptor

GST, glutathione S-transferase

GTP, guanosine 5'-triphosphate

HEPES, 4-(2-hydroxyethyl)-1-piperazineethanesulfonic acid

Hip or hpc, hippocampal formation

HPLC, high performance liquid chromatography

HRP, horseradish peroxidase

I-1 or inhibitor-1, protein phosphatase inhibitor-1

Indo, indolinone

IPTG, isopropyl-β-D-thiogalactopyranoside

IR, infrared

KO, knock-out

LTD, long-term depression

LTP, long-term potentiation

LC-MS/MS, liquid chromatography tandem mass spectrometry

MAPK, mitogen-activated protein kinase

MOPS, 3-(N-morpholino)-propanesulfonic acid

mRNA, messenger ribonucleic acid

MSN, medium-sized spiny neuron

NAc, nucleus accumbens

NAc-KO, targeted knock-out in the nucleus accumbens

NDS, normal donkey serum

NGS, normal goat serum

NMDA, N-methyl-D-aspartate

OF, open field

pA, polyadenylation

PBS, phosphate-buffered saline

PCR, polymerase-chain reaction

PDE, phosphodiesterase

PKA, cAMP-dependent protein kinase, protein kinase A

PKC, protein kinase C

PP-1, protein phosphatase 1

PP-2A, protein phosphatase 2A

PP-2B, protein phosphatase 2B, Ca^{2+}/calmodulin-dependent protein phosphatase, calcineurin

PR, progressive ratio

Quin, quinpirole

R26R, recombinant ROSA26 locus

RI, random interval

RIα, PKA regulatory subunit I alpha

RIβ, PKA regulatory subunit I beta

RIIα, PKA regulatory subunit II alpha

RIIβ, PKA regulatory subunit II beta

rAAV, recombinant adeno-associated virus

RM ANOVA, analysis of variance for repeated measures

Rosc, roscovitine

SDS-PAGE, sodium dodecyl sulfate polyacrylamide gel electrophoresis

SEM, standard error of the mean

Ser, serine

SKF, SKF81297

Str, striatum

TBS, Tris-buffered saline

TBS-T, TBS-Tween

TH, tyrosine hydroxylase

Thr, threonine

VTA, ventral tegmental area

WT, wild-type

CHAPTER ONE

INTRODUCTION

Remarkable advances in neuroscience research have provided the framework for our rapidly growing understanding of the biology of the central nervous system. More than ever, the fields of neurobiology and neuropsychiatry are converging, as changes in neuronal plasticity are increasingly appreciated as important biological processes that lead to many neuropsychiatric disorders, including drug addiction. It is clear that contextual, motor, and reward-based learning processes are crucial in reinforcing survival behaviors in animals. The key brain circuits that are involved in the execution of such learning processes include the basal ganglia and the mesolimbic reward system, regions which are also the targets of drugs of abuse. The long-term, compulsive use of addictive drugs is associated with potent and long-lasting memories of drug experience. While the network of brain circuitry that underlies the formation of the addictive state is highly complex, the long-standing drug-induced cellular and molecular neuroadaptations that occur in the mesolimbic system, including the ventral tegmental area (VTA) and nucleus accumbens (NAc), are key events in the process leading to drug addiction. Thus, it appears that the molecular substrates of motor and natural reward-based learning are hijacked and altered in response to drugs of abuse. The identification of neuroanatomical and cellular targets which

alter the effects of drugs of abuse and the plasticity of the reward system will likely prove beneficial in the development of novel therapeutic strategies for the treatment of drug addiction.

The neuronal protein kinase Cdk5 is emerging as an important regulator in the cellular, physiological, and behavioral responses to drugs of abuse. Cdk5 may affect the cellular responses to psychostimulants by modulating drug-induced changes in dopamine mediated signal transduction and cytoskeletal reorganization. In this regard, Cdk5, through its phosphorylation of various substrates, may serve to integrate a number of intracellular pathways that are targeted by psychostimulant drugs of abuse. Further research efforts, as well as the generation of novel animal models, will undoubtedly provide further insight into the biology of drug addiction as well as the role of Cdk5 in these processes.

Neuronal plasticity and drug addiction

The ability of the CNS to carry out complex functions such as learning and memory is via the malleability of the main processing unit of the nervous system—the neuronal synapse. At the synapse, presynaptic neurotransmitter release results in the activation of neurotransmitter receptors on corresponding postsynaptic membranes. "Fast neurotransmission" is mediated by neurotransmitters that bind ligand-gated ion channels that directly alter the excitability of the postsynaptic neuron. Examples of classical neurotransmitters

involved in "fast neurotransmission" include glutamate at AMPA, NMDA, and kainite receptors, GABA at $GABA_A$ receptors, and acetylcholine at nicotinic receptors. "Slow neurotransmission" is mediated by modulatory or nonclassical neurotransmitters that signal primarily through G-protein coupled receptors. Such "slow neurotransmitters" include the catecholamines (dopamine, norepinephrine, and epinephrine), serotonin, and various neuropeptides. However, metabotropic receptors exist for classical neurotransmitters as well, including mGluRs for glutamate, $GABA_B$ receptors for GABA, and muscarinic receptors for acetylcholine. Many neurotransmitter receptors are coupled to complex networks of intracellular signaling pathways in the postsynaptic compartment. Through modulation of these biochemical pathways, the physiological state of neurons can be altered such that they become either more or less responsive to neurotransmitter stimuli via ligand-gated ion channels. This process, by which synapses may be strengthened or weakened, is referred to as functional or synaptic plasticity and is an important component of CNS function. The main process by which synaptic strength is enhanced at synapses is known as long-term potentiation (LTP), while the counterpart, long-term depression (LTD) is a decrease in synaptic efficacy. LTP and LTD processes are basic properties of most synapses throughout the CNS that provide the basis for a number of properties involved in learning and memory.

It is likely that the regulatory mechanisms controlling neuronal plasticity in reward related regions are cellular targets of drugs of abuse (Hyman and Malenka, 2001; Nestler, 2001). The processes underlying drug addiction may be viewed as neuroadaptive responses to overwhelming reward-associated stimuli. These neuroadaptive responses may involve the processes of both functional and structural plasticity. Indeed, drugs of abuse induce LTP (Ungless et al., 2001; Thomas and Malenka, 2003) and alter neuronal morphology in the reward circuitry of the brain (Robinson and Kolb, 1999; Robinson et al., 2001). Consistent with this, chronic cocaine administration induces alteration in neuronal plasticity in dopaminergic projection neurons of the VTA (Liu et al., 2005).

Cdk5

Cdk5 is a neuronal proline-directed serine/threonine protein kinase that is activated through the association with either of the homologous neuron-specific regulatory cofactors, p35 or p39 (Tsai et al., 1994; Cai et al., 1997; Zheng et al., 1998). Cdk5 has been implicated in CNS development (Nikolic et al., 1996; Ohshima et al., 1996), as well as in the etiology of Alzheimer's disease (Patrick et al., 1999; Cruz et al., 2003) and other neurodegenerative diseases (Nguyen et al., 2001). Genetic ablation of the *cdk5* gene results in abnormal corticogenesis and perinatal lethality in mice (Ohshima et al., 1996). Furthermore, combined knock-out of the p35 and p39 genes results in an indistinguishable phenotype to the cdk5

knock-out (Ko et al., 2001). Cdk5 has been shown to be enriched in both the pre- and postsynaptic compartments (Tomizawa et al., 2002; Norrholm et al., 2003) and is involved in mediating neuronal plasticity (Dhavan and Tsai, 2001; Bibb, 2003). Recent studies have also demonstrated a presynaptic role for Cdk5 in neurotransmission (Tan et al., 2003; Tomizawa et al., 2003; Lee et al., 2004), and a number of substrates have been identified that implicate Cdk5 in the regulation of postsynaptic signal transduction pathways (Dhavan and Tsai, 2001; Bibb, 2003).

Cdk5 is expressed throughout regions of the central nervous system (**Figure 1.1**). Cdk5 levels are particularly high in cerebral cortex, striatum, hippocampus and hypothalamus, while comparatively lower in olfactory bulb and cerebellum. Cdk5 is also detected in homogenates from testis (**Figure 1.1**), consistent with previous reports (Tsai et al., 1994; Musa et al., 1998). In biology, several examples exist in which "brain-enriched" or "brain-specific" proteins are found in high levels in the reproductive system, these include fragile X mental retardation protein (FMRP) (Devys et al., 1993), Ma1 (Dalmau et al., 1999) and testis-brain RNA binding protein (TB-RBP or translin) (Han et al., 1995). It is enticing to think that the unique molecular signaling machinery of the nervous system has been borrowed for equally complex morphological and functional activities of reproductive tissues. Cdk5 levels are conspicuously absent from various peripheral tissues (**Figure 1.1**) consistent with previous reports (Hellmich

et al., 1992). However, it should be noted that there is some evidence that Cdk5 is involved in the regulation of secretory pathways in insulin-secreting pancreatic beta islet cells (Lilja et al., 2001; Wei et al., 2005). Interestingly, the monoclonal antibody against Cdk5 also detects a lower migrating cross-reactive band (~27 kDa) in peripheral tissues. This protein species is particularly abundant in lysates from lung and spleen. It is unclear what this protein species represents since there are no reports of specific degradation pathways for Cdk5, or alternatively spliced gene products. Further investigation may reveal if this lower migrating protein species is a functional *cdk5* gene product in peripheral tissue. For now, the investigation into the biology of Cdk5 activity is most well characterized and applicable to the function of the nervous system.

Dopamine

Dopamine is a monoamine neurotransmitter that functions in "slow neurotransmission," or the indirect modulation of neuronal activity. Dopamine was discovered by Arvid Carlsson and Nils-Ake Hillarp in 1952, and is derived from the amino acid, L-tyrosine. Dopamine is the precursor for the biosynthesis of norepinephrine and epinephrine, and was not believed to serve as a neurotransmitter itself for many years. Eventually, dopamine was shown to serve as a neurotransmitter and this feat, along with the signal transduction and behavioral effects downstream of dopamine signaling, was awarded the 2000

Nobel Prize in Physiology or Medicine. Today, we know that dopamine functions in a number of important roles in the brain, including the regulation of behavior, cognition, motivation and reward, mood, attention, and learning.

The synthesis of dopamine is governed by the mixed function monooxygenase, tyrosine hydroxylase (TH). TH is a tetrameric 56 kDa protein that catalyzes the conversion of L-tyrosine to L-DOPA. TH is enriched in the dopaminergic cells of the midbrain and its activity is modulated by phosphorylation in the N-terminus of the molecule (Fitzpatrick, 1999). Phosphorylation of Ser40 (by PKA, PKG PKC or CaMKII) and Ser19 (by CaMKII or MAPKAP2) and Ser31 (ERK or Cdk5) have been associated with increased enzyme activity (Campbell et al., 1986). Furthermore, Ser31 phosphorylation has been implicated in the stability of TH (Moy and Tsai, 2004) and the level of Ser31 TH phosphorylation is elevated in VTA of rats that have undergone cocaine self-administration (Kansy et al., 2004). These data indicate the potential for regulation of dopamine signaling through presynaptic regulation of TH activity. Interestingly, Cdk5 has been shown to be important regulator of presynaptic events including synaptic vesicle endocytosis (Tan et al., 2003; Tomizawa et al., 2003; Evans and Cousin, 2007).

Mesolimbic dopamine circuitry

Contextual, motor, and reward-based learning are important for survival behavior in animals. The cellular basis for the reinforcement of adaptive survival behavior includes dopaminergic modulation of neuronal activity. The dopamine system in the mammalian brain is the target of all psychoactive drugs of abuse and has many important neuromodulatory functions (Di Chiara et al., 1994). The primary dopaminergic output nuclei of the mammalian brain include the ventral tegmental area (VTA-A10), the substantia nigra pars compacta (SNc-A9), and the retrorubral field (RRF-A8). The striatum receives dopaminergic innervation from each of these regions. The projections from the SNc form the nigrostriatal dopamine system, while the projections from the VTA form the mesolimbocortical dopaminergic system. Medium-sized GABAergic inhibitory neurons of the striatum (medium spiny neurons) are the primary recipients of projections from dopaminergic nuclei of the SNc and the VTA. The medium spiny neurons constitute more than 95% of the neuronal population of the striatum. Dopaminergic terminals impinge on the necks of dendritic spines, often on the same spine receiving excitatory input from the cortex. Therefore, dopamine synapses are poised to modulate the fast glutamatergic neurotransmission, neuronal output, and plasticity. The well-characterized role of the nigrostriatal system is in the control of motor movements and acquisition of motor programs, while the mesolimbocortical system is commonly implicated in motivation and reward related behaviors.

Dopamine signal transduction

Dopamine mediates its modulatory effects on MSN function through the activation of two classes of dopamine receptors belonging to the G protein–coupled receptor (GPCR) superfamily. These dopamine receptors are classified as D1-like (D_1, D_5) and D2-like (D_2, D_3, D_4), according to their molecular and pharmacological properties, as well as G protein coupling. D1-like receptors are G_s coupled, while D2-like receptors are $G_{i/o}$ coupled (Andersen et al., 1990; Sibley et al., 1992). Medium spiny neurons of the striatum are known to express both families of dopamine receptors (Sibley et al., 1992), although whether individual neurons express more than one subtype of receptor remains controversial and the functional implications poorly understood. Nonetheless, there is segregation of receptor subtype expression between the two principal efferent pathways projection pathways from the striatum, the direct and indirect pathways. Direct pathway neurons express D_{1a} receptors while D_2 receptors are expressed in indirect pathway neurons. D_{1b}, D_3, and D_4 receptors are also found at lower levels in MSNs of the striatum. It is also important to note the presence of D_2 receptor expression on presynaptic corticostriatal glutamatergic terminals (Wang and Pickel, 2002), however the effect of dopamine on excitatory neurotransmission at corticostriatal synapses remains controversial. Nonetheless, the expression patterns and relative abundance of these dopamine receptor

subtypes are known to be quite diverse and determine the excitatory or inhibitory effects of dopamine signaling.

PKA signaling

Regulation of the generation of the second-messenger cAMP by adenylyl cyclase is the principal target of activation of GPCRs that are coupled to G_s and $G_{i/o}$ proteins. cAMP signaling is regulated at many levels. Adenylyl cyclases and phosphodiesterases are believed to regulate cAMP gradients in the cell. As the principal target of cAMP signaling, cAMP dependent kinase (PKA) is also subject to regulation. There are four kinds of subunits of the regulatory subunit for the PKA tetramer: RIα, RIIα, RIβ, and RIIβ. These regulatory subunits are responsible for catalytic subunit inhibition, cAMP responsiveness (Type I PKA K_{act} = 70nM, Type II K_{act} = 350nM), as well as subcellular localization. In fact, subcellular localization of AC, PDEs, and PKA all contribute to the spatio-temporal regulation of cAMP signaling.

Well characterized protein signaling complexes have been described by virtue of a family of protein scaffolds known as A kinase anchoring proteins (AKAPs). There are over a dozen AKAPs in the mammalian genome, and the PKA binding domain is also highly conserved between AKAP family members. However, subtle differences in protein sequences are believed to contribute to the differential affinity and specificity of the different AKAPs for PKA. The

association of AKAP with PKA is mediated through direct binding to the regulatory subunit. Each AKAP contains a unique targeting sequence that determines its localization and a consensus sequence for PKA binding. While most AKAPs are specific for Type II PKA (RIIα and RIIβ), several dual specificity AKAPs have been identified, which are capable of binding both types I and II PKA (Wang et al., 2001). Together, these AKAPs coordinate the association of PKA, PDEs, and phosphatases to specific subcellular complexes, facilitating the regulation of signal transduction. Importantly, disruption of these vital protein-protein interactions can have dramatic effects on the time course and magnitude of PKA signaling (Cantrell et al., 1999). Indeed, several reagents have been utilized to disrupt PKA binding to AKAPs (Carr et al., 1992). Among the most striking findings is that disruption of these associations in the brain is sufficient to impair a behavioral test of learning and memory (Moita et al., 2002). Since AKAPs direct PKA to specific targets upon activation, it is likely that the coordinated phosphorylation of specific cellular targets is necessary for the cellular mechanisms of memory formation. Indeed, cellular stimuli that disrupt or modulate PKA binding to AKAPs may serve as important regulators of cellular memory.

An important integrator of intracellular signaling pathways in dopaminoceptive neurons of the striatum is the protein DARPP-32 (dopamine and adenosine 3′, 5′-monophosphate-regulated phospho-protein, Mr 32 kDa)

(Greengard et al., 1999). DARPP-32 is enriched in almost all medium spiny neurons of the striatum (Ouimet et al., 1984; Ouimet and Greengard, 1990). Dopamine signaling through D1-like dopamine receptors activates adenylate cyclase, resulting in cAMP production and PKA-mediated phosphorylation of DARPP-32 at Thr34 (Hemmings et al., 1984b). This phosphorylation converts DARPP-32 into a potent inhibitor of protein phosphatase-1 (PP-1) (Hemmings et al., 1984a). PP-1 is a well-characterized serine/threonine protein phosphatase that regulates many phosphoproteins in the mammalian brain (Nairn and Shenolikar, 1992). Thus, activation of D1 receptors may lead to an increase in the phosphorylation state of an array of cellular phosphoproteins, including neurotransmitter receptors, ion channels, ion pumps, and transcription factors through regulation of PP-1 activity. The regulation of PP-1 activity by DARPP-32 is modulated by a number of neurotransmitters that target dopaminoceptive medium spiny neurons. For example, adenosine A2A receptor activation has been shown to increase phospho-Thr34 DARPP-32 levels (Svenningsson et al., 1998). In contrast, dopamine action on D2-like receptors leads to inhibition of PKA signaling, apparently through Gi protein–mediated inhibition of adenylate cyclase and a decrease in phospho-Thr34 DARPP-32 (Nishi et al., 1997; Lindskog et al., 1999). Furthermore, the dephosphorylation of phospho-Thr34 DARPP-32 in striatal tissue is catalyzed by Ca2+/calmodulin-dependent protein phosphatase PP-2B (or calcineurin) (Goto et al., 1986), which is highly enriched

in medium spiny neurons (Goto et al., 1986). Activation of ionotropic NMDA receptors by glutamate results in increased levels of intracellular Ca^{2+} and activation of PP-2B, leading to the dephosphorylation of phospho-Thr34 DARPP-32 (Halpain et al., 1990). Thus, DARPP-32 may affect the responsiveness and excitability of neurons responsible for fine motor control and motor- and reward-based learning in the neostriatum through the balancing of opposing inputs. In addition to the discovery of DARPP-32 as a substrate for PKA and inhibitor of PP-1, other observations have indicated that DARPP-32 serves as a convergence point of many signaling pathways. For example, it was shown that DARPP-32 could be phosphorylated by casein kinase II at Ser102 (Girault et al., 1989) and casein kinase I at Ser137 (Desdouits et al., 1995). Both of these phosphorylations have been suggested to enhance the ability of DARPP-32 to inhibit PP-1. Therefore, DARPP-32 may also integrate signals from multiple intracellular signaling pathways.

Discovery of Cdk5 as a regulator of dopamine-PKA signaling

Phosphopeptide map analysis of DARPP-32 immunoprecipitated from ^{32}P-labeled tissue suggested that it might serve as a substrate for additional protein kinases. The amino acid sequence of DARPP-32 includes five conserved proline-directed serine/threonine residues. Based on this observation, the proline-directed kinases MAPK and Cdk1 were evaluated for their ability to phosphorylate

DARPP-32 *in vitro*. While DARPP-32 served as a substrate for both kinases, only Cdk1 (isolated from sea star oocytes) consistently phosphorylated DARPP-32 to a stoichiometry near 1 mol ^{32}P/mol substrate (J.A. Bibb, unpublished observation). While interesting, these early findings were encumbered by the caveat that Cdk1 is associated with mitosis in mammalian cells and does not show significant expression in the postmitotic neurons of the CNS. However, as these studies were being conducted, Cdk5 was identified in neuronal tissue (Hellmich et al., 1992; Tsai et al., 1993). Since Cdk5 was identified on the basis of its high sequence homology to Cdk1, this new kinase provided an exciting new avenue of investigation.

In preliminary experiments conducted by J.A. Bibb using recombinant glutathione S-transferase (GST)-Cdk5 and GST-p21 (a truncated Cdk5-activating form of p35, provided by Jerry Wang), DARPP-32 was found to be an efficient substrate for Cdk5 *in vitro*. Furthermore, active kinase immunoprecipitated from striatal tissue caused an increase in the 32P-radiolabeling of DARPP-32 *in vitro*. This effect could be blocked through the use of the Cdk5 inhibitor, roscovitine, *in vitro*. Similarly, the use of Cdk5 immunoprecipitated from p35 knock-out mice showed reduced ^{32}P-radiolabeling of DARPP-32 *in vitro* (Bibb et al., 1999). Phosphopeptide mapping and phosphoamino-acid analyses demonstrated that both Cdk1 and Cdk5 phosphorylated DARPP-32 at the same site. The site of phosphorylation was identified as Thr75 of DARPP-32 by mass spectrometry and

Edman microsequencing of a tryptic phosphopeptide isolated by reverse phase HPLC. To confirm Thr75 as the site of phosphorylation, recombinant DARPP-32 containing a Thr75Ala mutation was generated. Neither Cdk5 nor Cdk1 phosphorylated this site-directed mutant *in vitro*, indicating that Thr75 was the only site of phosphorylation (J.A. Bibb, unpublished observation). A phosphorylation state–specific antibody to phospho-Thr75 DARPP-32 was generated in order to assess the physiological relevance of this site *in vivo*. The phosphorylation of DARPP-32 at Thr75 was reduced by inhibition of Cdk5 by roscovitine in striatal slices. Furthermore, reduced Cdk5 activity in p35 knock-out (p35 KO) mice correlated to a decrease in phospho-Thr75 levels in tissue homogenates from these animals (Bibb et al., 1999). At the same time, *in vitro* studies revealed that phosphorylation of DARPP-32 at Thr75 prevented it from serving as a substrate for PKA. Moreover, Cdk5-mediated phosphorylation of Thr75 converted DARPP-32 into an inhibitor of PKA. Inhibition of Cdk5 in acutely prepared striatal slices resulted in a reduction in phospho-Thr75 level (Cdk5 site) and a concomitant increase in phospho-Thr34 DARPP-32 (PKA site). These data suggested that the efficacy of dopamine signaling through D1 receptors could be controlled through the phosphorylation state of Thr75 of DARPP-32. Furthermore, roscovitine treatment induced an increase in the phosphorylation state of PKA substrates in wild-type striatal slices, but not in striatal tissue from DARPP-32 KO mice (Bibb et al., 1999). These studies

suggested that the roscovitine effect is mediated through the actions of DARPP-32 and that Cdk5-mediated phosphorylation of DARPP-32 reduces the efficacy of dopamine D1 receptor signaling through inhibition of the PKA pathway. Indeed, the ability of a D1 receptor agonist to induce phosphorylation of a number of PKA substrates was enhanced in p35 KO mice (Bibb et al., 1999). Thus, DARPP-32 may be the first molecule shown to function as either a protein phosphatase inhibitor or protein kinase inhibitor, depending on where it is phosphorylated. The fact that it inhibits the very kinase that converts it into a phosphatase inhibitor suggested an especially elegant regulatory equilibrium. Shortly after reduction of phospho-Thr75 DARPP-32 was shown to increase PKA activity, it was found that activation of PKA caused a decrease in phospho-Thr75 DARPP-32 (Nishi et al., 2000). At first, an attractive mechanism appeared to be direct PKA downregulation of Cdk5 activity. However, extensive analysis determined this not be the mechanism of PKA-mediated reduction in phospho-Thr75 DARPP-32 levels. Instead, studies indicated that PKA-dependent activation of protein phosphatase-2A (PP-2A) was responsible for the dephosphorylation of phospho-Thr75 DARPP-32.44 Interestingly, an acute dose of cocaine, which causes increased synaptic dopamine levels, was capable of raising phospho-Thr34 DARPP-32 levels through PKA activation and reducing phospho-Thr75 (Cdk5 site) levels, apparently via the PP-2A pathway (Nishi et al., 2000). These data suggested that a dynamic equilibrium existed where DARPP-

32 could be shunted to the PP-1 inhibition pathway (phospho-Thr34) provided phospho-Thr75 levels were low enough to permit PKA-dependent activation of PP-2A and dephosphorylation of Thr75. However, the physiological circumstances that could result in the converse shunting of DARPP-32 to PKA-inhibition remained unknown.

Cdk5 and drug addiction

It is well accepted that relapse to drug seeking and drug craving is due to long-standing effects of drug exposure on brain chemistry and CNS function (Hyman and Malenka, 2001; Nestler, 2001). These longstanding effects of drugs are due to the plasticity associated with the reward centers of the brain. The molecular mechanisms underlying the adaptation of the brain to drugs of abuse remain undefined for the most part. Nevertheless, Nestler and coworkers found that chronic administration of cocaine resulted in persistent, elevated expression of the Fos family transcription factor, ΔFosB, in reward-associated brain regions (Hope et al., 1994). This finding identified a potential marker of drug abuse plasticity in the reward system. Furthermore, the identification of a transcription factor warranted analysis to define target genes that are regulated by chronic drug treatment. In order to better understand how drug addiction may alter gene expression, a transgenic animal model was generated where ΔFosB overexpression was placed under the control of an inducible, striatal-specific,

tetracycline expression system (Chen et al., 1998). DNA microarray analyses were conducted on striatal tissue from mice that did or did not overexpress ΔFosB. Interestingly, the expression of Cdk5 was prominently enhanced as a result of overexpression of ΔFosB as assessed by DNA microarray analysis (Bibb et al., 2001). As the putative *cdk5* gene promoter region contains an AP-1 transcriptional regulation site (Ishizuka et al., 1995; Kumar et al., 2005), this finding suggested that Cdk5 was a transcriptionally regulated target gene of ΔFosB in the striatum. In collaborative studies, these results were confirmed using both inducible ΔFosB transgenic mice and rats chronically treated with cocaine. The mRNA and protein expression of Cdk5 and p35 were increased in response to increased ΔFosB expression and chronic exposure to cocaine.48 Furthermore, the phosphorylation state of Thr75 DARPP-32 was consistently elevated in each case. The functional significance of these findings was supported by pharmacology experiments that indicated that the ability of a D1 agonist to induce PKA phosphorylation of various substrates was reduced in striatal slices derived from rats treated chronically with cocaine (Bibb et al., 2001). As further evidence of the physiological relevance of this Cdk5-dependent depotentiation of D1 signaling, the locomotor effects of cocaine were found to be potentiated by the infusion of Cdk5 inhibitors into the striatum of cannulated rats (Bibb et al., 2001). This effect only became evident after multiple days of cocaine exposure. Thus, chronic cocaine-induced upregulation of *cdk5* gene

expression may lead to a decrease in the efficacy of D1 dopamine signaling. Indeed, animals treated with chronic cocaine showed reduced basal PKA activity, as assessed by examination of the phosphorylation state of PKA substrates, including the GluR1 subunit of the AMPA receptor. This decrease in basal PKA-dependent phosphorylation of GluR1 correlated with a reduction in kainate-sensitive AMPA current in striatal neurons (Bibb et al., 2001). These findings demonstrated that cocaine targeted Cdk5 expression and activity as a mechanism for regulating dopamine neurotransmission. It has been shown that drugs of abuse, including cocaine, methamphetamine, and opiates, alter dendritic spine density (Robinson and Kolb, 1999; Robinson et al., 2001). These structural alterations may represent long-term adaptive changes in neuronal circuitry. Evidence suggests that Cdk5 contributes to neuronal migration and neurite outgrowth through the modulation of cytoskeletal elements (Nikolic et al., 1996; Nikolic et al., 1998). Given this function of Cdk5 in neurodevelopment and cytoarchitectural modulation, the role of Cdk5 in modulating the morphological effects of drugs of abuse were investigated. Rats were given chronic cocaine either in the absence or presence of an intrastriatal infusion of roscovitine, and the striatal dendritic spine density was evaluated. Dendritic spine proliferation in medium spiny neurons in response to cocaine administration was attenuated by roscovitine (Norrholm et al., 2003), suggesting a role for this kinase in the regulation of morphological changes associated with cocaine exposure. Indeed,

chronic cocaine exposure may elicit an adaptive homeostatic response that irreversibly dedicates the affected neurons to a process of cytoarchitectural changes and dendritic spine formation. In this manner, changes in neuroplasticity associated with learning and memory may result in the formation of the addicted state. These studies suggest that Cdk5 may be a part of a global regulatory mechanism that couples normal and aberrant neurotransmission to the modulation of postsynaptic neuronal circuitry.

Cdk5 and reward-related behaviors

Cdk5 has been implicated in the regulation of reward-related behaviors through the use of infusion of pharmacological inhibitors into the reward pathway. These studies have raised the possibility that Cdk5 governs the neuroadaptations that are elicited by drug exposure, leading to altered behavioral responses to repeated cocaine exposure. Recently, we have reported that Cdk5 is involved in contextual learning and extinction through the regulation of NMDA receptor subunit constituency in the hippocampus (Hawasli et al., 2007). Together, these findings may suggest that the reward-related effects of drugs on dopamine signaling as well as the contextual learning associated with the hippocampal formation may be under the control of Cdk5.

Cdk5 activity has been shown to be determined by the availability of cofactor, as transgenic mice engineered to overexpress Cdk5 or p35 indicated

increased Cdk5 activity with p35 overexpression, not kinase overexpression (Takahashi et al., 2005). Likewise, transgenic mice overexpressing the truncated cofactor p25 have also been used as models of enhanced Cdk5 activity (Cruz et al., 2003). In the context of overexpression of p35, increase Cdk5-dependent phosphorylation of pThr75 DARPP-32 was associated with decreased phosphorylation of the PKA site, Thr34 DARPP-32 (Takahashi et al., 2005). These data support the notion that Cdk5-dependent phosphorylation of Thr75 DARPP-32 inhibits PKA activity (Bibb et al., 1999). Furthermore, these p35 overexpressing mice displayed reduced responses to psychostimulant exposure. These data indicate that Cdk5 may normally suppress or counteract processes involved in learning or drug-related plasticity.

Discussion

Regulation of biochemical signaling cascades is an important mechanism of controlling the response to chronic psychomotor drugs of abuse. Taken together, these studies indicate that the acute and chronic cellular effects of cocaine and dopamine neurotransmission are balanced and modulated by phosphorylation of DARPP-32 by Cdk5 and PKA, and that Cdk5 is involved in mediating the morphological effects of chronic cocaine. Since ablation of the *cdk5* gene locus results in perinatal lethality (Ohshima et al., 1996), many novel compounds have been developed to specifically inhibit Cdk5 activity (Meijer et

al., 1997; Gray et al., 1999). The majority of the studies described here have relied on the use of pharmacological inhibitors that inhibit Cdk5 *in vitro* and *in vivo*. However, many of these compounds also exert unwanted nonspecific effects on other cellular targets, including voltage-gated Ca^{2+} channels (Yan et al., 2002). The use of conditional knock-out technology holds the promise of providing a clearer understanding of the role of Cdk5 in the homeostasis that counteracts dopamine signaling. It is also interesting to speculate that Cdk5 may contribute to other undefined aspects of the cellular and physiological responses to drugs of abuse.

In order to study the involvement of Cdk5 in the regulation of behaviors associated with dopamine signaling and neuronal plasticity, we generated several novel conditional knock-out mouse models to mediate loss of Cdk5 in the adult brain. With these tools, we were able to identify numerous behavioral alterations that indicate the requirement for Cdk5 in governing reward-related motor output, motor learning, and emotional state. We also extended the role of Cdk5 in drug-related reward to the natural reinforcer, food. Furthermore, we were able to confirm Cdk5 as a negative regulator of dopamine signaling and identified specific post-synaptic knock-out of Cdk5 in neurons of the nucleus accumbens as crucial in the control of cocaine-related psychoactive and reinforcing properties. These studies were complimented by collaborative efforts that identified loss of

Cdk5 to result in increased intrinsic excitability of NAc neurons, as well as alter the dopamine-dependent modulation of firing rate.

In order to investigate possible biochemical mechanisms for Cdk5 modulation of dopamine signaling, we identified a novel Cdk5 phosphorylation site on the PKA regulatory subunit IIβ (RIIβ) and raised phosphorylation state-specific antisera to the site. This new target provides insight into the regulation of PKA signaling by Cdk5. In related studies, phosphorylation state-specific antisera were generated to both the PKA- and ERK- dependent phosphorylation sites of cAMP-specific phosphodiesterase 4 (PDE4). These reagents compliment other studies involving the Cdk5-dependent phosphorylation of PDE4 recently discovered by the Bibb laboratory. Furthermore, these reagents allow for the analysis of the regulation and crosstalk between PKA and ERK, as well as the involvement of Cdk5 in this pathway. Finally, the site of Cdk5-dependent phosphorylation of MEK1 was identified and confirmed as Thr292, rather than the previously reported Thr286. These data provide the foundation for investigation into novel mechanisms by which Cdk5 may regulate intracellular signaling pathways important in the control of motivation, motor function, reward-related behavior, and emotional state.

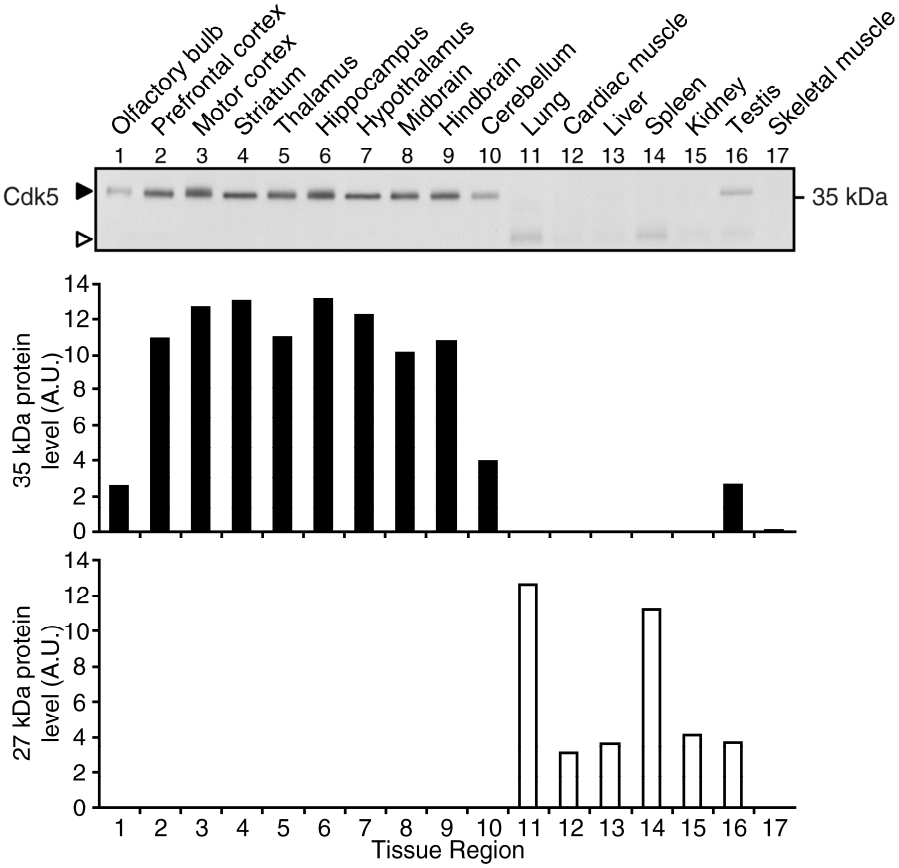

Figure 1.1. Evaluation of tissue distribution and expression level of Cdk5 in the adult mouse. Quantitative immunoblots of Cdk5 in homogenates from brain and peripheral tissues. Representative immunoblot of Cdk5 (top) and quantitation (bottom) are shown for 100 μg samples subjected to SDS-PAGE. Immunoblot shows the detection of native Cdk5 (closed arrowhead; apparent MW ~35 kDa) and a smaller, faster migrating species (open arrowhead; apparent MW ~27 kDa). Quantitation of both protein species in brain and peripheral tissue samples is shown at bottom.

CHAPTER TWO

REGULATION OF COCAINE REWARD, MOTIVATION, AND STRIATAL NEURON EXCITABILITY IN CONDITIONAL CDK5 KNOCK-OUT MICE

Summary

Cdk5 regulates dopamine neurotransmission and has been suggested to serve as a homeostatic target of chronic psychostimulant exposure. To study the role of Cdk5 in the modulation of the cellular and behavioral effects of psychoactive drugs of abuse, we developed Cre/*loxP* conditional knock-out systems that allow temporal and spatial control of Cdk5 expression in the adult brain. Here, we report the generation of Cdk5 conditional knock-out (cKO) mice employing the αCaMKII promoter driven Cre transgenic line (CaMKII-Cre). In this model system, loss of Cdk5 in the adult forebrain increased the psychomotor-activating effects of cocaine. Additionally, these CaMKII-Cre Cdk5 cKO mice show enhanced incentive motivation for food as assessed by instrumental responding on a progressive ratio schedule of reinforcement. Behavioral changes were accompanied by increased excitability of medium spiny neurons in the nucleus accumbens (NAc) in Cdk5 cKO mice. In order to study NAc-specific effects of Cdk5, another model system was utilized in which recombinant adeno-associated viruses (rAAV) expressing Cre recombinase caused restricted loss of Cdk5 in NAc neurons. Targeted knock-out of Cdk5 in the NAc (NAc-KO) facilitated cocaine-induced locomotor sensitization and conditioned place

preference for cocaine. These results suggest that Cdk5 acts as a negative regulator of neuronal excitability in the NAc and that Cdk5 may govern the behavioral effects of cocaine and motivation for reinforcement.

Introduction

Drugs of abuse induce persistent neuroadaptive alterations in synaptic plasticity within the mesocorticolimbic-striatal circuitry involved in reward-motivated behavior (Hyman and Malenka, 2001; Nestler, 2001; Ungless et al., 2001; Thomas and Malenka, 2003). Chronic cocaine exposure increases the expression of the transcription factor ΔFosB in these brain regions (Hope et al., 1994; Chen et al., 1997). An important target of ΔFosB is the neuronal proline-directed serine/threonine protein kinase Cdk5 (Bibb et al., 2001; Kumar et al., 2005). Cdk5 is activated upon association with either of the homologous cofactors p35 (Lew et al., 1994; Tsai et al., 1994) or p39 (Cai et al., 1997). This kinase regulates numerous aspects of neuronal function, including cAMP and Ca^{2+} signal transduction cascades (reviewed in Bibb, 2003), presynaptic machinery (Tan et al., 2003; Tomizawa et al., 2003; Evans and Cousin, 2007), and synaptic plasticity (Fischer et al., 2005; Centonze et al., 2006; Hawasli et al., 2007). In the striatum, Cdk5 controls dopamine neurotransmission through the regulation of the protein phosphatase-1 inhibitor, DARPP-32 (Bibb et al, 1999),

as well as presynaptic components of dopamine synthesis and release (Chergui et al., 2004; Kansy et al., 2004; Moy and Tsai, 2004). Thus, Cdk5 may regulate reward-related behaviors through numerous neurobiochemical pathways in the reward circuitry.

The perinatal lethality and congenital defects associated with Cdk5 or Cdk5-cofactor knock-out mice (Nikolic et al., 1996; Ohshima et al., 1996; Kwon and Tsai, 1998; Ko et al., 2001) have hampered the use of behavioral paradigms to study Cdk5 function. To circumvent this issue, we generated conditional knock-out systems that allow deletion of Cdk5 from specific brain regions in the adult animal, after normal CNS development. These models were specifically designed to avoid congenital issues of Cdk5 loss and allow the investigation of the effect of Cdk5 deletion from the mature brain on reward-related behavioral paradigms. Here, we report that CaMKII-Cre Cdk5 cKO mice showed enhanced locomotor responses to cocaine and intensified motivation for food reinforcement. Furthermore, NAc medium spiny neurons from Cdk5 cKO mice exhibited increased intrinsic excitability. These data suggest that Cdk5 activity within NAc neurons may be important in the modulation of reward-related behaviors.

Studies that have utilized pharmacological inhibitors of Cdk5 have suggested that inhibition of this kinase in the NAc enhances several behavioral responses to cocaine (Bibb et al., 2001; Taylor et al., 2007). However, such pharmacological approaches were unable to distingush the effects of Cdk5 inhibition in pre- versus

postsynaptic compartments. To investigate the role of Cdk5 specifically in NAc neurons in cocaine-related behaviors, we utilized targeted delivery of recombinant adeno-associated virus (rAAV) expressing Cre recombinase to the NAc of conditional Cdk5 mice. This approach allowed temporally-controlled and spatially-restricted loss of Cdk5 in the postynaptic compartment of NAc neurons. This manipulation produced an enhancement in the locomotor-activating effects of repeated cocaine exposure and facilitated cocaine-induced conditioned place preference. Taken together, these findings suggest that Cdk5-dependent modulation of neuronal excitability in the NAc is involved in the behavioral responses to cocaine, cocaine-associated stimuli, and motivation for food reinforcement.

Experimental Procedures

Animals and animal care

The conditional Cdk5 allele was generated using a Cre/*lox*P gene targeting strategy as described (Wattler et al., 1999). This floxed Cdk5 allele (fCdk5) is efficiently excised by Cre recombinase *in vivo* (Hawasli et al., 2007). fCdk5 mice were generated in 129/Sv and C57BL/6 hybrid mice and backcrossed several generations to C57BL/6. Mice were maintained on a mixed background of C57BL/6 and 129/Sv and were group-housed on a 12 hr light/dark cycle with

access to food and water *ad libitum*. All procedures were performed during the light cycle. Behavioral manipulations were approved by UT Southwestern Medical Center and Yale University Institutional Animal Care and Use Committees and conducted in accordance with the applicable portions of the National Institutes of Health *Guide for the Care and Use of Laboratory Animals*. All drugs and chemicals were obtained from Sigma-Aldrich (St. Louis, MO) unless otherwise noted.

Generation of conditional Cdk5 knock-out mice

Homozygous fCdk5 mice were bred with mice expressing Cre recombinase under the control of the αCaMKII promoter (Tsien et al., 1996) to generate Cdk5 conditional knock-out (cKO) mice. The CaMKII-Cre T50 line (provided by L.F. Parada, UT Southwestern Medical Center) was chosen in order to mediate recombination of Cdk5 in the postnatal forebrain. This line has been shown to exhibit Cre activity beginning postnatal day 18 (P18) proceeding through P60 (Luikart et al., 2005), thus circumventing developmental issues regarding loss of Cdk5. Littermate, homozygous fCdk5 mice lacking the CaMKII-Cre transgene served as controls. Adult (10–12 week old), male mice were utilized for all experiments. The transgenic CaMKII-Cre and R26R-EYFP mice (provided by A.J. Eisch, UT Southwestern Medical Center) were genotyped using PCR-based strategies.

PCR-based genotyping

Floxed and transgenic alleles were identified by PCR-based genotyping. The Cdk5 allele was detected using a strategy previously described (Hawasli et al., 2007) using the following oligonucleotide sequences: 5'-GCAGGCCTTCGTTCCTCCC-3' and 5'-CCTGACACGCTTCAGAGCC-3'. These oligos amplified a 304 bp wild-type and a 376 bp fCdk5 allele. The transgenic CaMKII-Cre genotyping was conducted using the following oligonucleotides: 5'-CCACACAGTCCTGCAGTATTGTG-3' and 5'-CATCAACGTTTTCTTTTCGGATC-3'. These oligos amplified a ~1.1 kb Cre transgene product. Oligonucleotides for the control target Gdf5 were included in all transgenic Cre reactions: 5'-GGAGCACTTCCACTATGGGAC-3' and 5'-AAAGAGTGAGGAGTTTGGGGAG-3' to amplify a 243 bp product. R26R-EYFP transgenic mice were genotyped as described (Soriano, 1999) using three oligonucleotides: 5'-AAAGTCGCTCTGAGTTGTTAT-3', 5'-GCGAAGAGTTTGTCCTCAACC-3', and 5'-GGAGCGGGAGAAATGGATATG-3'. These oligos amplified a 550 bp wild-type and 300 bp mutant allele.

Generation of NAc-specific Cdk5 knock-out mice using rAAV

Adeno-associated viral vectors were infused into the brain via stereotaxic surgical procedures as previously described (Hommel et al., 2003; Berton et al.,

2006). Vectors and rAAV were provided by R.J. DiLeone (Yale University) and expressed and purified by A.H. Hawasli (UT Southwestern Medical Center). Recombinant vectors encoding enhanced green fluorescent protein (EGFP), a Cre recombinase/EGFP chimeric protein (EGFPCre), or Cre were derived by cloning cDNAs into the pAAV-lacZ amplicon (Stratagene; La Jolla, CA). Serotype 2 recombinant adeno-associated viruses (rAAV) were generated using a modified triple transfection method in HEK293 cells, as previously described (Zolotukhin et al., 1999). After transfection, HEK293 cells were lysed and rAAV was purified via iodixanol density gradient to produce viral titers of 10^{11}–10^{12} pfu/ml.

These rAAV particles transduce neurons with high efficiency *in vivo* (Burger et al., 2004) and maintain detectable levels of expression in the brain for up to 12 months after infection (R.J. DiLeone, unpublished observations). NAc-specific Cdk5 knock-out (NAc-KO) was achieved in adult (6–8 week old), male homozygous fCdk5 mice via bilateral stereotaxic delivery of rAAV (~$4x10^8$ particles, 0.4 μl/hemisphere) to the NAc core (coordinates from bregma at skull surface: +1.6 to +1.9 mm anteroposterior, +1.5 mm lateral, −4.5 mm dorsoventral; 10° angle of entry). Surgical procedures were performed under aseptic conditions following anesthesia with Avertin (240 mg/kg). Delivery of rAAV expressing Cre produced focal, conditional knock-out of Cdk5 in the NAc, while littermate fCdk5 mice transduced with rAAV-EGFP served as controls.

Histological procedures and immunoblotting

In situ hybridizations for Cdk5 and Cre were conducted as described (Gold et al., 1997; Hawasli et al., 2007). B. Potts and S. Gold (UT Southwestern Medical Center) assisted in the execution of these experiments. Briefly, ^{35}S-UTP-labeled riboprobes were hybridized with fresh cryosections for 16–18 hr at 60 °C. Following hybridization, slides were washed in sodium chloride/sodium citrate buffer, dried, and exposed to film. Autoradiograms were scanned and semi-quantitative analysis was conducted using ImageJ software (NIH). Immunohistochemistry was performed essentially as described (Kansy et al., 2006). D.C. Lagace (UT Southwestern Medical Center) assisted with immunohistochemistry. Adult, CaMKII/R26R-EYFP mice were transcardially perfused with PBS and 4% paraformaldehyde (PFA). Brains were removed, post-fixed overnight in 4% PFA, and cryoprotected in 30% sucrose in PBS containing 0.1% sodium azide. Sections (35 μm) were prepared on a freezing microtome. Primary antibody incubations were conducted overnight at 4 °C using antibodies to GFP (1:1000, AbCam; Cambridge UK) and NeuN (1:100, AbCam). Slides were washed in PBS and incubated with Cy5 or Cy2-conjugated secondary antibody (1:200, Jackson ImmunoResearch; Westgrove, PA) before dehydration and coverslipping in DPX. Images were captured and analyzed using a scanning laser confocal microscope.

Immunoblotting was performed as previously described (Sahin et al., 2004). Tissue homogenates were prepared from control and Cdk5 cKO mice by acutely dissecting brain regions, transferring samples to screw-cap microcentrifuge tubes, and immediately freezing on dry ice. For NAc-KO and control samples, brains were removed into cold artificial cerebrospinal fluid (aCSF) containing (in mM): 124 NaCl, 4.5 KCl, 2 $CaCl_2$, 1 $MgCl_2$, 26 $NaHCO_3$, 1.2 NaH_2PO_4, and 10 D-glucose, brought to pH 7.4 by aeration with 95% O_2/5% CO_2, and 1 mm thick coronal slices were prepared using a matrix (Zivic-Miller, Pittsburgh, PA). The rAAV generated GFP signal was visualized in the NAc of tissue slabs under an epifluorescence microscope and NAc punches (1 mm diameter) were collected, transferred to screw-cap tubes, and frozen on dry ice. Samples were homogenized in boiling lysis buffer (50 mM NaF in 1.0% SDS) using a manual ultrasonic processor, boiled for 10 min, and protein concentration determined using a bicinchoninic acid (BCA) colorimetric protein assay (Pierce, Rockford, IL). Equal amounts of total protein from homogenates were resolved by SDS-PAGE on 10–15% isocratic gels and transferred onto nitrocellulose membranes (0.2 μm, Schleicher & Schuell, Keene, NH) overnight. Membranes were rinsed in water, then in TBS containing 0.01% Tween-20 (TBS-T) prior to western blotting. Antibodies were diluted in Blotto (5% Non-fat milk in TBS-T) with 0.02% sodium azide, except where noted. Membranes were probed with antibodies to Cdk5 (1:500, Santa Cruz; Santa Cruz, CA, C-8), β-actin (1:500,000, Abcam, AC-

15), GFP (1:5000, AbCam), Cre (1:10,000, Novagen), and phospho-Thr75 and total DARPP-32 (1:5,000, provided by P. Greengard, Rockefeller University). Membranes were washed and incubated with HRP-conjugated secondary antibodies (1:5000, Chemicon) and detected using ECL chemiluminescence (Amersham Biosciences; Piscataway, NJ). Membranes were exposed to autoradiographic film and resulting autoradiograms were scanned and analyzed using ImageJ (NIH). Exposure times ranged from 10 sec to 30 min. Quantitation consisted of calculation of band intensity by analysis of the area under the curve for each target. In all experiments, apparent phosphoprotein levels were adjusted to reflect relative levels of total protein loaded per lane. Where specified, these corrected values were further normalized to the means of indicated controls. Thus, Cdk5 protein levels are represented as values normalized to β-actin, while phospho-Thr75 is normalized to total DARRP-32.

Behavioral procedures

Cocaine-induced locomotor activity assay: Horizontal locomotor activity was monitored in standard polypropylene cages (15x25 cm) in chambers equipped with infrared photobeams to monitor activity using a computer (Photobeam Analysis Software, San Diego Instruments). Locomotor chambers were also equipped with light- and sound- attenuating surrounds. Locomotor activity was measured as sequential adjacent beambreaks and reported as locomotor counts.

The execution of repetitive, fine movements were measured as sequential single beambreaks and reported as stereotypy counts. In one experiment, a Latin-square crossover design was used to evaluate CaMKII-Cre Cdk5 cKO mice, with one testing session per day for 8 d (n = 10 per group). For each experimental day, animals were placed in the chamber and motor activity was recorded for 1 h, at which point a single intraperitoneal (i.p., 5 ml/kg) injection was delivered and the animal was returned to the chamber for 1 h. During the first 3 d mice were habituated to saline injections, and the next 5 d they were given injections of cocaine (0, 2.5, 5, 10, 20 mg/kg). Drug doses were randomized among the groups to prevent order or carryover effects on locomotor responses.

Instrumental responding and progressive ratio testing: Instrumental responding experiments for food reinforced reward in CaMKII-Cre Cdk5 cKO mice were performed using operant chambers for mice (16x14x14.5 cm) equipped with a food pellet dispenser and three nosepoke apertures. These experiments were conducted by J.J. Quinn and J.R. Taylor (Yale University). Throughout the experiment, only the left or right positions were reinforced, and the position of the active nosepoke was counterbalanced for all groups to prevent positional bias. Nosepokes were detected by photobeams within the receptacle linked to computer software (MedAssociates; St. Albans, VT). During the 5 d prior to the start of the experiment, all animals underwent food restriction to 85–90% of baseline weight (n = 16–20 per group). The animals were habituated to testing chambers and

pellet magazine before training. Animals were trained over fixed and random interval reinforcement schedules consisting of 5 d of each of the following: fixed-interval 20 sec (FI20), random-interval 40 sec (RI40), random-interval 60 sec (RI60), and reversal training, during which the active and inactive responses were switched and an RI60 schedule was used. Following training, the animals were tested for progressive ratio (PR) responding across 3 d. The PR sessions began with a fixed ratio (FR) 1 schedule for the first reinforcer and increased by 4 to obtain each subsequent reinforcer (*i.e.* 1, 5, 9…, X + 4 responses). The PR responding test was conducted as an open-session, such that the experiment was terminated when the animals reached its final breakpoint ratio. The breakpoint ratio was achieved when the animal discontinued responding in the active nosepoke for a continuous 5 min period. Weeks after the PR responding test, the same animals were utilized for the reinforcer devaluation experiment. In this experiment, animals were fed prior to PR responding for food-reinforced instrumental responding. The pre-feeding reinforcer devaluation experiment was performed by allowing animals to eat unlimited food pellets in a novel context for 1 h (with water available) before PR testing.

Cocaine-induced locomotor sensitization assay: Locomotor sensitization to cocaine (10 or 15 mg/kg) was examined in NAc-KO mice using an experimental design similar to that described above (see cocaine-induced locomotor activity). Some behavioral sensitization experiments were conducted by D. Theobald (UT

Southwestern Medical Center). In these experiments, subjects were habituated to saline for 4 d, followed by injection of cocaine over the following 5 d (n = 16–19 per group). For each experimental day, animals were placed in the chamber and motor activity was recorded for 30 min, at which point a single intraperitoneal (i.p., 5 ml/kg) injection was delivered and the animal was returned to the chamber for 1 h.

Cocaine conditioned place preference assay: The conditioned place preference assay was used to study NAc-KO responses to reward-associated stimuli. Place preference experiments were conducted by T. Sasaki (UT Southwestern Medical Center). The place preference chamber contained two large compartments with distinct visual and tactile cues, separated by a smaller, center compartment. Prior to drug conditioning, animals were placed in the center area to record exploration of all compartments for 20 min using computer software (MedAssociates). An unbiased, counterbalanced protocol was used to ensure that no preference for any compartment was observed in any group during the pre-training trial. For drug-context training sessions, partitions were put in place to confine subjects in a specific compartment of the apparatus. Alternating for 4 d, mice were conditioned to one compartment with saline or to the other compartment with cocaine (0, 2.5, 5, 20 mg/kg, i.p.) for 25 min (n = 9–19 per group). Mice were placed into the center area 24 h after the last conditioning session and the time spent in each compartment was recorded for 20 min. A

conditioning score was calculated for each animal by subtracting the time spent in the drug-paired compartment before training from the time spent after training.

Anxiety-related behavioral tests: The elevated plus maze (EPM), open field (OF), and dark light (D/L) habituation tests were used to assess the global emotional state and anxiety of experimental subjects, and were performed as previously described (Barrot et al., 2002; Green et al., 2006). Some anxiety experiments were conducted by T. Sasaki and A. Graham (UT Southwestern Medical Center). In brief, EPM and OF tests consisted of a single 5 min exposure to the testing apparatus. In the EPM, animals were placed in the center of a black, plexiglass elevated plus maze (each arm was 5x33 cm, with 25 cm walls on closed arms) in a dimly lit room for 5 min. Each session was videotaped for later analysis by an observer blind to the genotype of the mice. Time spent in the open and closed arms, number of open and closed arm entries, time spent in the middle, and number of explorations of the open arm (defined as placing head and two limbs into open arm without full entry) were calculated. The OF test consisted of a square arena (44x44 cm) in which the latency to enter the center of the arena, time spent in center vs. periphery, and distance traveled in each area were recorded by automated video-tracking software (Ethovision, Noldus Information Technology, Wageningen, Netherlands). For the OF test, the center region encompassed a 14x14 cm square in the middle of the box, whereas the peripheral region included all areas within 5 cm of the edge. The D/L apparatus consists of

MedAssociates mouse place preference box linked to MedAssociates photobeam data acquisition software (MedPC). Mice were placed in the dark side for 2 min, and then the door between the compartments was opened to allow the animal to freely explore either the light or dark side for 10 min. Anxiety-like behavior was measured based on the latency to enter the light side, time spent in light vs. dark side, exploration and activity in light and dark side.

Preparation of acute striatal slices and electrophysiology

Acute slices and whole-cell patch clamp recordings were performed in CaMKII-Cre Cdk5 cKO mice, according to methods previously described (Zhong et al., 2003). The electrophysiological analyses were performed by P. Zhong and Z. Yan (SUNY Buffalo). Briefly, mice were anesthetized by inhaling 2-bromo-2-chloro-1,1,1-trifluoroethane (1 ml/100g) and decapitated. Brains were then quickly removed, iced and sliced with a VP1000S Vibrotome (Leica; Nussloch, Germany). Slices (400 μm) were incubated for 1–5 hr at room temperature (20–22 °C) in a $NaHCO_3$-buffered saline bubbled with 95% O_2, 5% CO_2. To measure intrinsic excitability, current-clamp recordings were conducted using patch electrodes filled with an internal solution containing (in mM): 60 K_2SO_4, 60 N-methyl-D-glucamine, 40 HEPES, 4 $MgCl_2$, 0.5 BAPTA, 12 phosphocreatine, 2 Na_2ATP, 0.2 Na_3GTP, 0.1 leupeptin, pH 7.2–7.3, 265–270 mOsm/L. Slices were positioned in a heated (30 °C) perfusion chamber attached to the fixed-stage of an

upright microscope (Olympus; Center Valley, PA) and submerged in continuously flowing oxygenated aCSF. Cells were visualized with a 40x water-immersion lens and illuminated with near infrared (IR) light, and the image was detected with an IR-sensitive CCD camera. Recordings were made with Multiclamp 700A amplifier (Axon Instruments; Sunnyvale, CA) that was controlled and monitored with a computer running pClamp (v. 8) with a DigiData 1322A interface (Axon Instruments). Tight seals (2–5 GΩ) from visualized neurons were obtained by inducing negative pressure. The membrane was disrupted with additional suction, and the whole-cell configuration was obtained. The access resistances ranged from 10–15 MΩ.

Statistical analysis

Experimental data were analyzed using two-way ANOVA followed by Bonferroni test, ANOVA followed by Tukey or Neuman-Keuls test, or Student's *t*-test using GraphPad Prism 4.0 and SPSS 12.0 for Windows software. We employed a paired *t*-test where appropriate (i.e., time in drug side before and after training, etc.). Two-way ANOVA for repeated measures (RM) was employed where appropriate (*i.e.*, response to repeated injections, performance on consecutive days, etc.). Data are reported as mean ± *SEM* for each measure. Each sample size is indicated. A value of $p \leq 0.05$ was considered statistically significant.

Results

Generation of a conditional Cdk5 knock-out mouse model

To achieve conditional loss of Cdk5, the endogenous gene encoding the protein kinase was first replaced with a targeted allele in which *loxP* sites flank exons 2–5 (**Figure 2.1*A***). This fCdk5 allele is subject to excision by Cre recombinase, resulting in knock-out of Cdk5. The transgenic line expressing Cre under the control of the αCaMKII promoter (CaMKII-Cre) was employed to mediate excision of Cdk5 in the adult brain. Using this transgenic strategy, recombination of the fCdk5 allele was achieved throughout the forebrain of adult CaMKII-Cre/fCdk5 transgenic mice (**Figure 2.1*B***). Cdk5 cKO mice showed significant reduction in Cdk5 mRNA in striatum (32.4 ± 4.8%), cortex (39.5 ± 5.3%), and hippocampus (26.1 ± 4.7%) in comparison to littermates lacking the CaMKII-Cre transgene (**Figure 2.1*B***). No alteration was observed in the level of Cdk5 mRNA in the cerebellum of cKO mice (101 ± 4.9% of littermate control). These data indicate that Cdk5 was selectively decreased throughout structures of the adult forebrain in Cdk5 cKO mice. The decrease in striatal Cdk5 mRNA corresponded to a similar decrease in protein level in striatal tissue lysates (50.7 ± 17.0% compared to littermate control, **Figure 2.1*C***). Decreases in Cdk5 protein also correlated well with reduced Cdk5 activity in tissue homogenates from inducible Cdk5 conditional knock-out mice (Hawasli et al., 2007). Furthermore Cdk5 cKO mice showed a decrease in Cdk5-dependent phosphorylation of Thr75

DARPP-32 in striatal tissue lysates (62.9 ± 0.05% of littermate control; **Figure 2.1*C***). Consequently, transgenic CaMKII-Cre Cdk5 cKO mice showed reduction in Cdk5 mRNA, protein, and kinase activity in forebrain structures.

To further define the activity of the CaMKII-Cre, this Cre line was crossed to a transgenic reporter line that expresses enhanced yellow fluorescence protein (EYFP) following Cre-mediated recombination (R26R-EYFP) (Srinivas et al., 2001). The R26R-EYFP mouse harbors a *loxP* flanked stop-EYFP cassette at the R26R locus. Cre-mediated excision of this stop signal results in fluorescence due to EYFP expression. Cre activity was visualized in ~60% of the cells of the dorsal striatum and NAc of CaMKII-Cre/R26R-EYFP mice at 10–12 weeks of age (**Figure 2.1*D***), consistent with previous observations for this transgenic line (Monteggia et al., 2007). These data suggest that the CaMKII-Cre transgene mediates Cdk5 knock-out in a mosaic population of neurons within the striatum.

Effect of conditional Cdk5 knock-out in adult forebrain on psychomotor stimulant effects of cocaine

To assess the effect of loss of Cdk5 on the locomotor-activating effects of cocaine, a randomized Latin-square dose response experiment was conducted using transgenic Cdk5 cKO mice. Mice were habituated to locomotor activity chambers and received i.p. injections of saline for 3 days. On each of the subsequent 5 days, mice were given a single injection of cocaine (2.5, 5, 10, or 20

mg/kg) or saline and locomotor responses were recorded for 60 min. Statistical analyses revealed a significant effect of treatment in both control and Cdk5 cKO mice ($F(4,76) = 10.8$; $p < 0.0001$, two-way RM ANOVA). Animals displayed elevated responses to escalating doses of cocaine administration (**Figure 2.2*B*-*F***). No difference between genotypes was detected in response to saline injection (94.1 ± 14.0 for control vs. 153.8 ± 37.0 for cKO; **Figure 2.2*B***). There was no significant effect of genotype ($F(1,76) = 2.8$; $p = 0.1$) and no interaction between genotype and treatment day ($F(4,76) = 2.1$; $p = 0.1$). However, conditional loss of Cdk5 produced a dramatic elevation in response to 20 mg/kg cocaine compared to control mice (330 ± 80.3 for control vs. 739.7 ± 207.2 for cKO; **Figure 2.2*F***). This enhancement in locomotor activity in response to cocaine in Cdk5 cKO was evident, but not statistically significant, in response to the 10 mg/kg dose as well (180.9 ± 53.3 for control vs. 313.7 ± 133.2 for cKO; **Figure 2.2*E***). These data indicate that Cdk5 loss in the forebrain produced an enhancement in locomotor responsiveness to acute exposure to a high dose of cocaine. These findings provide direct evidence for the involvement of Cdk5 in the regulation of behavioral responses to cocaine.

Sterotypic responses are known to compete with locomotor activity in response to psychostimulants. Therefore, we also monitored stereotypic activity in the randomized Latin-square dose response experiment (**Figure 2.3**). There were no differences between control and Cdk5 cKO mice in stereotypic

movements in response to cocaine injection at any dose ($F(1,76) = 0.3$; $p = 0.6$) and no interaction between genotype and treatment day ($F(4,76) = 0.9$; $p = 0.5$). Notably, stereotypic movements in both genotypes displayed dose-dependence, and increased with escalating doses of cocaine administration in both control and Cdk5 cKO mice ($F(4,76) = 41.2$; $p < 0.0001$, two-way RM ANOVA; **Figure 2.3*B-F***). These data indicate that there are no differences between control and Cdk5 knock-out mice in the time spent executing repetitive, fine movements (stereotypy) in response to cocaine administration.

Effect of Cdk5 loss in adult forebrain on motivation for food-reinforced progressive ratio responding

Drugs of abuse activate the neural circuitry involved in normal incentive motivation for reinforcers such as food (Kelley and Berridge, 2002). Instrumental responding on progressive ratio schedules has been widely used to study motivation. To evaluate the involvement of Cdk5 in motivation, CaMKII-Cre Cdk5 cKO mice and littermate controls were trained to nosepoke for food reinforcement and tested for three consecutive days under a progressive ratio schedule of reinforcement which provides a measure of how hard an animal is willing to work for the reward. Cdk5 cKO mice did not differ from controls in their acquisition of instrumental responding (**Figure 2.4*A***). In contrast, loss of Cdk5 produced dramatically elevated active responses compared to controls on all

days tested on progressive ratio responding (3209.1 ± 662.6, 1886.2 ± 533.9, and 1901.7 ± 546.0 for cKO vs. 1057.1 ± 214.0, 375.3 ± 80.7, and 432.6 ± 133.1 for control on day 1, 2, and 3, respectively; **Figure 2.4*B***). Cdk5 cKO mice also showed significantly elevated inactive responses on day 1 (471.1 ± 117.5 for cKO vs. 194.7 ± 43.3 for control; **Figure 2.4*B***), although this effect did not persist over the second and third day of testing. Most striking was that Cdk5 cKO mice achieved significantly higher breakpoints compared to controls over all 3 days of testing (142.0 ± 17.5, 92.3 ± 14.9, and 101.3 ± 16.2 for cKO vs. 79.2 ± 9.3, 46.2 ± 6.1, and 47.0 ± 7.5 for control on days 1, 2, and 3, respectively; **Figure 2.4*C***). These data indicate that loss of Cdk5 in the adult forebrain increases the motivation for goal-directed instrumental responding for appetitive reinforcement.

We also sought to specifically explore motivational influences on goal-directed responding in Cdk5 cKO mice by assessing the ability of post-training reinforcer devaluation to alter progressive ratio responding. This satiety-induced reinforcer devaluation experiment was conducted by switching the motivational state from hunger to satiety via pre-feeding the animals prior to progressive ratio testing. Pre-feeding prior to testing dramatically reduced the breakpoints achieved in control and Cdk5 cKO mice and eliminated the difference between groups (27.1 ± 5.2 for control vs. 40.4 ± 9.5 for cKO; **Figure 2.4*D***). These data indicate that reduction in incentive motivation for reinforcement completely eliminated the enhanced breakpoint ratio achieved by Cdk5 cKO mice. No

differences in weight were observed between groups (**Figure 2.5*A***), suggesting that the enhanced performance in Cdk5 cKO mice was not likely attributed to alterations in appetite or hunger. Furthermore, Cdk5 cKO and control mice consumed the same amount of food during pre-feeding, suggesting that there was likely no difference in hunger or appetite prior to testing (**Figure 2.5*B***). Taken together, these data indicate that loss of Cdk5 increased the motivation to obtain reinforcement, likely through enhancement in incentive value. Thus, Cdk5 may govern aspects of reward processing in the mesocorticolimbic-striatal circuitry that are important for natural reinforcers.

Neurons in the NAc from Cdk5 cKO mice exhibit increased excitability

To understand possible mechanisms involved in these behavioral effects, we examined the effect of Cdk5 loss on the physiological state of NAc neurons. For this analysis, patch clamp recordings were performed in NAc medium spiny neurons from CaMKII-Cre Cdk5 cKOs to examine the potential changes in their intrinsic excitability. When compared to cells recorded from control mice, loss of Cdk5 did not alter the current-voltage relationship (**Figure 2.6*A***), resting membrane potential, or action potential waveform properties (**Table 2.1**) in NAc medium spiny neurons. However, there was a dramatic increase in the intrinsic excitabilty of NAc neurons as measured by the number of spikes evoked by injection of depolarizing current steps (**Figure 2.6*B***). Loss of Cdk5 increased the

firing rate of NAc neurons by 126–210% in response to 180–240 pA current injections, compared to NAc neurons from control mice (**Figure 2.6*C***). In addition, cells from Cdk5 cKO slices displayed a reduced threshold to elicit a spike compared to controls (137.6 ± 5.3 pA in cKO vs. 158.3 ± 4.2 pA in control), as well as a decreased latency to fire in response to 180 pA current injection (**Table 2.1**). Thus, NAc neurons from Cdk5 cKO mice show increases in neuronal excitability. These data suggest that Cdk5 exerts an inhibitory effect on the basal intrinsic excitability of NAc neurons that may be related to behavioral responses to rewarding stimuli, including cocaine and natural reinforcers like food.

Generation of NAc-specific Cdk5 knock-out mouse model

To investigate the role of Cdk5 specifically in neurons of the NAc, we delivered rAAV expressing Cre recombinase to the NAc of fCdk5 mice to excise the Cdk5 allele (**Figure 2.7*A***). rAAV expressing EGFP served as the control vector as previously described (Berton et al., 2006). RNA *in situ* hybridization analysis on serial coronal brain sections of homozygous fCdk5 mice transduced with Cre indicated a circumscribed loss of Cdk5 mRNA within the NAc that precisely overlaid the area of Cre expression (**Figure 2.7*B***). These rAAV vectors are not subject to retrograde transport when delivered to striatal brain regions (Burger et al., 2004). Thus, these results indicate that KO of Cdk5 occurred

specifically within the postsynaptic compartment of NAc neurons (NAc-KO). Delivery of the Cre vectors into wild-type animals exhibited no such effects on Cdk5 expression (data not shown). To evaluate NAc-KO at the protein level, the EGFP signal present in the EGFPCre and the control EGFP vector was used to visualize the specific population of transduced neurons using an epifluorescence microscope. Immunoblots of tissue punch homogenates from EGFPCre fields showed a reduction in Cdk5 protein level to 55.0 ± 5.1% of control (**Figure 2.7*C***). In contrast, transduction by the control EGFP vector had no effect on Cdk5 expression in the NAc (107 ± 7.28% of naïve control). Thus, we achieved control of Cdk5 expression in NAc neurons by rAAV-mediated Cdk5 NAc-KO.

Effect of NAc-specific loss of Cdk5 on cocaine-induced behavioral sensitization

Previous studies have suggested that Cdk5 contributes to the development and expression of locomotor sensitization to cocaine (Bibb et al., 2001; Taylor et al., 2007). However, these studies utilized pharmacological inhibition of Cdk5 that likely had both pre- and postsynaptic effects in the NAc. In order to investigate the role of Cdk5 specifically in the postsynaptic compartment of striatal neurons, we utilized rAAV-mediated Cre delivery to the NAc. Notably, NAc-KO did not alter spontaneous activity or anxiety compared to controls (**Figure 2.8**). With this NAc-KO strategy, we were able to study the effect of selective, postsynaptic Cdk5 loss on locomotor responses to cocaine. Adult,

fCdk5 mice were targeted with rAAV expressing EGFP or Cre (EGFPCre or Cre) into the NAc and assessed for cocaine-induced locomotor sensitization to 10 and 15 mg/kg cocaine doses (**Figure 2.9**). Following habituation to saline injections in the locomotor chambers, mice were injected with 10 mg/kg cocaine for 5 consecutive days and locomotor responses were recorded for 60 min (**Figure 2.9*A***). There was a main effect of treatment day on locomotor responses in the first 30 min after saline injection and 5 days of cocaine ($F(5,160) = 7.85$; $p < 0.0001$, two-way RM ANOVA) and locomotion increased over consecutive days to repeated cocaine injections. However, Cdk5 NAc-KO mice showed significantly higher locomotor counts as early as day 3 of cocaine treatment (336.4 ± 126.3 vs. 52.2 ± 7.3 for saline) whereas the control mice only showed increases in locomotion on day 5 of cocaine (300.1 ± 101.8 vs. 58.1 ± 14.3 for saline; **Figure 2.9*A***). These data indicate that Cdk5 loss in the postsynaptic compartment of the NAc enhanced the behavioral sensitization to 10 mg/kg cocaine exposure.

When mice were analyzed for the development of sensitization using a higher dose of 15 mg/kg cocaine, no such differences between EGFP and Cre animals were appreciated (**Figure 2.9*B***). Both groups showed robust locomotor sensitization to this higher cocaine dose ($F(5,165) = 51.3$; $p < 0.0001$, two-way RM ANOVA), with both genotypes exhibiting progressive increases in locomotor activity over subsequent challenge days. These effects were observed on day 3

for both control mice (501.6 ± 83.9 vs. 74.8 ± 11.9 for saline) and Cdk5 NAc-KO mice (496.8 ± 83.1 vs. 74.2 ± 10.8 for saline). Statistical analyses revealed no main effect of genotype ($F(5,165) = 0.0$; $p = 1.0$) and no interaction between genotype and treatment day ($F(5,165) = 0.6$; $p = 0.7$). Furthermore, the overall level of behavioral sensitization to 5 days of 15 mg/kg cocaine exposure was not altered between genotypes (663.2 ± 91.3 for control vs. 751.6 ± 98.0 for NAc-KO). Taken together, these data indicate that loss of Cdk5 specifically from the postsynaptic compartment of NAc neurons caused a leftward shift in the threshold to induce behavioral sensitization, but did not alter the maximal behavioral responses to repeated cocaine exposure.

Effect of NAc-specific Cdk5 KO on expression of cocaine conditioned place preference

Drug addiction involves associative learning processes where the reinforcing properties of drugs become associated with environmental cues. To assess the role of Cdk5 in this aspect of reward-related learning that likely has relevance for recidivism, Cdk5 NAc-KO mice were analyzed for cocaine conditioned place preference (**Figure 2.10**). In this paradigm, cocaine exposure is paired with a distinctive context in order to associate cocaine reinforcement with specific contextual cues. After cocaine conditioning, the degree of cocaine reinforcement is inferred by the amount of time the mice spend in the previously

drug-associated context. Before conditioning, there was no preference for the compartment that was to be paired with cocaine at any dose in either control or NAc-KO mice ($F(3,101) = 0.2$; $p = 0.9$, two-way ANOVA). When conditioned with a low dose of cocaine (2.5 mg/kg), Cdk5 NAc-KO mice displayed a significant increase in time spent in the drug-paired context (644.7 ± 41.4 during post-training vs. 520.5 ± 23.1 for pre-training; **Figure 2.10*A***), while no place preference was found in control animals (574.7 ± 42.8 during post-training vs. 522.5 ± 35.9 for pre-training; **Figure 2.10*A***). These data indicate that postsynaptic loss of Cdk5 in NAc neurons may facilitate cocaine-induced associative learning. Training with either 5 or 20 mg/kg cocaine induced significant increases in the amount of time spent in the cocaine-associated compartment in both control and NAc-KO mice (**Figure 2.10*A***). Furthermore, analysis of the conditioning score for each group indicated that training induced a significant preference at all cocaine doses in Cdk5 NAc-KO mice compared to saline, while control mice showed preferences following only 5 and 20 mg/kg training doses in comparison to saline (**Figure 2.10*B***). Taken together, these data suggest that deletion of Cdk5 from neurons of the NAc reduced the threshold for cocaine-conditioned place preference. This finding is consistent with the enhanced psychomotor effects of cocaine seen in Cdk5 NAc-KO mice in the locomotor sensitization assay and further supports the notion that Cdk5 regulates

cocaine-related behavioral responses, at least in part, through activity in striatal neurons of the NAc.

Discussion

The present study demonstrates that loss of Cdk5 in the adult forebrain enhances the locomotor activating properties of cocaine, augments motivation for food reinforcement, and increases intrinsic neuronal excitability in the NAc. Enhancements in the psychoactive properties of cocaine were also induced by selective loss of Cdk5 in postsynaptic compartments of the NAc. These findings are consistent with the hypothesis that Cdk5 regulates dopamine neurotransmission in the NAc and serves as a homeostatic target of chronic psychostimulant exposure. Two model systems were employed here that allowed restricted loss of Cdk5 activity: first, a transgenic Cdk5 cKO system was developed that allowed temporal and spatial control of Cdk5 expression selectively in the adult forebrain. Second, rAAV was used to induce loss of Cdk5 restricted to the postsynaptic compartment of NAc neurons in adult animals (*i.e.,* NAc-KO). This targeted deletion of Cdk5 in the NAc facilitated cocaine-induced locomotor sensitization and conditioned place preference for cocaine. Together these results provide compelling evidence that Cdk5 acts as a key negative regulator of neuronal excitability in the NAc through postsynaptic mechanisms

that may underlie enhanced neuroadaptive and motivational properties of addictive drugs and natural reinforcers.

While previous studies have utilized the infusion of Cdk5 inhibitors into the brain in combination with behavioral assessments (Bibb et al., 2001; Chen and Chen, 2005; Taylor et al., 2007), the development of conditional Cdk5 knock-out model systems allowed for direct evaluation of the role of Cdk5 in the psychoactive properties of cocaine and reward-motivated behavior. Indeed, these approaches circumvent the limitations of Cdk5 inhibitors, including the inability to localize the effects of Cdk5 inhibition to either pre- or postsynaptic compartments and the possibility of nonspecific pharmacological effects. Furthermore, inhibition of Cdk5 catalytic activity may not affect structural or activity-independent roles of the protein, which have recently been appreciated (Hawasli et al., 2007). Thus conditional knock-out strategies provide a powerful platform from which to evaluate the role of Cdk5 in reward-related behavior. In the present study, conditional Cdk5 knock-out allowed the restricted and selective loss of Cdk5 in adult brain to be more directly linked to behavioral response to rewarding stimuli.

The reinforcing and rewarding properties of drugs of abuse are associated with potent activation of the mesocorticolimbic-striatal circuitry controlled by dopamine neurotransmission. Cdk5 negatively regulates dopamine signal transduction (Bibb et al., 1999) and pharmacological inhibition of Cdk5 in the

NAc enhances several locomotor and motivational responses to cocaine (Bibb et al., 2001; Taylor et al., 2007). Here, we show that CaMKII-Cre Cdk5 cKO mice, in which Cdk5 is deleted in the adult brain, display potentiated locomotor responses to cocaine. Specifically, loss of Cdk5 throughout the forebrain, including the mesocorticolimbic-striatal circuitry, increased the locomotor response to the highest dose of cocaine in a randomized dose-response study. These data are consistent with previous studies where Cdk5 inhibition enhanced locomotor responses to cocaine (Bibb et al., 2001; Taylor et al., 2007) and suggest that Cdk5 activity in the adult forebrain is involved in the modulation of the psychoactive effects of cocaine exposure.

Dopamine neurotransmission plays important roles in multiple reward-related behavioral processes in addition to those invoked by addictive drugs. To investigate whether Cdk5 is also involved in non-drug reward-related behavior, we evaluated the consequences of loss of Cdk5 on instrumental responding for food reinforcement. Cdk5 cKO mice displayed increased incentive motivation for food-reinforcement measured by progressive ratio responding. It should be noted that while the CaMKII-Cre Cdk5 cKO model system avoids the possible confounds of congenital abnormalities and pharmacological nonspecificity, the loss of Cdk5 is not complete in this model system (see **Figure 2.1**). Nonetheless, the observations made here are consistent with Cdk5 inhibition enhancing cocaine-induced potentiation of conditioned reinforcement and progressive ratio

responding for cocaine (Taylor et al., 2007) and strongly suggest that Cdk5 activity influences reward-motivated processes that involve dopamine signaling in the NAc.

The development of locomotor sensitization may model aspects of the neuroadaptive processes that occur in the mesocorticolimbic-striatal circuitry in response to repeated drug exposure. In previous studies, pharmacological inhibition of Cdk5 in the NAc enhanced the maximal activity level to repeated cocaine exposure (Bibb et al., 2001; Taylor et al., 2007). However, as mentioned above, these pharmacological manipulations cannot distinguish pre- versus postsynaptic effects of Cdk5 inhibition. Furthermore, the effect of pharmacological inhibitors is restricted to catalytic activity, whereas knock-out removes the protein with consequences for both activity-dependent and independent functions of Cdk5. In the current study, selective postsynaptic knock-out of Cdk5 in neurons of the NAc using infusions of rAAV lowered the threshold for cocaine-induced locomotor sensitization. The maximal activity level achieved after repeated cocaine exposure was, however, not affected. Based on the behavioral differences in these models, it may be speculated that Cdk5 activities in the pre- versus postsynaptic compartments of the mesocorticolimbic-striatal circuitry have complementary, yet possibly distinct actions. Although we are cautious in drawing conclusions from such different models, the present data derived from NAc-specific KO suggest that Cdk5 activity in NAc neurons may

regulate the threshold for the development of neuroadaptations in response to drugs of abuse.

Such drug-induced neuroadaptations also influence the formation of associations between the rewarding properties of the drug and environmental stimuli. We therefore tested Cdk5 NAc-KO in this form of reward-related learning using the conditioned place preference paradigm. Similar to the effects on locomotor sensitization, selective loss of Cdk5 in the NAc reduced the threshold dose required to induce a conditioned place preference for cocaine. Notably, consistent with the findings from the locomotor sensitization experiment, the maximal behavioral responses to a high dose of cocaine were not affected by Cdk5 NAc-KO. rAAV-mediated NAc-specific loss of Cdk5 allowed the role of this kinase to be assessed in a specific compartment of the mesocorticolimbic-striatal circuitry and alleviated the need for transgenic Cre mice. However, it should be noted that this viral approach for spatially-restricted transgene delivery is dictated by serotype, viral-receptor, and promoter considerations (Shevtsova et al., 2005). Nonetheless, these data suggest that Cdk5 in the NAc is critical for regulating the threshold or sensitivity of the effects of cocaine on neuroplasticity and reward-related learning.

Striatal medium spiny neurons are the primary output of the mesocorticolimbic-striatal circuitry that mediates behavioral responses to reward-related stimuli. At this critical point of convergence, the signal transduction

cascades activated by cocaine result in increased striatal excitability (Dong et al., 2006). Indeed, dopamine regulates striatal neuron firing through PKA-dependent signaling (Hernandez-Lopez et al., 1997) and chronic cocaine exposure has also been reported to decrease the excitability of rat striatal neurons (Zhang et al., 1998). Since the signaling mechanisms underlying decreases in striatal excitability in cocaine-exposed animals remain unknown, we performed an electrophysiological analysis of the properties of NAc neurons from Cdk5 cKO mice. This experiment revealed a dramatic increase in intrinsic excitability in NAc medium spiny neurons following a loss of Cdk5 suggesting that Cdk5 not only has inhibitory influences on dopamine neurotransmission, but also on the intrinsic firing properties of NAc neurons. Moreover, these findings implicate Cdk5 in the regulation of striatal neuron responsiveness to excitatory neurotransmission, such as that mediated via glutamatergic input from cortical afferents. The present studies illustrate the functional relevance of regulation of striatal excitability in the mesocorticolimbic-striatal circuit and suggest cocaine-regulated targets, such as Cdk5, may influence the electrophysiological properties of striatal output neurons. Since Cdk5 controls the efficacy of dopamine and PKA-dependent signaling via the phosphorylation of DARPP-32 at Thr75 in the striatum (Bibb et al., 1999; Benavides and Bibb, 2004), the current data support the hypothesis that Cdk5 may modulate striatal neuron excitability via regulation of PKA activity. Future studies will undoubtedly identify additional mechanisms

by which Cdk5 may regulate cocaine sensitivity and motivation. Here we demonstrate that elevation in striatal neuron intrinsic excitability in Cdk5 cKO mice is associated with parallel enhancements in behavioral responses to reinforcing stimuli, either drugs or food. These findings underscore the importance of understanding how Cdk5 alters the functional properties of ion channels that mediate striatal neuron firing, as these mechanisms may serve as novel targets for the treatment of addiction and disorders of motivation.

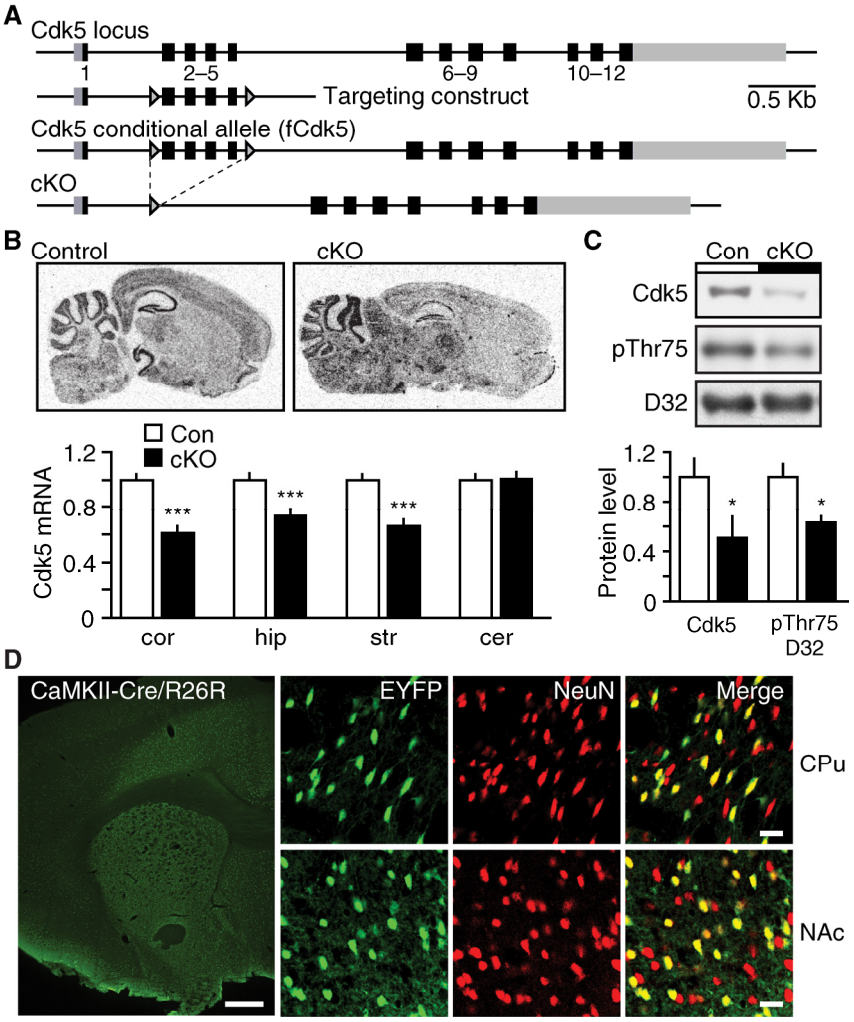

Figure 2.1. Generation of conditional Cdk5 knock-out mouse model. **A**, Diagram depicting targeting strategy for generation of conditional Cdk5 allele. The targeted fCdk5 allele contains *loxP* sites (arrowheads) flanking exons 2-5. **B**, Utilization of transgenic CaMKII-Cre to mediate excision of Cdk5 in adult brain. Representative *in situ* hybridization of sagittal brain sections from control and Cdk5 conditional knock-out (cKO) mice using Cdk5 riboprobe. Graph depicts normalized Cdk5 mRNA levels (± *SEM*) in cortex (cor), hippocampus (hip), striatum (str), and cerebellum (cer) in control mice (Con) and Cdk5 cKO mice (***$p < 0.001$ compared to control, Student's *t*-test, n = 5–7 per group). **C**, Quantitative immunoblots of Cdk5 and phospho-Thr75 DARPP-32 (pThr75 D32) in striatal homogenates from control and cKO mice. Representative immunoblots (top) and quantitation (bottom) are shown for each (*$p < 0.05$ compared to control, Student's *t*-test, n = 5–8 per group). **D**, Immunostaining for EYFP

(green) and the neuronal marker, NeuN (red), in CaMKII-Cre/R26R-EYFP reporter mice. Cre activity is shown in EYFP-positive cells (green) in the caudatoputamen (CPu), nucleus accumbens (NAc), and cortex at low magnification (left). EYFP/NeuN double-positive cells (yellow) are shown throughout the CPU and NAc at high resolution (right). Scale bars are 500 μm (left, low magnification) and 20 μm (right, high magnification).

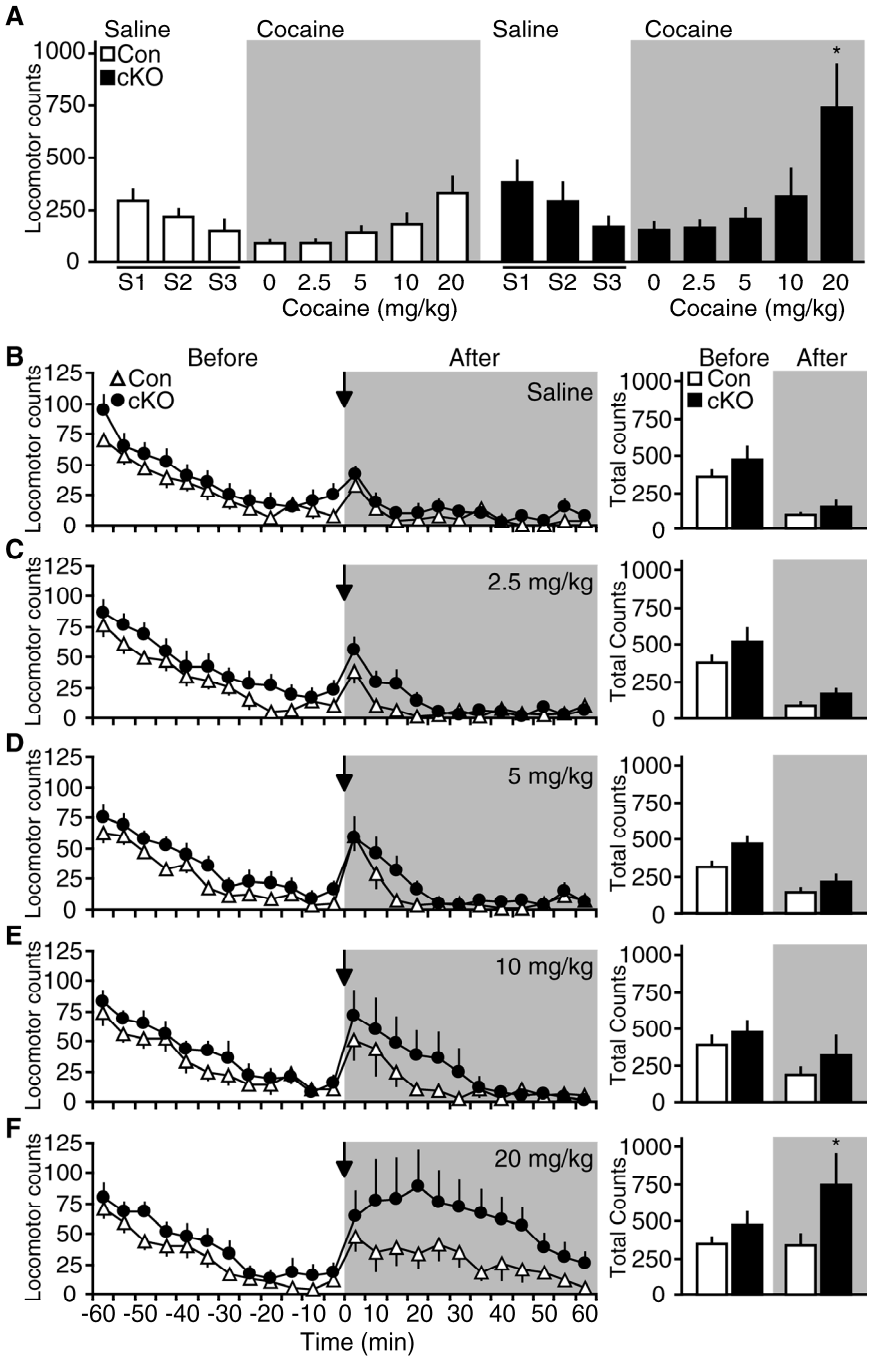
A
Saline
Cocaine
Saline
Cocaine
Con
cKO
Locomotor counts
1000
750
500
250
0
*
S1 S2 S3 0 2.5 5 10 20
Cocaine (mg/kg)
S1 S2 S3 0 2.5 5 10 20
Cocaine (mg/kg)
B
Before
After
Con
cKO
Saline
Locomotor counts
Total counts
C
2.5 mg/kg
D
5 mg/kg
E
10 mg/kg
F
20 mg/kg
-60 -50 -40 -30 -20 -10 0 10 20 30 40 50 60
Time (min)

Figure 2.2. Effect of transgenic Cdk5 cKO on cocaine-induced locomotor activity. **A**, Locomotor responses of control (Con) and CaMKII-Cre Cdk5 cKO (cKO) mice to saline and cocaine injections in Latin-square dose response experiment. Mice were habituated to saline injections for 3 consecutive days (S1–3), followed by cocaine injections in the Latin-square dose-response (grey background). Graph depicts mean locomotor counts (± *SEM*) for 60 min after injection with saline or the drug dose indicated (*$p < 0.05$ compared to control, post hoc Bonferroni, n = 10 per group). **B**, Time course of locomotor activity in response to administration of saline. Graph on left depicts mean locomotor counts (± *SEM*) over 60 min before (white background) and after (grey background) injection of control or cKO groups. Arrow denotes time of injection in each graph. Cumulative locomotor counts (± *SEM*) over 60 min are displayed in histograms at right (*$p < 0.05$, Student's *t*-test, n = 10 per group). **C**, Locomotor activity response to injection of 2.5 mg/kg cocaine over the same time course as summarized as in **B.** **D**, Response to injection of 5 mg/kg cocaine over the same time course as **B** with data summarized in histograms (right). **E**, Response to injection of 10 mg/kg cocaine over the same time course and summarized as in **B.** **F**, Locomotor activity response to injection of 20 mg/kg cocaine over the same time course as **B** with data summarized in histograms (right).

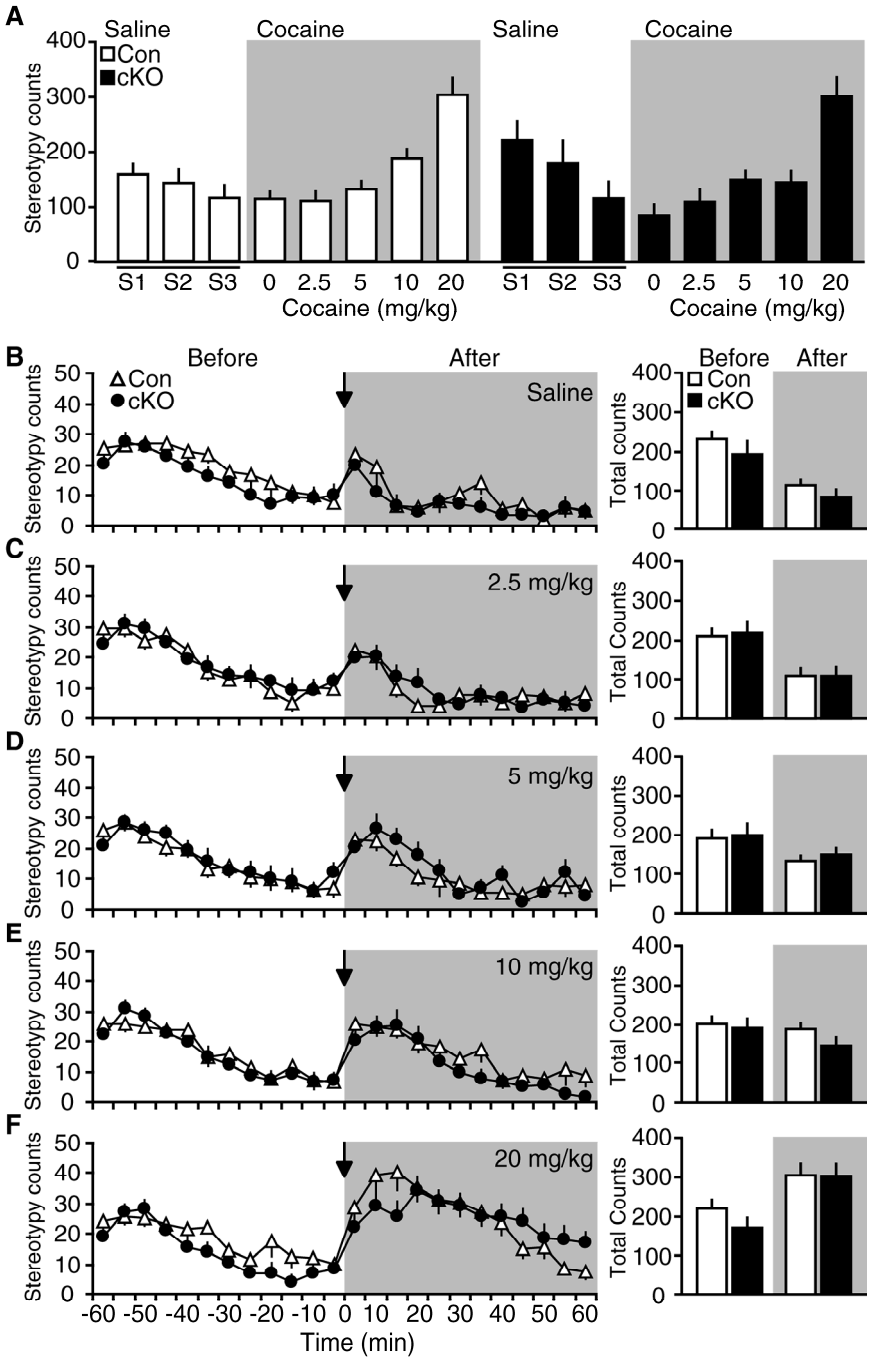
A
Saline
Cocaine
Saline
Cocaine
Con
cKO
Stereotypy counts
S1 S2 S3 0 2.5 5 10 20
Cocaine (mg/kg)
B
Before
After
Saline
Total counts
C
2.5 mg/kg
Total Counts
D
5 mg/kg
E
10 mg/kg
F
20 mg/kg
-60 -50 -40 -30 -20 -10 0 10 20 30 40 50 60
Time (min)

Figure 2.3. Effect of transgenic Cdk5 cKO on stereotypic responses to cocaine exposure. **A**, Stereotypy counts of control (Con) and CaMKII-Cre Cdk5 cKO (cKO) mice to saline and cocaine injections in Latin-square dose response experiment. Mice were habituated to saline injections for 3 consecutive days (S1–3), followed by cocaine injections in the Latin-square dose-response (grey background). Graph depicts mean stereotypy counts (± *SEM*) for 60 min after injection with saline or the drug dose indicated (n = 10 per group). **B**, Time course of stereotypic activity in response to administration of 20 mg/kg cocaine. Graph on left depicts mean stereotypy counts (± *SEM*) over 60 min before (white background) and after (grey background) injection of control or cKO groups. Arrow denotes time of injection in each graph. Cumulative stereotypy counts (± *SEM*) over 60 min are displayed in histograms at right (n = 10 per group). **C**, Stereotypy counts in response to injection of 2.5 mg/kg cocaine over the same time course as summarized as in **B.** **D**, Response to injection of 5 mg/kg cocaine over the same time course as **B** with data summarized in histograms (right). **E**, Response to injection of 10 mg/kg cocaine over the same time course and summarized as in **B.** **F**, Stereotypy response to injection of 20 mg/kg cocaine over the same time course as **B** with data summarized in histograms (right).

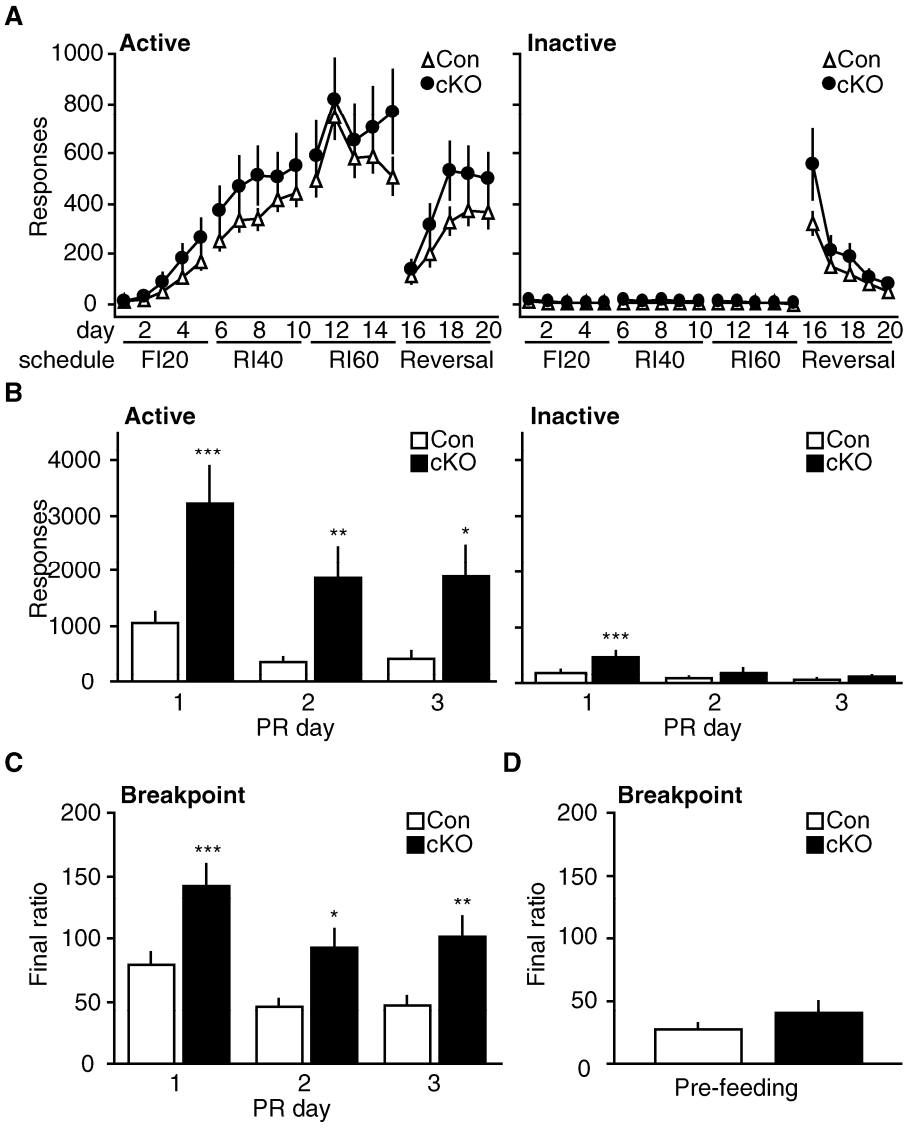

Figure 2.4. Effect of Cdk5 cKO on acquisition and performance of instrumental responding for reward. **A**, Performance for control (Con) vs. cKO mice in active (left) and inactive (right) nosepoke responses during training for instrumental responding. Day and training schedule (as described in the behavioral procedures) is denoted along the x-axis. **B**, Performance for control (Con) vs. cKO mice for food reinforcement under a progressive ratio (PR) schedule. Graphs depict active (left) and inactive (right) nosepoke responses (± *SEM*) for three consecutive days of PR testing (*p < 0.05, ** p < 0.01, *** p < 0.005 compared to control, post hoc Tukey, n = 16–20 per group). **C**, Breakpoints achieved for control vs. cKO mice during 3 days of PR responding.

Graphs show mean final ratios achieved ± *SEM* (*p < 0.05, **p < 0.01, ***p < 0.001 compared to control, post hoc Tukey, n = 16–20 per group). **D**, Performance in progressive ratio instrumental responding following pre-feeding.

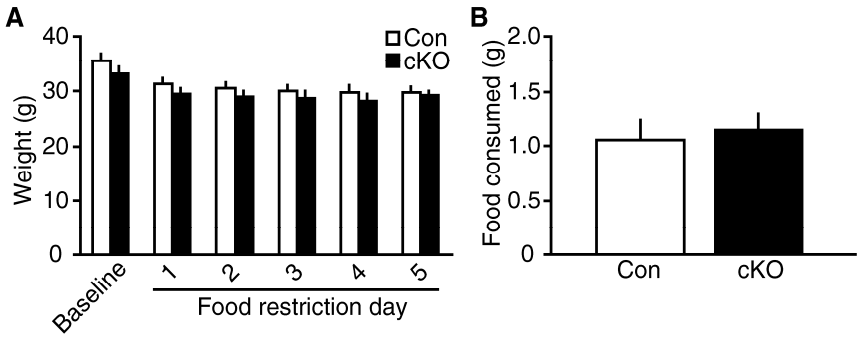

Figure 2.5. Effect of Cdk5 cKO on weight change, hunger, or appetite in progressive ratio experiments. **A**, Baseline and weight change in Cdk5 cKO mice over the first 5 days of food restriction prior to instrumental performance evaluation. **B**, Amount of food pellets consumed during 1 hr pre-feeding session prior to reinforcer-devaluation PR responding in control vs. cKO mice. Graphs depict mean ± *SEM* for each measure (n = 16–20 per group).

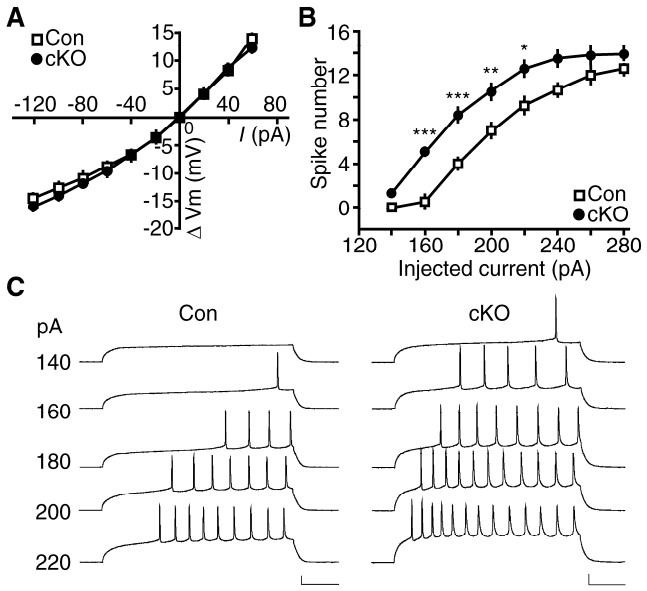

Figure 2.6. Effect of Cdk5 cKO on intrinsic membrane excitability of NAc neurons. **A**, Current-voltage graphs in NAc neurons from control (Con) and cKO mice showing no effect on passive membrane properties. **B**, Analysis of intrinsic excitability of NAc neurons from control vs. cKO mice. Graph shows mean spike number ± *SEM* in response to different current injections (*$p < 0.05$, **$p < 0.01$, ***$p < 0.001$ compared to control, post hoc Bonferroni, n = 7–8 per group). **C**, Representative traces of action potential firing evoked by depolarizing current pulses (140–280 pA; 500 ms) in NAc neurons from control and cKO mice. Scale bars: 20 mV, 100 ms.

Table 1. Membrane properties of NAc medium spiny neurons from Control and Cdk5 cKO mice.

	Control	Cdk5 cKO
Resting membrane potential (mV)	–81.8 ± 2.2	–78.7 ± 1.0
Rheobase (pA)	158.3 ± 4.2	137.6 ± 5.3*
Latency to first spike (ms)	312.8 ± 45.3	155.0 ± 20.5*
Spike threshold (mV)	–42.8 ± 0.7	–41.2 ± 1.2
Spike amplitude (mV)	72.4 ± 3.4	70.3 ± 2.5
Spike halfwidth (ms)	1.4 ± 0.2	1.5 ± 0.3

Rheobase value was determined as the smallest current injection that elicited a single spike. Latency to first spike was measured from 180 pA current injection. Values are expressed as mean ± *SEM*. *$p < 0.05$, Student's *t*-test, n = 7–8 per group.

Table 2.1. Membrane properties of NAc medium spiny neurons from control and Cdk5 conditional knock-out mice. Rheobase value was determined as the smallest current injection that elicited a single spike. Latency to first spike was measured from 180 pA current injection. Values are expressed as mean ± *SEM*. *$p < 0.05$, Student's *t*-test, n = 7–8 per group.

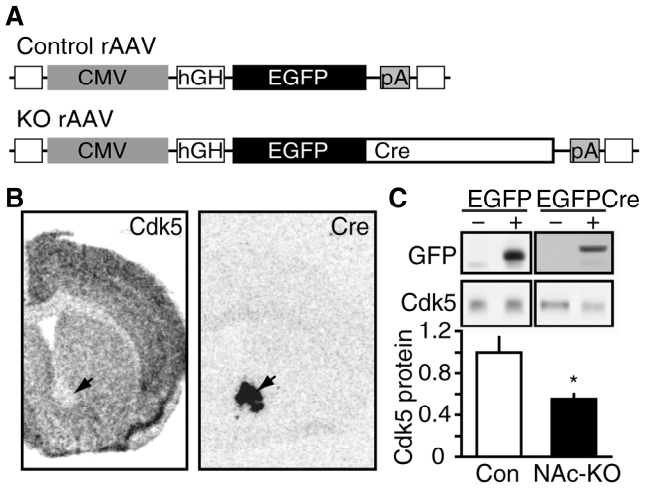

Figure 2.7. Generation of NAc-specific Cdk5 knock-out mouse model. **A**, Diagram depicting recombinant viral vectors to mediate excision of Cdk5 in NAc. Viral constructs contain CMV promoter (CMV), human growth hormone intron (hGH), SV40 polyadenylation sequence (pA), and inverted terminal repeats (open squares). The control vector contains an enhanced green fluorescent protein (EGFP) cassette, while the knock-out (KO) vector expresses a chimeric EGFPCre protein. **B**, Representative *in situ* hybridization analysis of rAAV mediated NAc-specific knock-out of Cdk5. Arrows indicate corresponding NAc regions of rAAV transduction in adjacent sections hybridized with Cdk5 (left) and Cre (right) riboprobes after rAAV-EGFPCre delivery. **C**, Quantitative immunoblotting of rAAV-mediated NAc-KO. Representative immunoblots of GFP and Cdk5 in homogenates from mice transduced with rAAV expressing EGFP (left) or EGFPCre (right) are shown in the top panels. GFP immunoblots show detection of EGFP (~28 kDa) in control samples and EGFPCre (~70 kDa) in NAc-KO samples. Quantitation of Cdk5 levels in NAc lysates transduced with EGFP (Con) vs. EGFPCre (NAc-KO) is shown at bottom (*$p < 0.05$, Student's *t*-test, n = 4 per group).

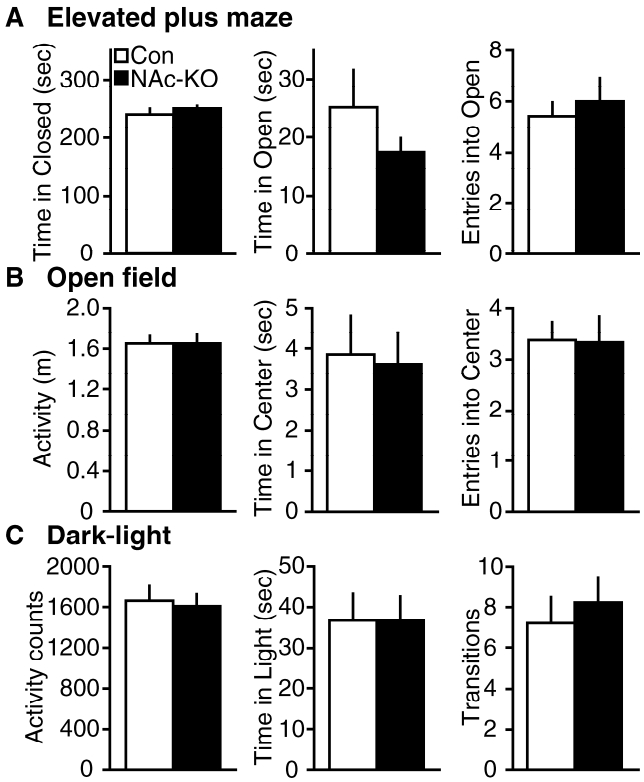

Figure 2.8. Effect of Cdk5 NAc-KO on anxiety-related behavior. Comparison of control (Con) and NAc-KO mice for performance in the **A**, Elevated plus maze; **B,** Open field; and **C**, Dark-light box. Graphs represent mean ± *SEM* for each measure ($p > 0.05$ compared to control, Student's *t*-test, n = 28–48 per group).

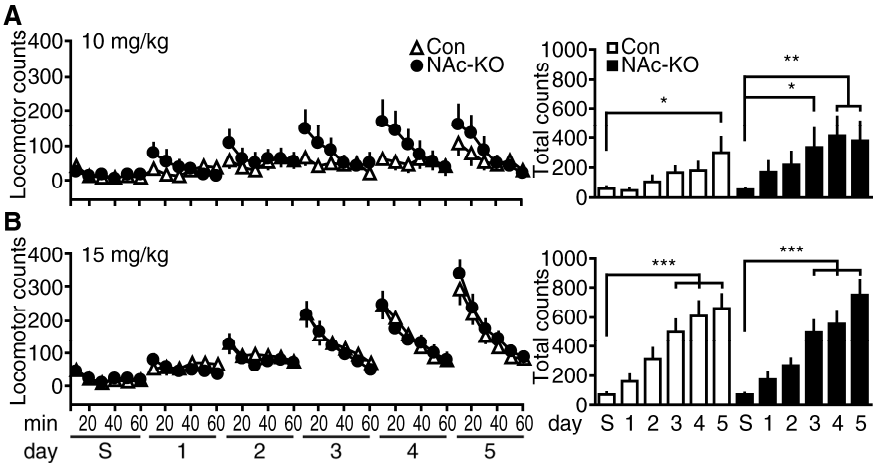

Figure 2.9. Effect of NAc-specific Cdk5 KO on locomotor sensitization to repeated cocaine exposure. **A**, Locomotor activity in response to saline injection (S), followed by repeated 10 mg/kg cocaine injection over 5 consecutive days (1–5). Mean locomotor counts (± *SEM*) in 10 min bins for 60 min immediately following injection for each day are shown for control (Con) vs. NAc-KO groups (left). Data for the first 30 min following injection are summarized in histograms (right, *$p < 0.05$, **$p < 0.01$ compared to saline, post hoc Tukey, n = 17 per group). **B**, Locomotor sensitization to 15 mg/kg cocaine in control (Con) and NAc-KO mice. Time course locomotor activity and data summaries are shown as in **A** (***$p < 0.001$ compared to saline, post hoc Tukey, n = 16–19 per group).

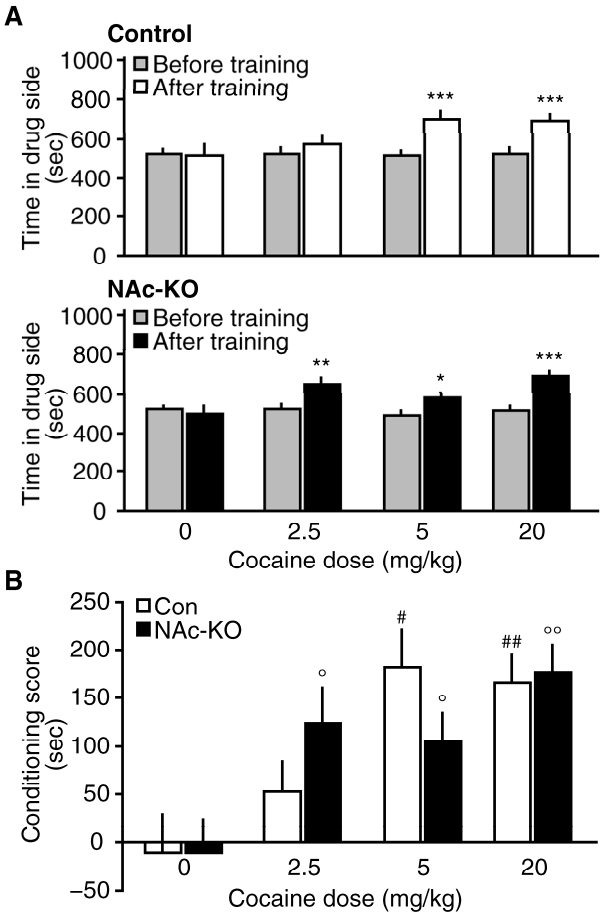

Figure 2.10. Effect of NAc-specific Cdk5 KO on cocaine conditioned place preference. A, Time spent in drug-paired compartment for control and NAc-KO mice. Top graph depicts performance of control mice before (grey) and after (white) cocaine training at the indicated cocaine doses. Bottom graph depicts Cdk5 NAc-KO mice performance before (grey) and after (black) cocaine training. Mean time spent in drug compartment is indicated (± *SEM*) for each group at each training dose of cocaine (*$p < 0.05$, **$p < 0.01$, ***$p < 0.001$, paired *t*-test, n = 9–19 per group). **B**, Analysis of conditioning scores calculated from performance before and after training for each dose indicated. Graph depicts mean conditioning score (± *SEM*) in control (Con, $^{\#}p < 0.05$, $^{\#\#}p < 0.01$ compared to saline, post hoc Neuman-Keuls, n = 9–19 per group) vs. Cdk5 NAc-KO ($^{\circ}p < 0.05$, $^{\circ\circ}p < 0.01$ compared to saline, post hoc Neuman-Keuls, n = 12–18 per group) mice for the cocaine dose indicated.

CHAPTER THREE

REGULATION OF MOTIVATION, MOTOR LEARNING, AND ANTIDEPRESSANT-LIKE BEHAVIOR IN TAMOXIFEN-INDUCIBLE CDK5 CONDITIONAL KNOCK-OUT MICE

Summary

Cdk5 has been implicated in many aspects of neuronal function. Since Cdk5 is expressed ubiquitously throughout the brain, Cdk5 may be involved in numerous networks and pathways that regulate various aspects of behavior. Investigation into the role of Cdk5 in the expression of certain behaviors has been hampered by the perinatal lethality of constitutive Cdk5 knock-out mice. We utilized novel tamoxifen-inducible conditional knock-out (CKO) model systems to investigate the effect of loss of Cdk5 in the adult brain on a battery of behavioral paradigms to assess sensory function, motivation, motor function and motor learning, emotional state and response to the psychostimulant cocaine. We show that tamoxifen-inducible Cdk5 CKO, achieved by the use of the Prp-CreER^{T} transgenic, produces increased motivation, locomotor activity and improvement in the motor learning. Furthermore, Cdk5 CKO mice have increased responses to the psychoactive properties of cocaine. Interestingly, Cdk5 CKO mice also display an antidepressant-like behavioral phenotype in forced swim and tail suspension tests. These findings are accompanied by alteration in

the state of PKA signaling in the striatum as well as altered dopaminergic responsiveness. These results suggest that Cdk5 may act as a regulator of neuronal circuitry of brain regions that govern various types of behavior related to motor control and emotional state. These findings form the foundation for future investigation into the specific role Cdk5 plays in the neural circuits and mechanisms that control these behaviors, and underscore the promise of Cdk5 as a pharmacotherapeutic target for neuropsychiatric disorders involving altered motor and emotional states.

Introduction

Plasticity in the neural circuitry of the brain contributes to the execution of various behaviors. It is therefore likely that the regulatory mechanisms controlling neuronal plasticity and synaptic function, underlie alterations in behavioral profiles. Cdk5 has been implicated as a molecular target of drug-induced plasticity that may affect behavioral responses to drugs (Bibb et al., 2001). Cdk5 is a proline-directed serine/threonine kinase that has also been called neuronal cyclin-dependent-like protein kinase (Nclk) and tau protein kinase II (TPKII). Cdk5 is expressed predominantly in the CNS and is enriched in both the pre- and post-synaptic compartments (Tomizawa et al., 2002; Norrholm et al., 2003) and is believed to be involved in mediating neuronal plasticity (Dhavan and

Tsai, 2001; Bibb, 2003). Cdk5 has been implicated in CNS development (Nikolic et al., 1996; Ohshima et al., 1996) as genetic ablation of the *cdk5* gene results in abnormal corticogenesis and perinatal lethality in mice (Ohshima et al., 1996). Furthermore, combined knock-out of the *p35* and *p39* genes results in a phenotype indistinguishable from that of the *cdk5* knock-out (Ko et al., 2001). Previous studies have implicated Cdk5 activity as an important regulatory of learning and memory. However, most of these studies have employed constitutive knock-out mice that have robust congenital cellular and cytoarchitecture defects (Ohshima et al., 2005). The perinatal lethality and congenital defects associated with constitutive knock-out mice (Nikolic et al., 1996; Ohshima et al., 1996; Kwon and Tsai, 1998; Ko et al., 2001) have hampered the use of behavioral paradigms to study Cdk5 function. Thus, an approach that allows for temporal and spatial control of Cdk5 activity in the brain could clarify the role of this kinase in various behaviors. More recent studies have employed conditional knock-out technology to implicate loss of Cdk5 in the regulation of NMDAR function and hippocampal-dependent learning and memory (Hawasli et al., 2007). This approach has uncovered novel insight into the regulation of behaviors by Cdk5 and is far superior to previous approaches.

Experimental procedures

Animals and animal care.

The conditional Cdk5 allele was generated using a Cre/*lox*P gene targeting strategy and genotyped as described in Chapter Two. The fCdk5 mice were maintained on a mixed 129/SVxC57BL/6 background and were group-housed on a 12 hr light/dark cycle with access to food and water *ad libitum*. In one experiment, we utilized male, 6-month old C3H/HeJ mice (Jackson Laboratory). Behavioral manipulations were approved by UT Southwestern Medical Center Institutional Animal Care and Use Committee and conducted in accordance with the applicable portions of the National Institutes of Health *Guide for the Care and Use of Laboratory Animals*. All drugs and chemicals were obtained from Sigma-Aldrich (St. Louis, MO) unless otherwise noted.

Generation of tamoxifen-inducible conditional Cdk5 knock-out mice.

Homozygous fCdk5 mice were bred with mice expressing a chimeric Cre recombinase–modified estrogen receptor (ER) under the control of the neuronal prion protein promoter to generate Cdk5 conditional knock-out (CKO) mice. The *PrP*-Cre-ER^{T} transgenic line (provided by P. Chambon, Institut de Génétique et de Biologie, Moléculaire et Cellulaire, Strasbourg, France) was selected in order to mediate inducible recombination in the adult brain as previously reported for this transgenic line (Weber et al., 2001). Adult (6-12 week old), male mice were

utilized for all experiments. The offspring of all crosses were genotyped for the *PrP*-Cre-ER^{T} transgene, as well as the fCdk5 allele. Homozygous, fCdk5 animals that were positive for the *PrP*-Cre-ER^{T} transgene were dubbed "Cdk5 conditional knock-outs" (Cdk5 CKO). For induction of recombination in these mice, the administration of intraperitoneal (i.p.) injections of tamoxifen (1.0–3.0 mg; T), or 4-hydroxytamoxifen (0.1–1.0 mg; HT) was conducted for 1-15 days. Sunflower oil vehicle (V) was administered as a control in some experiments. Littermate, homozygous fCdk5 mice that were negative for the *PrP*-Cre-ER^{T} transgene served as control subjects (Con). The notation for drug exposure is as follows: Cdk5 CKO administered tamoxifen = CKO^{T}; control mouse administered 4-hydroxytamoxifen = Con^{HT}; CKO administered vehicle = CKO^{V}, etc. At varying time points following the final injection, animals were either sacrificed for tissue collection or slices were prepared as described under the "*Preparation of acute striatal slices and slice pharmacology*" section. The optimal tamoxifen or 4-hydroxytamoxifen treatment regime was determined through the use of mRNA *in situ* hybridization analysis of Cre-mediated *cdk5* gene ablation, as previously described (Hawasli et al., 2007). We empirically determined 10 consecutive day of Tam (100 mg/kg) or 15 d of 4-OH-Tam (66 mg/kg) to yield reliable and robust decrease in Cdk5 mRNA throughout the brain.

PCR-based genotyping

Floxed and transgenic alleles were identified by PCR-based genotyping. The Cdk5 allele was detected using the strategy described in Chapter Two. The transgenic Prp-CreER^T genotyping was conducted as described (Hawasli et al., 2007) using the following oligonucleotides: 5'-CAACCGAGCTGAAGCATTCTGCC-3' and 5'-CATCAACGTTTTCTTTTCGGATC-3'. These oligos amplified a 420 bp CreER^T transgene product. PCR reactions also included control oligos for growth differentiation factor 5 (GDF5): 5'-GGAGCACTTCCACTATGGGAC-3' and 5'-AAAGAGTGAGGAGTTTGGGGAG-3' which amplified a 243 bp GDF5 product.

Histological procedures and immunoblotting.

In situ hybridizations for Cdk5 and Cre were conduced as described in Chapter Two. Quantitative immunoblots were performed using the methods and reagents described in Chapter Two. In addition, membranes were probed with antibodies to phospho-Thr34 DARPP-32 (1:5,000, provided by P. Greengard, Rockefeller University), p35 (1:1000, Santa Cruz, C-19), phospho-Ser845 (1:500, PhosphoSolutions) and total GluR1 (1:1,000 Calbiochem). The polyclonal antibody to ΔFosB (1:600, PGU-NFB01-06) was provided P. Ulery and E. Nestler

(UT Southwestern Medical Center). Some primary antibodies required incubation overnight at 4°C. Quantitation was conducted as described in Chapter Two.

Immunoprecipitation (IP)–kinase assays were conducted as previously reported (Bibb et al., 1999; Hawasli et al., 2007). Briefly, striatal lysates from adult tamoxifen-inducible Cdk5 CKO mice and littermate controls were prepared in RIPA buffer containing (in mM): 65.2 Tris base, pH 7.4, 150 NaCl, 2 EDTA, 50 NaH_2PO_4, 50 NaF, and 0.1% TritonX-100, 0.1% SDS, and 0.5% Deoxycholate, and protease inhibitor cocktail (Sigma P8340). Cdk5 was and immunoprecipitated with Cdk5-agarose (C-8, Santa Cruz) and the product was then tested for activity *in vitro* for incorporation of [γ-^{32}P]-ATP into Histone H1. Samples were resolved by SDS-PAGE and imaged and analyzed using Storm PhosphoImager (Amersham).

Behavioral procedures.

SHIRPA protocol: The SHIRPA primary behavioral screen was conducted with littermate control and Cdk5 CKO^{HT} mice as previously described (Rogers et al., 1997). This protocol consists of 40 measures of basic neurological function conducting in three paradigms. First, animals were placed in an inverted beaker for observation for 5 min. During this time, animals were scored for body position (flat, on side, prone, sitting or standing, rearing, repeated jumping), movement (absent, slow, moderate, vigorous, extreme), respiration rate (irregular,

shallow, normal), and body tremor (absent, mild, marked). Mice were then transferred to a polypropylene rat cage (25x 45x20 cm) for measures of transfer arousal (comatose, prolonged freezing, extended freezing, brief freezing, momentary freeing, no freezing, "manic" movement), locomotor activity (number of 8 cm segments traversed in 30 sec), palpebral closure (wide-open, semi, closed), piloerection (none, present), gait (normal, abnormal, limited, no movement), pelvic elevation (flat, touching, normal, elevated), tail elevation (dragging, horizontal, elevated), touch escape (none, mild, moderate, vigorous), and positional passivity (tail, neck, supine, hind legs, none). Finally, the mice were removed from the arena and observed for trunk curl or limb grasping, with visual placing (none, nose, whisker, before whisker, early), grip strength (none, slight, moderate, active, strong), and wire maneuver hindleg activity (active, difficult, none and fall within sec, falls immediately) determined using a metal rod. Body tone (flaccid, slight, extreme resistance), pinna reflex (none, active, hyperactive), corneal reflex (none, single, multiple eyeblink), toe pinch (none, slight, moderate, brisk, very brisk withdrawal), skin color (blanched, pink, red), heart rate (slow, normal, fast), limb tone (none, slight, moderate, marked, extreme), abdominal tone (flaccid, slight, extreme), lacrimation (absent, present), salivation (absent, present) and provoked biting (absent, present) were assessed with the animal scruffed and restrained. Data are represented as percent of subjects achieving score.

Visual platform test: The visual platform test was performed in a water maze with the help of C.M. Powell (UT Southwestern Medical Center) according to published protocol (Hawasli et al., 2007) with slight modification. Briefly, animals were placed in a pool of opaque water with a submerged platform marked by a visual target. The test consisted of 4 trials conducted in a single day, separated by 25 min between trials. Latency to reach the visual platform was measured for each trial. Each trial was concluded when the animal reached the target or at the end of 60 sec. If the animal failed to reach the platform, it was manually placed on the submerged platform and allowed to remain there for an additional 60 sec. Data are represented as mean latency to find platform (± *SEM*) for each of the four trials.

Locomotor activity: Horizontal motor activity was monitored according to the methods described in Chapter Two. Locomotor activity (sequential adjacent beambreaks), stereotypy (repetitive single beambreaks), and total activity (sum of locomotion and fine movement) were recorded using a computer (Photobeam Analysis Software, San Diego Instruments). Animals were placed into apparatus for 60 or 90 min for analysis of spontaneous locomotor activity. For cocaine-induced locomotor activity test, animals were placed in the cage and motor activity recorded for 2 h, at which point a single i.p. injection was delivered and the animal replaced in the chamber for an additional 2 h. Data are represented as average activity in 5 or 10 min bins ± *SEM*.

Rotarod motor learning: The rotarod task was utilized to assess motor coordination and motor learning. The apparatus consists of a rotating rod that accelerates linearly from 0 to 45 rpm in 60sec. The time spent on the rod was monitored by a device triggered when the animal fell of the rod (IITC Life Science, Woodland Hills, CA). Five trials were performed separated by at least 25 min in one day, for 4 consecutive days. The mean latency to fall from the rod was reported ± *SEM* for each trial.

Cocaine-conditioned place preference: The place preference assay was conducted as described in Chapter Two. Data are represented as average time spent in the drug paired context before and after drug conditioning ± *SEM* for each group and drug dose.

Anxiety-related tests: The elevated plus maze (EPM), open field (OF), and dark light habituation (D-L) tests were conducted as described in Chapter Two.

Depression-related tests: The forced swim test (FST) and tail suspension test (TST) were used to assess the depressive phenotype of the animals. The FST was conducted with the help of A. Graham (UT Southwestern Medical Center) according to previously reported methods (Porsolt et al., 1977). In brief, the FST was conducted in a single session by placing mice in glass beakers containing 25 °C water for 10 min. Activity was videotaped and scored manually by an experimenter blind to genotype. Only the last 4 min of the response was scored for quantification of latency to immobility and total immobility time. In the TST,

mice were suspended from the tail to a strain-gauge. The TST test was conducted with the help of R. Reister and H.K. Gershenfeld (UT Southwestern Medical Center) as described (Liu and Gershenfeld, 2001). Each animal was tested in a single session and the time of immobility during the 6 min trial was recorded. The computer also monitored the force of movements during the trial, and reported the values in arbitrary units. Data are presented as mean ±*SEM* for each measure.

Contextual fear conditioning: Mice were placed in a plexiglass shock box with clear front and rear walls (MedAssociates) for 5 min. This experiment was conducted by C.M. Powell (UT Southwestern Medical Center). Briefly, two-second, 0.5 mA foot shocks were delivered at 2 min intervals for training trial. Freezing behavior, defined as a lack of motion except for respiration, was monitored at 5-sec intervals by an observer blind to the genotype. Baseline freezing was reported as the freezing during the first two minutes of the training session before the delivery of any foot shock. Twenty-four h after training, contextual and cue learning were assessed by monitoring freezing behavior upon re-exposure to training apparatus (context) or the training sound (cue) for 5 min. Data are presented as freezing time (% total) ± *SEM* during each phase of the experiment.

Voluntary wheel running: Mice were housed individually in cages equipped with a freely-moving wheel connected to an electronic counter. Activity

was monitored daily for 21 consecutive days. Mice learned to run in the wheels over the first 3–7 days. The data represent the mean activity over a 10 day period after the acquisition of stable running behavior. Computer-generated white noise was used to drown out ambient noise over the course of the experiment. Data are reported as mean wheel revolutions ±*SEM* in 6 min interval.

Preparation of acute striatal slices and slice pharmacology.

Acute striatal slices and pharmacology experiments were performed as described (Sahin et al., 2006) with slight modification. Adult tamoxifen-inducible Cdk5 mice and littermate controls were utilized for slice preparation after at least two-week washout from the last day of 4-OH-Tam delivery. Briefly, animals were decapitated and the brains transferred to cold aCSF containing (in mM): 124 NaCl, 4.5 KCl, 2 $CaCl_2$, 1 $MgCl_2$, 26 $NaHCO_3$, 1.2 NaH_2PO_4, and 10 D-glucose, brought to pH 7.4 by aeration with 95% O_2/5% CO_2. Coronal sections (300–350 μm thick) were prepared in ice-cold modified aCSF using a manual vibratome and striatum microdissected under constant oxygenation in ice-cold aCSF. Striatal slices were transferred immediately to a netwell submerged in aCSF at 30^{o}C bubbled with 95% O_2/5% CO_2. After two, 30 min recovery incubations, pharmacological agents were applied with a change of buffer. In dopamine signaling experiments, slices were incubated in the presence of adenosine deaminase (5 μg/ml, Roche) during recovery and dopamine pharmacology. At

the conclusion of the treatment, slices were transferred to screw-cap centrifuge tubes and frozen in dry ice and stored at −80 °C until analysis. Treatments were conducted in tandem, with vehicle-equivalent, drug-free controls for each treatment. Data are represented as normalized phospho-target/total protein level relative to drug-free control.

Monoamine quantitation in striatal samples.

Striatal tissue samples were collected from control and Cdk5 CKO^{HT} mice, two weeks after the last injection of drug. Tissue samples were microdissected, washed in cold PBS, transferred to screwcap microcentrifuge tubes, and weighed before storage at −80 °C. Monoamine quantitation was performed by ESA Laboratories (Chelmsford, MA). Frozen samples were lysed in 0.2 M PCA, sonicated and centrifuged prior to loading into refrigerated auto-sampler. The instrument consisted of a fully automated isocratic HPLC-coulometric electrochemical detection system with a pump, autosampler, column oven, and Coulochem III Model 5300 detector (ESA Biosciences, Chelmsford, MA), equipped with MD-150 (3 x 150 mm; 3 μl) column and Model 5020 guard cell and Model 5014B analytical cell. The mobile phase (MDMT-2) contained (in mM): 90 NaH_2PO_4, 50 citric acid, 1.7 l-octane sulfonic acid, 0.05 EDTA, and 10% acetonitrile, pH ~3.0. This mobile phase was designed to allow analysis of low levels of monoamines and metabolites by HPLC-ECD. The flow rate was 0.6

ml/min, run at room temperature. The potentials were as follows (in mV): E_1 -150, E_2 +200, and E_3 +350. The calibration curve consisted of 6 standards (1, 5, 10, 50, 100, 500, 1000 ng/ml). The concentration was calculated from the standard curve generated by the instrument.

Statistical analysis.

Experimental data were analyzed using the approaches described in Chapter Two. In some instances, the Wilcoxon Mann-Whitney *t*-test for nonparametric values was utilized. Data are reported as mean ± *SEM* for each measure. Each sample size is indicated. A value of $p \leq 0.05$ was considered statistically significant.

Results

Generation of a tamoxifen-inducible conditional Cdk5 knock-out mouse model

To achieve Cdk5 CKO, the endogenous gene encoding the protein kinase was first replaced with a targeted allele in which *LoxP* sites flank exons 2-5 (see **Figure 2.1*A***). In order to mediate excision of Cdk5 throughout the adult brain, we employed an inducible Cre recombinase transgenic animal (*PrP*-Cre-ER^T). This inducible Cre construct utilizes a chimeric fusion protein, composed of Cre recombinase and a mutated estrogen receptor (ER^T). The activity of this ligand-

dependent chimeric recombinase is induced by the synthetic ER antagonist, tamoxifen (Tam) or 4-hydroxytamoxifen (4-OH-Tam), yet remains insensitive to endogenous 17β-estradiol (E2) (Feil et al., 1997). As a result, Cre activity is only induced in response to intraperitoneal administration of Tam or 4-OH-Tam. The expression of this Tam-inducible form of Cre is under the control of the neuron-specific prion promoter (*PrP*) (Weber et al., 2001). In the *PrP*-Cre-ER^T line, Cre activity was robust in the hippocampal formation, cortex, striatum and cerebellum, as we have previously reported (Hawasli et al., 2007). Experiments were conducted to empirically determine the optimal Tam dosing paradigm for Cdk5 knock-out (**Figure 3.1*A***). We found that Tam caused a dose-dependent decrease in Cdk5 mRNA throughout the brain when administered i.p. for 10 consecutive days (**Figure 3.1*A***). The effect was most dramatic after a course of 100 mg/kg (~3 mg Tam/mouse/day) in adult male Cdk5 CKO mice, resulting in robust decrease in Cdk5 mRNA mice throughout the brain (**Figure 3.1*A***). These results were consistent with our previous report of Cdk5 loss induction by a 15-day course with 66.0 mg/kg 4-OH-Tam (~1 mg 4-OH-Tam/mouse/day) (Hawasli et al., 2007). FISH analysis of Con^T and CKO^T striatal slices shows clear expression of Cre and reduction in Cdk5 mRNA in striatal neurons of Cdk5 CKO mice (**Figure 3.1*B***). Furthermore, Cdk5 CKO mice administered Tam (CKO^T) show a show a decrease in protein levels in the striatal lysates (**Figure 3.1*C***). Notably, there is a more robust and reproducible decrease in striatal Cdk5 protein

level in Cdk5 CKO mice administered 4-OH-Tam (66.5 ± 3.0% reduction compared to controls, **Figure 3.1*D***). Furthermore, decreases in Cdk5 protein also correlated well with reduced Cdk5 activity in tissue homogenates (61.1 ± 10.6% compared to controls, **Figure 3.1*E***), as previously reported (Hawasli et al., 2007). Consequently, tamoxifen-inducible Cdk5 CKO produced a dramatic reduction in Cdk5 mRNA, protein, and kinase activity throughout regions of the adult brain. Thus, we have generated a model system in which Cdk5 is specifically recombined in the adult brain, allowing for the investigation of the requirement for Cdk5 in various aspects of behavior.

Effect of tamoxifen-inducible conditional Cdk5 knock-out on general behavior battery

The most commonly utilized measure of motor function is spontaneous locomotor activity in the open-field (Holland and Weldon, 1968). The use of a standardized behavioral battery is of great utility in the characterization of transgenic mouse models. The well-described SHIRPA protocol (Rogers et al., 1997) encompasses two stages for detailed phenotype assessment, with a third stage allocated for specialized phenotype screening for specific neurological deficits. The primary observational screen provides measures of sensory and autonomic function, muscle and motor neuron function, as well as spinocerebellar and neuropsychiatric function. To assess the effect of loss of Cdk5 on the this

behavioral batter, 4-hydroxytamoxifen dosed Cdk5 conditional knock-out mice and littermate controls were subjected to the SHIRPA protocol observational battery (**Figure 3.**). When compared to control mice, Cdk5 CKO mice struggled much more violently when held by the tail. Once placed in the viewing-jar, Cdk5 CKO mice were more likely to sit compared to control mice (**Figure 3.*A***). However, no differences were observed between control and Cdk5 CKO in movement (moderate), respiration rate (normal), or body tremor (mild).

When transferred to the arena in the SHIRPA protocol, Cdk5 CKO mice did not differ from controls in transfer arousal (mild), locomotor activity, gait (normal), pelvic elevation (normal), or tail elevation (normal). Furthermore, both genotypes had eyes wide open with no piloerection. No differences were detected between genotypes in trunk curl (absent), limb grasping, visual placing, grip strength, (moderate), body tone, pinna reflex, corneal reflex, or toe pinch. In the wire manouever, Cdk5 CKO mice were more likely to achieve an active hindleg grip than control mice (**Figure 3.*B***). In supine restraint, no differences were observed in skin color (pink), heart rate (normal), limb tone (moderate), abdominal tone (slight resistance), lacrimation (none), or salivation (slight) between control and Cdk5 CKO mice. Neither genotype showed impairment in the righting reflex or contact righting reflex. However, Cdk5 CKO mice were less likely to turn and climb the grid compared to control mice in the negative geotaxis test (**Figure 3.*C***).

No differences were observed between Cdk5 CKO and control mice in measures of fear, irritability, aggression or vocalization, or fecal boli or urination during viewing jar or arena portions of the protocol. Cdk5 CKO mice displayed a significant reduction in weight compared to control mice (28.4 ± 0.5 g for CKO vs. 30.3 ± 0.8 g for Con). Interestingly, this difference emerged after the induction of Cdk5 knock-out, as both genotypes began at the same weight for 4-OH-Tam dosing 30 days prior (29.7 ± 0.8 g for CKO vs. 29.7 ± 1.0 g for Con). The response of subjects to experimenter approach indicated that control mice were more likely than Cdk5 CKO^{HT} to display robust escape from experimenter finger stroke (Wilcoxon-Mann-Whitney, $p < 0.01$; **Figure 3.*D***). These data indicate that Cdk5 CKO mice are similar to their control littermates in measures of sensory and motor function. The Cdk5 CKO mice appear less likely to execute some tasks (e.g., negative geotaxis), but are much more effective in tasks associated with motivation to escape (e.g., tail restraint, wire maneuver). Conversely, Cdk5 CKO mice were not as likely to escape the approach of an experimenter's hand. Further investigation into the behavioral response of these animals was necessary to discern their phenotype.

Effect of tamoxifen-inducible conditional Cdk5 knock-out on visual acuity and fear conditioning

Interestingly, the Prp-CreER^T transgenic line was characterized for its expression and activity in retina (Weber et al., 2001). Thus it is possible that the light sensitivity in Cdk5 CKO stems from alteration in visual perception. In order to test the sight of these animals directly, we conducted a visual platform task in the Morris Water Maze (**Figure 3.**). Cdk5 CKO mice and control mice both learn to navigate to the visual platform over repeated trials. The transgenic line C3H/HeJ mice are homozygous for the retinal degeneration mutation *Pde6b*rd, which causes loss of vision in adulthood. Indeed, these mice were impaired in their ability to navigate the visual platform test compared to controls (**Figure 3.**). Thus, Cdk5 CKO mice are not altered in their basic visual capabilites.

In order to determine if Cdk5 CKO mice are able to associate visual stimuli with contextual learning, we used a hippocampal-dependent learning task, contextual fear conditioning. The acquisition of this associative task was tested 24 h after a training protocol involving three foot shocks. In this experiment, animals were exposed to a context and given a mild footshock. Twenty-four h later, they were returned to the context to assess the level of recall that the context was previously associated with the footshock. Re-exposure of the mice to the training context after 24 h induced robust freezing behavior compared to baseline in both controls (79.5 ±4.2% vs. 6.1 ± 2.0%) and Cdk5 CKO^T (84.3 ± 5.1% vs. 5.7 ± 1.7). Next, the mice are placed in a new context, but given a cue that was previously paired to the context and footshock. As shown, Cdk5 CKO mice

showed enhanced cue-induced fear (49.0 ± 6.8 vs. 25.2 ± 5.6 for controls, $p < 0.05$), indicating that sensory processing through the amygdala is likely altered in Cdk5 CKO mice compared to controls. These findings are somewhat inconsistent with our previous reports that Cdk5 CKO mice display enhanced contextual fear conditioning (Hawasli et al., 2007). Nonetheless, these data provide compelling evidence that Cdk5 CKO visual sensory systems are intact and that the animals are capable of perceiving stimuli to consolidate fear-associated memories.

Effect of tamoxifen-inducible Cdk5 CKO on anxiety related behaviors

Adult, fCdk5 mice, with or without the Prp-CreER^{T} transgene were assessed for anxiety in three separate tasks (**Figure 3.4**). We utilized the elevated plus maze, open-field test, and dark-light habituation task in order to assess the effect of conditional loss of Cdk5 on anxiety-related behaviors. Performance in the elevated plus maze was unaltered by conditional knock-out of Cdk5 in CKO^{HT} mice (**Figure 3.4*A***). The amount of time spent in open and closed arms and the number of entries into the open arm were not significantly different between control and Cdk5 CKO mice. Cdk5 CKO mice spent 244.6 ± 5.2 sec and 23.8 ± 4.2 sec in the closed and open arms, respectively, compared to 232.6 ± 9.4 sec and 26.6 ± 5.0 sec for controls (**Figure 3.4*A***). Likewise, the number of entries into the open arm was not statistically different between control and Cdk5 CKO mice (6.2 ± 0.8 for controls vs. 4.8 ± 0.5 for cKO, $p > 0.05$, Student's *t*-test). These

data suggest that loss of Cdk5 has no effect on anxiety-related behavior in the elevated plus test.

Cdk5 CKO mice showed several indications of higher anxiety compared to controls in the open-field test. The arena was divided into several areas, with specific monitoring of the extreme center and periphery of the apparatus. The open-field test showed no difference in the amount of time spent in the extreme center of the arena by either genotype (**Figure 3 4*B***). The measure of time in the center of the arena was highly variable in the control group and likely contributed to the lack of statistical significance in this test between groups (5.3 ± 1.6 sec for controls vs. 2.7 ± 0.6 sec for cKO, $p = 0.1$, Student's *t*-test). Conversely, there was a significant difference in the amount of time Cdk5 CKO mice spent in the periphery of the apparatus compared to controls (244.2 ± 7.1 sec for CKO vs. 210.3 ± 9.0 sec for controls, $p < 0.01$). These data indicate that Cdk5 CKO mice avoided the center of the arena much more than control animals. Furthermore, there was a trend for a significant decrease in the number of visits to the center arena made by Cdk5 CKO mice compared to controls (2.7 ± 0.6 for CKO vs. 4.1 ± 0.6 for controls, $p = 0.1$). Together, these data suggest that conditional loss of Cdk5 in the brain results in performance in the open-field task consistent with increased anxiety.

The dark-light habituation task showed that Cdk5 CKO mice spent significantly less time in the light side of the apparatus (19.0 ± 6.0 sec for cKO vs.

80.4 ± 17.7 sec for controls, $p < 0.01$), also indicating an anxiogenic phenotype in Cdk5 CKO mice (**Figure 3.4*C***). Furthermore, there was a trend for reduced transitions into the light side by Cdk5 CKO mice compared to controls (5.8 ± 1.6 for cKO vs. 11.1 ± 2.2 for controls, $p = 0.06$). Taken together, these findings indicate that Cdk5 cKO mice display increased anxiety phenotypes in both open-field and dark-light tests. Notably, there was no significant difference in novelty-induced activity in Cdk5 cKO mice compared to controls in either the open-field or dark-light tests of anxiety.

These findings demonstrate the anxiogenic effect of Cdk5 loss in the adult brain. However, both tests in which Cdk5 mice were shown to have behavioral performances consistent with increased anxiety were performed in bright light conditions as a means of increasing the anxiogenic properties of the task. The Prp-CreER^T transgene that was used to mediate recombination of Cdk5 in the adult brain has been shown to have robust activity in the retina (Weber et al., 2001). Cdk5 has also been reported to function in the retina (Hirooka et al., 1996; Yamazaki et al., 2002). Thus, it is possible that Cdk5 loss in the visual system may alter light sensitivity in the adult animal. These findings are difficult to differentiate, as avoiding a brightly lit arena is normally interpreted as increased anxiety in these tests. Further investigation may reveal the effect of lighting conditions on the performance of these Cdk5 cKO mice in tests of anxiety.

Effect of tamoxifen-inducible conditional Cdk5 knock-out in adult brain on locomotor activity

The most commonly utilized measure of motor function is spontaneous locomotor activity in the open-field (Holland and Weldon, 1968). To assess the effect of loss of Cdk5 on the locomotor activity, Tam and 4-OH-Tam dosed animals were exposed to locomotor activity chambers. Cdk5 CKO mice do not display novelty or anxiety-related alterations in behvaior, as we have previously reported that condtional knokcout of Cdk5 does not alter total distance traveled during a 5 min exposure to an open field apparatus (Hawasli et al., 2007). However, Cdk5 CKO mice do not explore the light side of a dark-light habituation chamber as much as control mice (see **Figure 3.*C***). This may be related to light sensitivity, as this test is conducted at bright lighting conditions (> 250 lux).

In order to get a broader measure of general locomotor activity, animals were observed over 60-90 min in locomotor activity chambers (**Figure 3.5**). Cdk5 CKO mice displayed elevated activity over the middle of the testing session, but reached similar levels by the end of the test, suggesting habituation (**Figure 3.5*A***). Furthermore, Cdk5 CKO mice did not differ from their littermate controls in initial locomotor activity in the chambers. Taken together, these data indicate that Cdk5 CKO mice have aleration in the rate of habituation of locomotor activity. This paradigm requires handling prior to the expermineter, and any

experimenter-induced stress may effect the behavior tested. In order to remove this confound from the evaluation of locomotor activity, we recorded locomotor activity over the entire 24 hour circadian cycle in activity chambers (**Figure 3.5*C***). In this approach, Cdk5 and control mice displayed normal circadian changes in locomotor activity, with striking increase activity with the onset of the dark cycle (subjective night) compared to light cycle (subjective day). After habituation to the activity chambers, locmotor activity was recorded for 3 consecutuive days. No difference was observed in the level of activity in Cdk5 CKO mice in comparison to their littermate controls in mean activity over the 24 hour day (**Figure 3.5*C*)**. These data suggest that the locomotor effect of Cdk5 CKO in the lococmtor activity asssay may be related to increased stress response from handling. Indeed, stress has been linked to hyperactivity phenotypes in mice (Kavaliers and Ossenkopp, 1986; Strekalova et al., 2005). These findings provide direct evidence of the involvement of Cdk5 in the regulation of fine locomotor activity and habituation rates rather that gross activity levels.

Effect of tamoxifen-inducible Cdk5 CKO on motor performance in rotarod task

Cdk5 has been implicated in the regulation of dopamine signaling in the striatum. Therefore, we sought to investigate the effect of loss of Cdk5 on motor output using the accelerating rotarod task. This paradigm measures the ability of the mouse to coordinate movement and stay on a rotating horizontal rod as its

rotation speed in increased. This task has been shown to require both the striatum and the cerebellum, and is dependent on dopamine release in the striatum (Bertolucci-D'Angio et al., 1990; Emerich et al., 1993). Cdk5 CKO mice were indistinguishable from control mice during the first trials on the rod (**Figure 3.*A***). However, over subsequent trials, Cdk5 CKO showed superior performance in the task and stayed on the rod longer than control mice. This effect was maintained over subsequent days of testing. Interestingly, the inter-trial performance was enhanced in Cdk5 CKO mice, suggesting improved retrieval (**Figure 3.*A***). Furthermore, the time spent on the rod by Cdk5 CKO mice was greater than control mice over the final 10 trials of testing (119.0 ± 4.2 sec vs. 84.8 ± 3.0 sec for controls, **Figure 3.*B***). These data indicate that the ability to coordinate motor output is significantly enhanced in mice lacking Cdk5.

Effect of Cdk5 CKO on response to cocaine exposure

We previously reported that conditional Cdk5 knock-out using the CaMKII-Cre transgenic produced increased locomotor responses to cocaine exposure, and nucleus accumbens-specific loss using rAAV-Cre caused a shift in the threshold for cocaine place preference (see Chapter Two). Here, we sought to determine the effect of Cdk5 loss using the tamoxifen-inducible Prp-CreER^{T} system on cocaine-related locomotor and stereotypic activity. Tamoxifen-inducible Cdk5 CKO mice showed more robust behavioral responses to

experimenter handling than the CaMKII-Cre Cdk5 CKO mice (data not shown). We chose to conduct a single challenge of 20 mg/kg cocaine to observe the psychoactive effects on Cdk5 CKO mice (**Figure 3.**). After 2 h habituation to the activity chambers, animals were injected with cocaine and returned to the chambers for an additional 2 h. As described before, Cdk5 CKO and control mice habituate to activity chambers to the same extent after 90-120 min (**Figure 3.*A***). However, Cdk5 CKO mice showed dramatic increase in stereotypic movements compared to controls in the 60 min following challenge with 20 mg/kg cocaine (426.6 ± 81.9 in CKO vs. 209.0 ± 33.7 in controls, **Figure 3.7*B***). No such difference was observed when Cdk5 CKO and control mice were injected with saline (data not shown). Stereotypic movements are often associated with intense activation of the dopamine pathway (Karler et al., 1995), and increases in stereotypy measures may be on a continuum of the locomotor activating effects of dopaminergics. Thus, Cdk5 CKO mice appear to display increased sensitivity to the psychoactive properties of cocaine compared to control mice.

Effect of tamoxifen-inducible Cdk5 CKO on cocaine conditioned place preference

As previously discussed, drug addiction involves associative learning processes where the reinforcing properties of drugs become associated with environmental cues. We utilized tamoxifen-inducible Cdk5 CKO mice to investigate the effect of global loss of Cdk5 in the brain on conditioned place

preference for cocaine (**Figure 3.*A***). As before, this paradigm estimates the degree of cocaine reinforcement inferred from the amount of time the mice spend in a previously drug-associated context. Before conditioning, there was no preference for the compartment that was to be paired with cocaine at any dose in either control or Cdk5 CKO^T mice ($F(3,101) = 0.23$, $p = 0.87$, two-way ANOVA). Administration of saline caused no significant change in the time spent in either context in control or Cdk5 CKO^T mice. However, when conditioned with 10 mg/kg dose of cocaine, Cdk5 CKO^T mice displayed a significant increase in time spent in the drug-paired context (644.7 ± 41.4 during post-training vs. 520.5 ± 23.1 for pre-training), while no place preference was found in control animals (574.7 ± 42.8 during post-training vs. 522.5 ± 35.9 for pre-training). Training with 20 mg/kg cocaine induced significant increases in the amount of time spent in the cocaine-associated compartment in both control and CKO^T mice (**Figure 3.*B***). These data indicate that the loss of Cdk5 in CKO^T mice enhances reward-related learning, consistent with our previous observations (see **Figure 2.10**). Taken together, these data indicate that the drug reinforcing properties of cocaine may be greater after loss of Cdk5 in the reward pathway, consistent with our previous observations (see Chapter Two). Furthermore, these data suggest that the ability of cocaine to induce stereotypic movements in this model system does not negatively affect drug reinforcing properties, but enhances reinforcement.

Dopamine-PKA signaling in tamoxifen-inducible Cdk5 CKO

Cdk5 negatively regulates PKA signaling in the striatum through the direct phosphorylation of a number of key substrates, including DARPP-32 and tyrosine hydroxylase (Kansy et al., 2004). In order to examine the effect of Cdk5 loss in the striatum on PKA signaling, acute striatal slices were prepared from Cdk5 CKO and control mice (**Figure 3.A**). Basally, there was a significant increase in the phosphorylation of PKA substrates (*i.e.* pS845 GluR1 and pT34 D32). Although control slices exhibited robust increase in PKA dependent phosphorylation of pSer845 GluR1 and pThr34 DARPP-32 in response to the dopamine D1-receptor agonist, SKF81297 (1 μM, 5 min, **Figure 3.9*A***), no such increase was observed in slices from Cdk5 CKO mice following the same treatment (**Figure 3.A**). These results indicate that the basal state of PKA signaling was elevated in Cdk5 CKO striatum, and dopamine-dependent modulation of PKA towards these key substrates was occluded. These data may indicate tolerance to the cellular effects of dopamine D1-receptor signaling, despite sensitization to the behavioral effects of cocaine.

In order to explore the mechanism by which these behavioral effects may be achieved, we investigated the catecholamine levels in striatal samples from Cdk5 CKO and control mice (**Table 3.**). In this analysis, free levels of catecholamines are quantitated by HPLC against standards for dopamine (DA),

3,4-dihydroxyphenylacetic acid (DOPAC), homovanilic acid (HVA), norepinephrine (NE), serotonin (5-HT), and 5-hydroxyindoleacetic acid (5-HIAA). No differences were observed in the levels of DA or its metabolites in striatal samples of Cdk5 CKO and control mice. Likewise, there were no differences in NE or 5-HT levels in either genotype. Interestingly, there was a significant increase in the 5-HT main metabolite, 5-HIAA, in Cdk5 CKO mice compared to controls (641.2 ± 15.6 ng/g in CKO vs. 537.5 ± 11.6 ng/g in controls, $p < 0.001$). This result indicates that the steady-state metabolism of 5-HT may be increased in Cdk5 CKO striatum. Notably, increased serotonin levels have been associated with agitation and hypervigilance, as well as hypomania and hyperresponsive reflexes (Howland, 1996; Isbister and Buckley, 2005). Furthermore, serotonin signaling is an important aspect of cocaine reinforcement (Tella, 1995; Hall et al., 2004; Barot et al., 2007).

Effect of tamoxifen-inducible Cdk5 CKO on depressive behavior

Emotional fortitude and vigilance are important adaptations of the reward pathway. Drugs of abuse often dysregulate the neural circuits that govern emotional states mood. The forced swim test and tail suspension test are routinely employed to judge antidepressant action of pharmacotherapeutic agents. In these tests, latency to stop swimming or struggling is inferred as a measure of despair. Agents that increase the latency to stop swimming or struggling have

antidepressant efficacy (Porsolt et al., 1977). In order to investigate the state of despair in our model, we subjected Cdk5 CKO and control mice to the FST and TST (**Figure 3.**). In the FST, Cdk5 CKO mice displayed an increase latency to have become immobile, and decreased time spent immobile compared to controls (**Figure 3.*A***). Cdk5 CKO mice took nearly three times as long to become immobile compared to controls (148 ± 33 sec for CKO vs. 48 ± 24 sec for controls, $p < 0.05$, Student's *t*-test). Furthermore, control mice spent nearly four times as long immobile compared to Cdk5 CKO mice (109 ± 17 sec vs. 29 ± 17 sec for CKO, $p < 0.01$). These data indicate that conditional loss of Cdk5 produced antidepressant-like behavioral profile in the forced swim test. Cdk5 CKO mice also displayed increased time spent struggling in the TST (**Figure 3.*B***). The mice exhibited more forceful movements in the TST, as measure by the strain gauge attached to the apparatus (135.8 ± 1.7% higher in CKO compared to controls 100 ± 1.1%, $p < 0.05$). These results indicate that loss of Cdk5 confers antidepressant characteristics in these behavioral paradigms. Increased serotonin □ ô □ ì □ Ì □ μ □ ¥ are commonly used antidepressant therapeutics. Indeed, Cdk5 CKO mice displayed behavioral phenotypes consistent with elevated serotonin signaling, indicating that an interesting avenue of research to explore may be the regulation of serotonin signaling in the brain by Cdk5.

Evaluation of voluntary wheel running in tamoxifen-inducible Cdk5 CKO mice

We reported altered voluntary locomotor activity and responsiveness to stimuli in tamoxifen-inducible Cdk5 CKO mice. Taken together, these data indicate that Cdk5 CKO mice have alerations in the rate of habituation of locomotor activity. These data also indicate that the basal locomotor activity is not significantly altered over the 24h day.. In order to investigate the effect of voluntary execrise, we recorded wheel-running activity over the entire 24 h circadian cycle in control and Cdk5 CKO^{HT} mice (**Figure 3.**). In this approach, Cdk5 and control mice displayed normal circadian changes in activity, with a striking increase activity with the onset of the dark cycle (subjective night) compared to light cycle (subjective day), reminiscent of the locomotor activity presented in **Figure 3.5*C***. However, after acquisition of the behavior, Cdk5 CKO mice displayed dramatically reduced steady-state levels of voluntary wheel-running compared to controls. The effecct was most dramatic during the dark cycle, during which time activity levels in both controls and CKO mice were higher than during the light cycle.

In related studies, we investigated the effect of voluntary wheel-running on the level of Cdk5 and associated proteins in the striatum. There was no significant affect of one week of voluntary wheel running on absolute levels of Cdk5, p35 or pThr75 DARPP-32 in striatal samples (**Figure 3.**). However, there was a significant increase in the level of ΔFosB in this brain region after running

(75.4 ± 24.6 % for 35 kDa and 46.0 ± 14.8 % for 37 kDa forms over controls, $p < 0.05$ for each). This finding is not unexpected, as previous studies have implicated this molecule in the acquisition and execution of voluntary exercise (Werme et al., 2002). Nontheless, we show that as little as one week of exposure to voluntary wheel running is sufficient to induce significant increases in the accumulation of ΔFosB in the motor circuitry. These data suggest that depsite not being an early target of voluntary wheel running, Cdk5 may regulate the excecution or motivation for reward.

Discussion

We report here the development of tamoxifen-inducible conditional Cdk5 knock-out model systems in which Cdk5 loss is achieved in spatially restricted regions of the adult nervous system. This allowed for the investigation of the direct effects of Cdk5 knock-out in the adult animal on the behavioral profile testing motor function and emotional states. Previous behavioral investigations have utilized the infusion of Cdk5 inhibitors into the brain (Bibb et al., 2001; Norrholm et al., 2003; Chen and Chen, 2005; Taylor et al., 2007). While pharmacological agents have provided insight into the role of Cdk5 in reward processing, their limitations include the localization of the effects to specific regions. In the current study, it has been possible to investigate the consequence

of more global loss of Cdk5 activity in the brain. While this approach, like the pharmacological approach, limits the ability to localize the effects to either pre- or postsynaptic compartments or brain circuits, it has provided a wealth of new avenues to implicate Cdk5 in the control of behaviors likely mediated through circuits outside the basal ganglia. Moreover, the loss of the Cdk5 protein has made it possible to observe the impact of putative structural or activity-independent roles of the kinase in these behaviors, as has been recently suggested (Hawasli and Bibb, 2007). Thus, the use of tamoxifen-inducible Cdk5 CKO mice has allowed for the loss of the *cdk5* gene in adult mice to be more directly linked to behavioral profiles.

We have shown that conditional loss of Cdk5 in the adult brain produced elevated spontaneous locomotor activity, motor learning, and antidepressant-like behavioral profiles. These behavioral changes were accompanied by increased basal state of PKA signaling in striatal samples and augmented responses to direct dopamine receptor activation. Furthermore, catecholamine levels displayed elevated serotonin turnover in striatal samples. These findings illustrate the importance of Cdk5 in the control of various behaviors and in the control over the function of striatal neurons that may regulate motor and emotional behaviors.

Previous studies have reported that loss of Cdk5 in the adult brain contributes to enhanced responses to cocaine (see Chapter Two) as well as increased contextual learning and extinction (Hawasli et al., 2007). These studies were the

first to utilize conditional knock-out technology to investigate the role of Cdk5 in the control of behaviors in the adult animal. These model systems benefit from the ability to discern the contribution of various activity dependent and activity independent roles of Cdk5. Early studies using Cdk5 inhibitors have implicated Cdk5 in the regulation of striatal function via regulation of the D1R-PKA-DARPP-32-PP-1 pathway (Bibb et al., 1999). Since these original studies, several groups have found evidence for the involvement of Cdk5 in the regulation of psychostimulant exposure (Narita et al., 2005; Wedzony et al., 2005; Taylor et al., 2007). Although the bulk of these earlier works utilized Cdk5 inhibitors, some studies have utilized DARPP-32 phosphomutant mice to investigate the requirement of the individual phosphorylation sites in the behavioral responses to psychostimulant and antipsychotic drugs (Svenningsson et al., 2003). Mutation of the Cdk5 site of DARPP-32 failed to affect the responsiveness to psychostimulants. These data are in conflict with the notion that Cdk5 is important in the responses of the D1-PKA-PP1 pathway in response to drugs of abuse. However, it is important to note that one study indicated altered behavioral adaptation of T75A-D32 mice in response to repeated cocaine exposure (Zachariou et al., 2006). Clearly, the biochemical and cellular targets underlining the effect of Cdk5 in the reward circuitry and elsewhere remains to be fully elucidated. Taken together, the findings in this chapter highlight the complexity of the regulation of Cdk5 activity in the brain and provide the basis

for future studies attempting to examine the mechanism underlying Cdk5 knock-out behaviors.

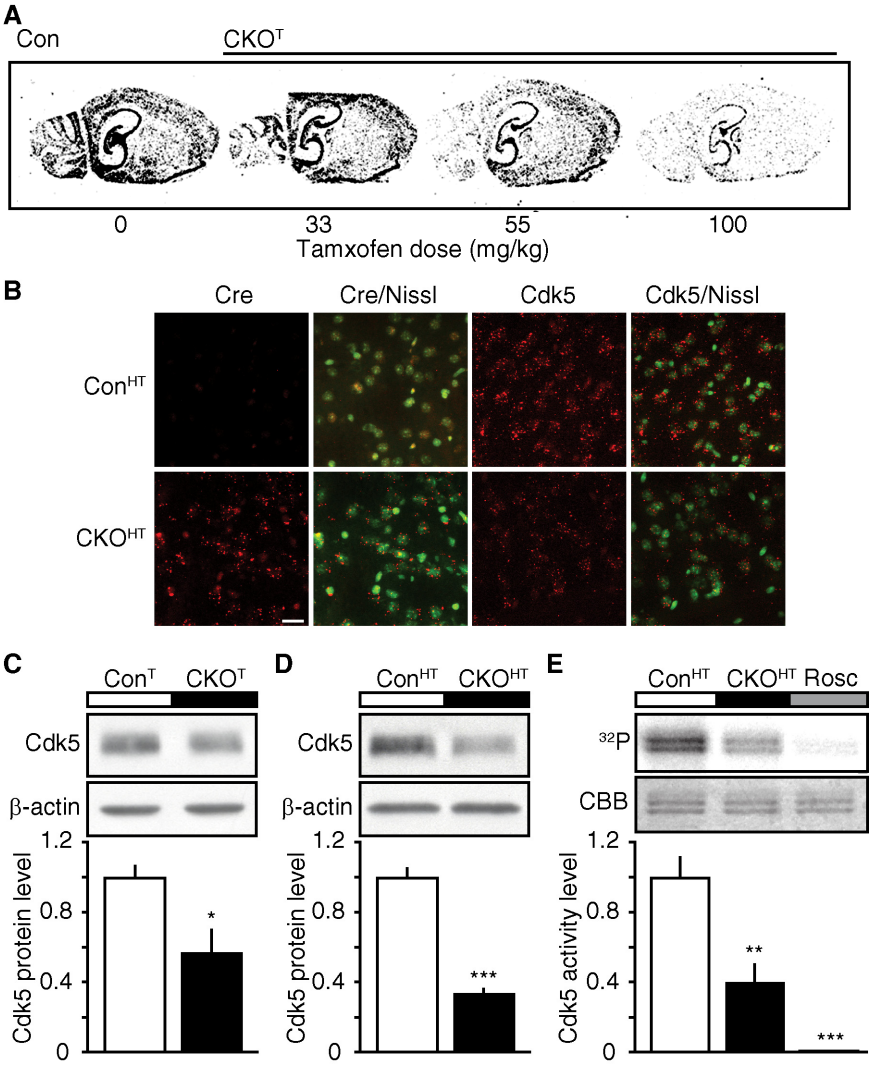

Figure 3.1. Generation of Tamoxifen-inducible Cdk5 conditional knock-out mouse models. **A**, Radiolabeled in situ analysis of tamoxifen dose response in Cdk5 CKO^{T} mice. Animals were administered Tam at indicated doses for 10 consecutive days. **B**, Fluorescence in situ hybridizations for Cdk5 and Cre mRNA in striatal regions in control (Con^{HT}) and Cdk5 CKO^{HT} mice administered 66 mg/kg 4-hydroxytamoxifen for 15 consecutive days. Nissl counterstains are shown for each. Scale bar 20 μm. **C**, Quantitative immunoblot analysis of striatal samples from CKO^{T} and Con^{T} mice administered tamoxifen. Representative immunoblots (top) and bar graph of quantitation (bottom) are shown for each. **D**, Quantitative immunoblot analysis of striatal samples from CKO^{HT} and Con^{HT} mice administered 4-hydroxytamoxifen. **E**, Cdk5 kinase activity

immunoprecipitated from striatal samples of Con^{HT} and CKO^{HT}. Treatment of immunoprecipitate from control samples with Roscovitine (Rosc, 10 μM) prior to kinase assay is also shown (*$p < 0.05$, **$p < 0.01$, ***$p < 0.001$ compared to controls, Student's *t*-test, n = 6–9)

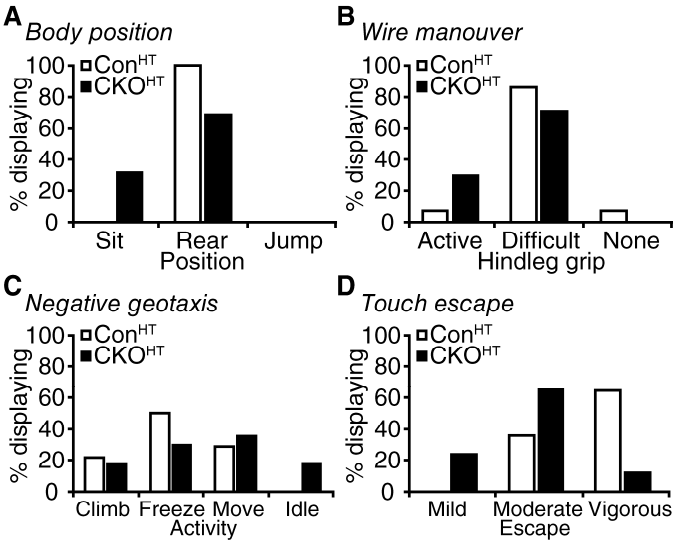

Figure 3.2. SHIRPA analysis of Tamoxifen Cdk5 CKO mice. **A**, Performance of control and Cdk5 CKO^{HT} mice in body position portion of SHIRPA analysis. **B**, Hindleg grip performance in wire maneuver task by control and Cdk5 CKO^{HT} mice. **C**, Activity in negative geotaxis task in control and Cdk5 CKO mice administered 4-hydroxytamoxifen. **D**, Performance of control and Cdk5 CKO^{HT} mice in touch escape test in SHIRPA analysis (n = 14–17 per group).

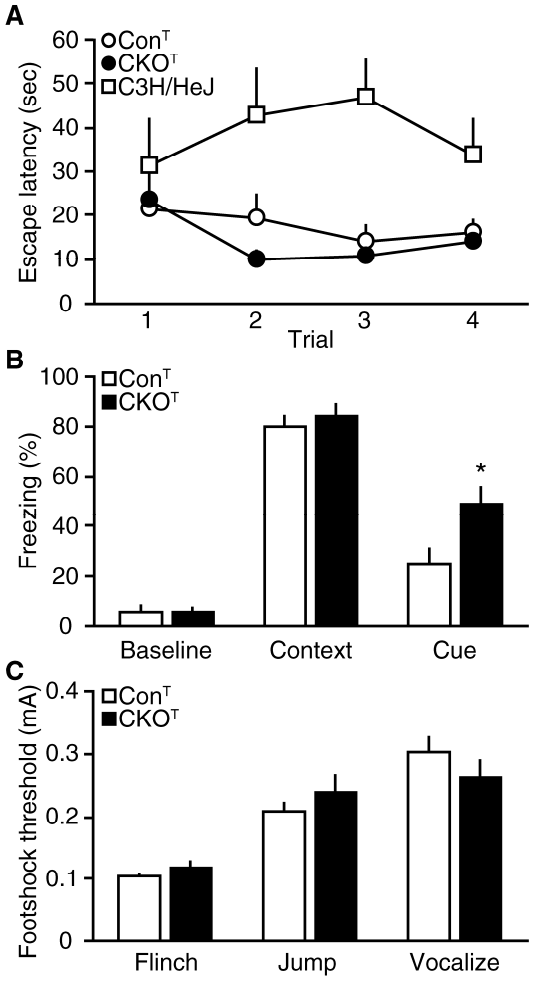

Figure 3.3. Effect of Tamoxifen Cdk5 CKO on visual acuity, conditioned fear, and nociception. **A**, Comparison of performance of control (Con^T) and Cdk5 CKO^T mice for performance in visual platform test in water maze. Time spent searching for the submerged platform during each trial are shown (n = 8–12 per genotype). Performance of blind C3H/HeJ mice are also shown during each trial (n = 5). **B**, Performance of Cdk5 CKO mice in fear conditioning memory. Baseline freezing time is shown along with context and cue re-exposure 24 h after training. Mean freezing time (% of total time ± *SEM*) during each phase is shown (*$p < 0.05$, Student's *t*-test compared to controls, n = 8–12 per group). **C**, Nociception in control and Cdk5 CKO mice. Performance in footshock threshold to flinch, jump, and vocalize. Graph represents mean shock intensity (± *SEM*) necessary to observe each measure (n = 8–12 per group).

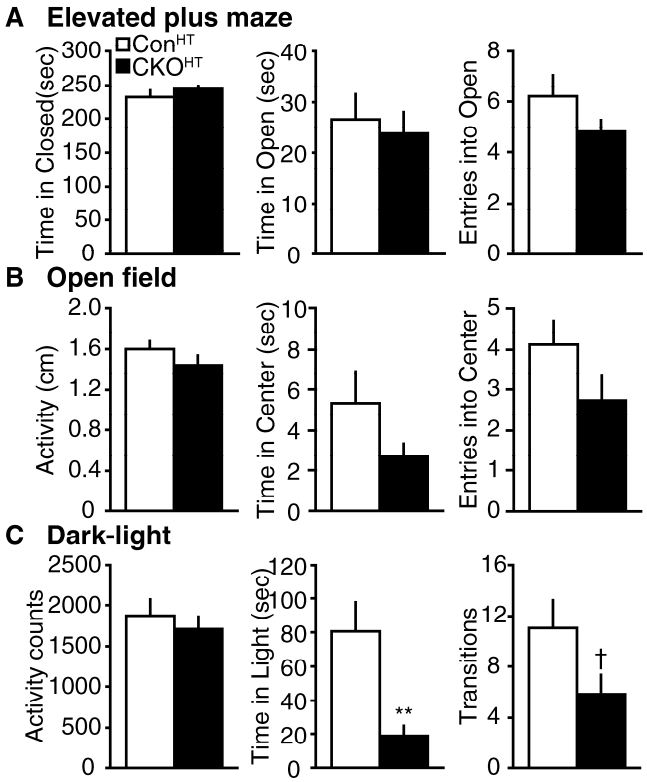

Figure 3.4. Effect of Tamoxifen Cdk5 CKO on anxiety-related behavior. A, Comparison of control (Con^{HT}) and Cdk5 CKO^{HT} mice for performance in the elevated plus maze. Time in each arm of the task and the number of entries into the open arm are shown (n = 35–37 per group). **B**, Performance of Cdk5 CKO^{HT} mice in open field task. Mean distance traveled (± *SEM*) during the task is shown, along with time in center arena and number of entries into center arena (n = 37–38 per group). **C**, Performance of control and Cdk5 CKO^{HT} mice in dark-light habituation box. Mean locomotor activity counts (± *SEM*) during the task are shown, along with time spent in light and number of dark-light transitions (n = 16–17 per group). Graphs represent mean ± *SEM* for each measure ($^{\dagger}p = 0.06$, $^{**}p < 0.01$ compared to control, Student's *t*-test).

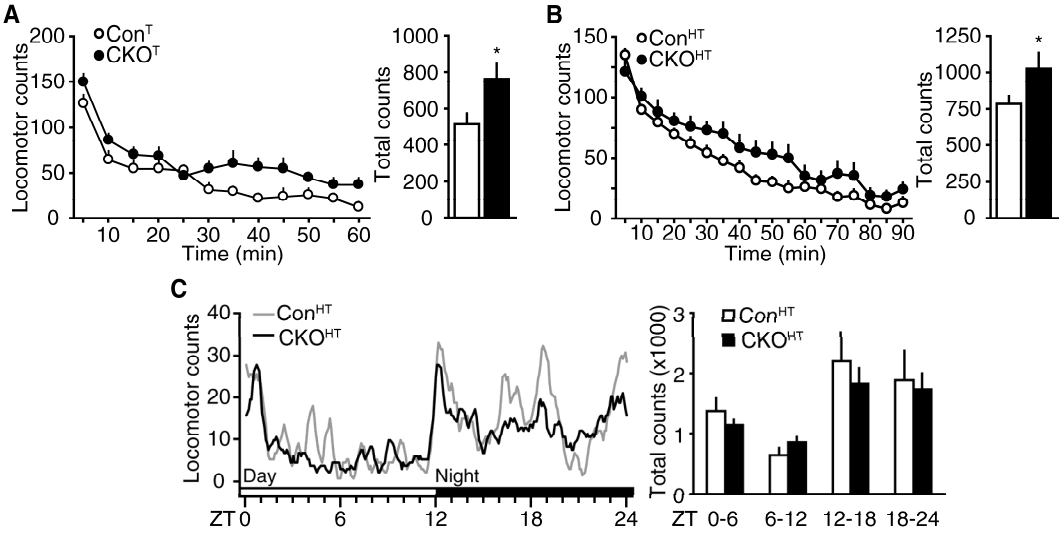

Figure 3.5. Effect of Tamoxifen Cdk5 CKO on spontaneous locomotor activity. **A**, Time course of spontaneous locomotor activity in tamoxifen-treated Cdk5 CKO mice. Graph on left depicts mean locomotor counts in 5 min bins (± *SEM*) over 60 min. Cumulative locomotor counts (± *SEM*) over 60 min are displayed in bar graph at right (*$p < 0.05$, Student's *t*-test, n = 12 per group). **B**, Time course of spontaneous locomotor activity in 4-hydroxytamoxifen-treated Cdk5 CKO mice. Graph on left depicts mean locomotor counts (± *SEM*) over 90 min. Cumulative locomotor counts (± *SEM*) over 90 min are displayed in histograms at right (*$p < 0.05$, Student's *t*-test, n = 17–19 per group). **C**, Time course of home cage circadian locomotor activity in 4-hydroxytamoxifen-treated Cdk5 CKO mice. Graph on left depicts locomotor counts (30 min moving period) over 24 h interval for control (grey line) and Cdk5 CKO (black line) mice. Zeitgeber time (ZT) is indicated on abscissa along with boxes indicating light conditions (white = day; black = night). Cumulative locomotor counts (± *SEM*) over 6 h bins are displayed in histograms at right.

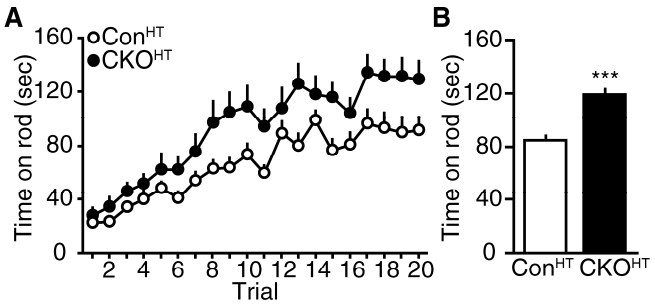

Figure 3.6. Effect of Tamoxifen Cdk5 CKO on rotarod performance and motor learning. **A**, Locomotor performance 4-hydroxytamoxifen treated control (Con^{HT}) and Cdk5 knock-out (CKO^{HT}) mice on accelerating rotarod. Graph depicts mean time on rod (± *SEM*) in each session conducted over 4 consecutive days (RM ANOVA, genotype X trial interaction $p < 0.01$). **B**, Bar graph representation of mean performance over final 10 sessions are shown (***$p < 0.001$ compared to Con^{HT}, Student's *t*-test, n = 17-25).

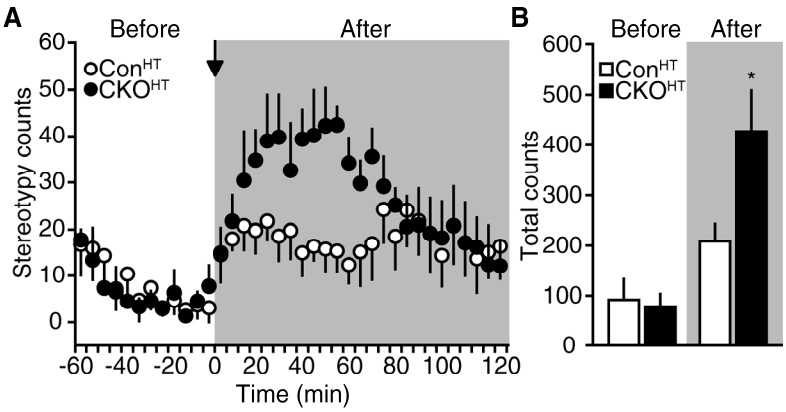

Figure 3.7. Effect of Tamoxifen Cdk5 CKO on stereotypic movements after cocaine exposure. **A**, Time course of stereotypic movements in Cdk5 CKO^{HT} mice in response to 20 mg/kg cocaine injection. Graph depicts stereotypy counts in 5 min bins over 60 min before (white background) and 120 min after (grey background) cocaine injection. **B**, Cumulative stereotypy counts (± *SEM*) over 60 min before and after injection are displayed in histogram at right (*$p < 0.01$, Student's *t*-test, n = 5 per group).

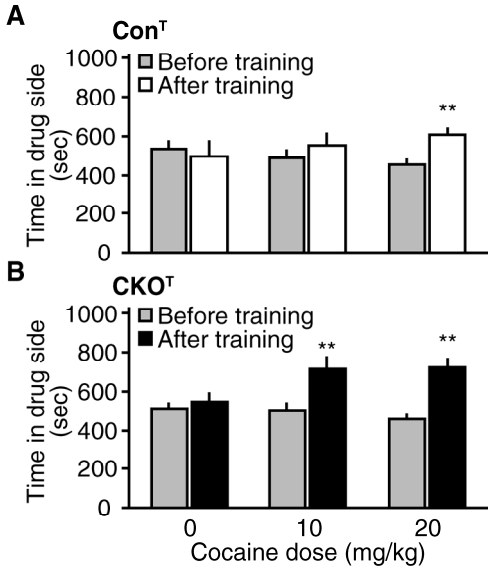

Figure 3.8. Effect of Tamoxifen Cdk5 CKO on cocaine-induced conditioned place preference. **A**, Performance of control mice (Con^T) in cocaine conditioned place preference assay. Graph depicts time spent in drug-paired compartment before (grey) and after (white) cocaine training at the indicated cocaine doses. Mean time spent in drug compartment is indicated (± *SEM*) for each group at each training dose of cocaine (**$p < 0.01$, paired *t*-test, n = 5–6 per dose). **B**, Performance of Cdk5 CKO^T mice in cocaine conditioned place preference assay as in **A**. Graph depicts CKO^T mice performance before (grey) and after (black) cocaine training. Mean time spent in drug compartment is indicated (± *SEM*) for each group at each training dose of cocaine (**p < 0.01, paired *t*-test, n = 7–9 per dose).

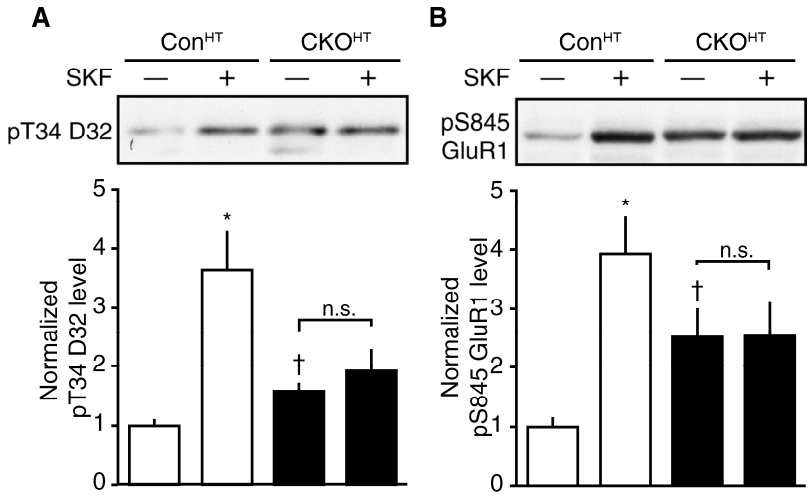

Figure 3.9. Effect of Tamoxifen Cdk5 CKO on phosphorylation of PKA substrates and dopamine-D1 receptor signaling in the striatum. **A**, Quantitative immunoblots of striatal slices from 4-hydroxytamoxifen treated control (Con^{HT}) and Cdk5 knock-out (CKO^{HT}) mice incubated with the D1 receptor agonist, SKF 81297 (SKF; 1uM, 5 min) or without. Representative immunoblots of phospho-Thr34 D32 are shown (top) with quantitation (bottom). Graph depicts mean normalized phospho/total protein level (*$p < 0.05$ versus control, Student's *t*-test; †$p < 0.05$, Student's *t*-test versus Con^{HT} control, n = 5–8). **B**, Quantitative immunoblots of phospho-Ser845 GluR1 as in **A**. Representative immunoblots (top) and graph of quantitation normalized phospho/total protein level is shown (bottom; *$p < 0.05$ versus control, Student's *t*-test; †$p < 0.05$, Student's *t*-test versus Con^{HT} control; n.s., not significant versus CKO^{HT} control, n = 5–8).

Table 1

Monoamine levels in dorsal striatum samples of control and Cdk5 CKO^{HT} mice

Monoamine	Control	Cdk5 CKO^{HT}
DA	10.5 ± 0.9†	11.1 ± 0.8†
DOPAC	1.6 ± 0.3†	1.8 ± 0.4†
HVA	1.1 ± 0.04†	1.1 ± 0.09†
NE	27.6 ± 4.1‡	31.8 ± 6.4‡
5-HT	418.5 ± 25.6‡	416.0 ± 26.2‡
5-HIAA	537.5 ± 11.6‡	641.2 ± 15.6‡**

DA, dopamine; DOPAC, 3,4-dihydroxyphenylacetic acid; HVA, homovanilic acid; NE, norepinephrine; 5-HT, serotonin; 5-HIAA, 5-hydroxyindoleacetic acid. †mg/g tissue; ‡ng/g tissue.
**p<0.001, Student's *t*-test, n = 6 per group.

Table 3.1. Monoamine levels in dorsal striatum samples of control and Tamoxifen Cdk5 CKO mice. Striatal lysates subjected to HPLC for quantitation of monoamine levels. Abbreviations: DA, dopamine; DOPAC, 3,4-dihydroxyphenylacetic acid; HVA, homovanilic acid; NE, norepinephrine; 5-HT, serotonin; 5-HIAA, 5-hydroxyindoleacetic acid. †Values indicate mg/g tissue; ‡Values indicate ng/g tissue. **p<0.001, Student's *t*-test, n = 6 per group.

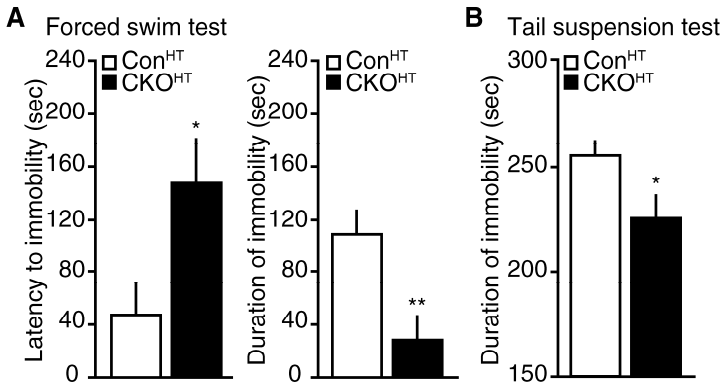

Figure 3.10. Effect of Tamoxifen Cdk5 CKO on behavioral despair. **A**, Performance of Cdk5 CKO^{HT} mice in forced swim test. Graph depicts duration and latency to immobility for control (Con^{HT}) and CKO^{HT} mice. Mean time for each measure (± *SEM*) is indicated for each group (*$p < 0.05$, **$p < 0.01$, Student's *t*-test, n = 11-13 per genotype). **B**, Performance of 4-hydroxytamoxifen treated Cdk5 CKO mice in tail suspension test. Graph depicts mean duration of immobility (± *SEM*) for each group (*$p < 0.05$, Student's *t*-test, n = 9-12 per group).

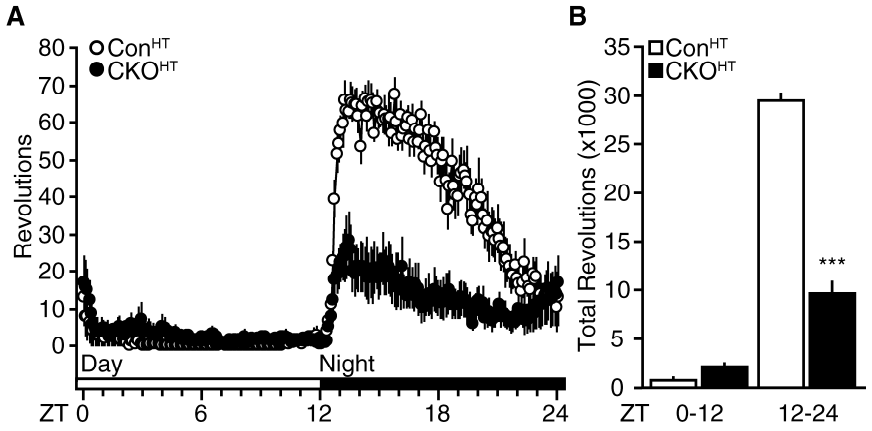

Figure 3.11. Effect of Tamoxifen Cdk5 CKO on voluntary circadian wheel-running behavior. **A**, Analysis of wheel-running activity recorded after acquisition of stable running in control (Con^{HT}) and Cdk5 CKO^{HT} mice. Mean wheel revolutions counts (± *SEM*) in 6 min bins over 24 h period are shown for Con^{HT} and CKO^{HT} groups. Time of day labels in Zeitgeber time (ZT), as well as graphically as day (open bar) and night (closed bar), appear on abscissa. **B**, Bar graph representation of total revolutions during 24 h period. Graph depicts mean revolutions (± *SEM*) during light (ZT 0–12) and dark (ZT 12–24) (*$p < 0.05$ compared to controls, Student's *t*-test, n = 6 per genotype).

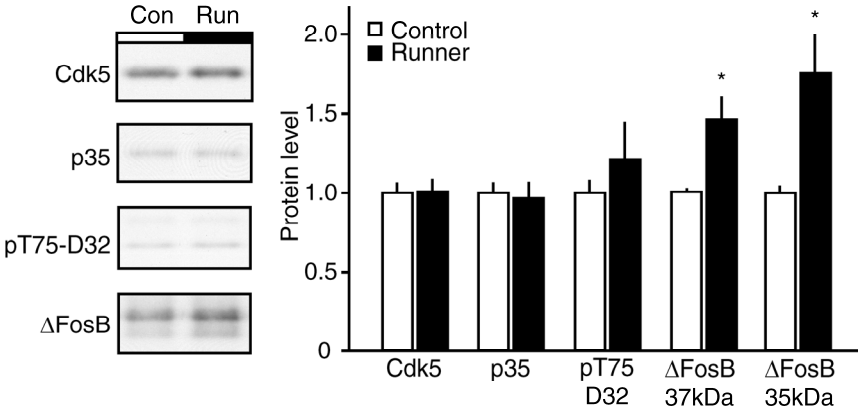

Figure 3.12. Analysis of striatal levels of Cdk5 after voluntary running. Quantitative immunoblot analysis of striatal samples from mice undergoing voluntary wheel running for one week. Representative immunoblots (left) and quantitation (right) are shown for each target (*$p < 0.05$ compared to control non-runner, Student's *t*-test, n = 6 per group).

CHAPTER FOUR

REGULATION OF PKA SIGNAL TRASNDUCTION THROUGH CDK5-DEPENDENT PHOSPHORYLATION OF PKA REGULATORY SUBUNIT RIIβ

Summary

Cdk5 is an important regulator of dopamine-PKA signaling in striatal tissue via its phosphorylation of DARPP-32 at Thr75. Here, we show that CaMKII-Cre conditional Cdk5 knock-out (cKO) mice have enhanced behavioral response to repeated cocaine exposure and altered behavioral responses to dopaminergic drugs. We found that PKA activity in striatal tissue from Cdk5 cKO mice was altered basally and in response to cocaine exposure relative to controls.

Interestingly, inhibition of Cdk5 in T75A-DARPP-32 phosphomutant mice leads to the activation of PKA signaling indistinguishable from wild-type mice. This finding predicts that there exists novel mechanisms by which Cdk5 regulates PKA signaling. Using a candidate search, we found that Cdk5 directly phosphorylates the PKA regulatory subunit II β (RIIβ) *in vitro*. The site of Cdk5-dependent phosphorylation was identified by mass spectrometry and confirmed by site-directed mutagenesis as Thr69 of RIIβ. Basal levels of pThr69 RIIβ, as detected by novel phosphorylation state-specific antisera, were detected in various

regions of the adult rodent brain. Furthermore, the level of pThr69 RIIβ was reduced in striatal samples from Cdk5 cKO mice. In wild-type striatal tissue I, pThr69 RIIβ levels were resistant to modulation by various pharmacological manipulations. Functionally, we found that pThr69-RIIβ served as a more efficient substrate for mu-calpain-mediated cleavage compared to dephospho-RIIβ *in vitro* and altered binding to an AKAP motif. These findings demonstrate a novel mechanism by which Cdk5 may regulate PKA signaling in the striatum. Furthermore, the modulation of striatal neuron excitability by dopaminergic agents was altered in Cdk5 cKO mice. These findings identify a novel target by which Cdk5 may regulate PKA signaling in the striatum which may be important for the cellular and behavioral responses to dopamine signaling and drug addiction.

Introduction

Neuroadaptations in cAMP signaling in the mesolimbic dopamine system likely underlie the behavioral consequences of chronic cocaine exposure and are important for the conversion to addiction (Self, 2004). There are numerous molecular changes that occur in the reward circuitry following drug exposure, most notably the accumulation ΔFosB, a transcription factor involved in/important for (Hope et al., 1994). The neuronal enriched kinase Cdk5 is a

downstream effector of ΔFosB (Bibb et al., 2001; Kumar et al., 2005). In the striatum, Cdk5 is found both pre- and post-synaptic compartments of dopaminergic neurons (Bibb et al., 1999; Chergui et al., 2004). Indeed, Cdk5 has been implicated as a regulator of the behavioral effects of dopaminergic drugs (Bibb et al., 2001; Taylor et al., 2007), likely through control of dopamine-PKA signaling (Bibb et al., 1999) and synaptic plasticity (Hawasli et al., 2007). To date, the exact cellular mechanism responsible for these Cdk5-dependent regulatory effects remain to be fully elucidated.

In a recent study, Cdk5 was shown to phosphorylate WAVE1 and to regulate actin cytoskeletal remodeling pathways (Kim et al., 2006). These pathways may serve as mechanistic explanations for the previous studies implicating Cdk5 in cocaine-mediated morphological alterations (Norrholm et al., 2003). Furthermore, this work highlights the interplay between Cdk5 and PKA signaling pathways. Previous work by our group identified DARPP-32 as a direct substrate of Cdk5, turning DARPP-32 into a potent inhibitor of PKA (Bibb et al., 1999). While this pathway is well positioned to subserve cocaine-elicited alterations in PKA signaling efficacy in striatal tissue (Bibb et al., 2001), its application is restricted to DARPP-32 expressing cells. The use of Cdk5 inhibitors, including roscovitine, have proven to be effective activators of PKA signaling (Kansy et al., 2004; Kim et al., 2006). While the decrease in DARPP-32 phosphorylation and disinhibition is an attractive explanation, there is

significant evidence that this regulation of PKA exists in DARPP-32 deficient tissue as well (Kansy et al., 2004).

The subcellular localization of PKA is dependent upon interaction of regulatory subunit RII with specific A-kinase anchoring proteins (AKAPs). These interactions are crucial for the proper spatial regulation of PKA signaling. Previous work has implicated a role for cyclin-dependent protein kinase mediated phosphorylation of RII subunits in AKAP binding (Keryer et al., 1993). Cdk1 (cyclin B-p34^{cdc2}) has also been shown to phosphorylate RIIα at T54 (Keryer et al., 1998). This phosphorylation caused an electrophoretic mobility shift in RIIα in SDS-PAGE and caused a solubilization or redistribution of the protein in HeLa cells. These data provide compelling evidence for the notion that Cdks control PKA signaling through the regulation of regulatory subunit subcellular localization. This alteration in localization is likely coincident with re-association with new protein-protein complexes in the cytosol. In this chapter, we explore novel roles of Cdk5 in the regulation of PKA signaling.

Experimental Procedures

Chemicals and enzymes

All chemicals were from Sigma, except where indicated. Cdk5 and p25-His6 were co-expressed in insect Sf9 cultures using baculovirus vectors and

affinity-purified by K. Hayashi (UT Southwestern Medical Center), as previously described (Saito et al., 2003). The rat catalytic subunit of PKA was from New England Biolabs. Cell culture reagents were from Invitrogen. Dithiothreitol, isopropyl-β-D-thiogalactopyranoside, and ATP were from Roche Applied Science. [γ-^{32}P]ATP was from PerkinElmer Life Sciences. Peptides and phosphopeptides were provided by H. Ball (Protein Chemistry Technology Center, UT Southwestern Medical Center). Trypsin was from Promega. Roscovitine was provided by L. Meijer (Centre National de la Recherche Scientifique, Roscoff, France). Indolinone A and Indolinone B were provided by F. Gillardon (Boehringer Ingelheim Pharma, Ingelheim, Germany). NMDA was from Tocris. Forskolin was from LC Laboratories. U0126 was from Promega.

Animals and animal care

The CaMKII Cdk5 cKO mice and littermate controls were generated and utilized as described in Chapter Two. Adult, male C57BL/6 mice (Charles River) were used in experiments. For some experiments, wild-type and Thr75Ala-DARPP-32 mutant mice (Svenningsson et al., 2005) were utilized (provided by P. Greengard). These mice were backcrossed to C57BL/6 and maintained as separate breeders. For all experiments, male, adult 10-12 week old mice were used. All manipulations were approved by UT Southwestern Medical Center and Rockefeller University Institutional Animal Care and Use Committees and

conducted in accordance with the applicable portions of the National Institutes of Health *Guide for the Care and Use of Laboratory Animals*.

Behavioral procedures

Cocaine-induced locomotor sensitization assay: Locomotor sensitization to cocaine (15 or 20 mg/kg) was examined in CaMKII-Cre Cdk5 cKO mice and littermate controls according to the methods and experimental design described in Chapter Two.

Dopamine receptor agonist treatment and locomotor activity: Horizontal motor and stereotypic activity was monitored in standard polypropylene cages as described in Chapter Two. The response to D1 or D2 was assessed using a cumulative dose regimen, in which each animal was given an increasing dose of the drug followed by behavioral testing. This within session dose response was performed by placing animals in the cage and activity recorded for 1 hr, at which point a single i.p. injection (5 ml/kg) was delivered and the animal replaced in the chamber for an additional hour. This was repeated for injections of SKF81297 (1, 3, 10 mg/kg) over the next three hours. Animals were habituated to saline injection on the day before SKF81297 administration. In separate experiments, the locomotor suppressant effects of quinpirole were assessed using novelty-induced locomotor activity. Animals which had not undergone habituation were monitored for locomotor activity for 10 min in the apparatus, after which they

were returned to home cages. After 20 min, a single injection of quinpirole (0.3, 1.0 mg/kg) was injected s.c. and the animals were returned to the home cage. After 30min, the animals were replaced into the locomotor activity chambers for 10 min. Data are represented as average activity in 5 or 10 min ± *SEM*.

Chronic cocaine exposure in Cdk5 cKO mice

Adult, male control and CaMKII Cdk5 cKO mice were utilized for chronic cocaine exposure experiment. In this experiment, animals were given a single i.p. injection of 15 mg/kg cocaine in a novel cage with minimal bedding and without food or water for 3 h daily for 1, 3, or 10 consecutive days. All animals were habituated to handling, novel context, and saline injection for at least 3 d prior to the administration of cocaine. All animals received at least 7 injections total.

Preparation of acute striatal slices and slice pharmacology

Acute striatal slices were prepared from C57BL/6, and littermate control and CaMKII Cdk5 cKO mice as described in Chapter Three. In one experiment, littermate wild-type control and T75A D32 mutant mice (provided by P. Greengard) were utilized for the preparation of acute striatal slices. For some experiments, striatal slices were pre-incubated with calpeptin (20 μM, Calbiochem) for 30 min prior to the addition of NMDA (100 μM). As before,

samples were transferred to screw-cap tubes, frozen on dry ice, and stored at –80°C until analysis.

Immunoblot analysis of cell and tissue homogenates and cellular fractionation

Quantitative immunoblotting and analysis were performed as described in Chapter Two. Frozen cell pellets and striatal tissue samples were homogenized in boiling lysis buffer (50 mM NaF in 1.0% SDS) using a manual ultrasonic processor and boiled for 10 min. For the cocaine exposure experiment, mice were sacrificed 30 min after the last injection of cocaine and brains were removed and 1 mm thick coronal slices were prepared using a matrix, as described in Chapter Two. In one experiment, we utilized striatal samples from adult (20 week old) RIIβ KO and littermate control mice that were provided by T. Czyzyk and G.S. McKnight (University of Washington). Protein concentrations were determined and quantitative immunoblotting was performed as described in Chapter Two.

For subcellular fractionation, cell culture pellets or tissue samples were lysed in homogenization buffer (HB) containing (in mM): 320 sucrose, 10 Tris base, pH 7.4, 150 NaCl, 5 EDTA, 5 EGTA, pH 7.4, 50 NaF with protease inhibitor cocktail (1:250, Sigma P8340). Lysates were prepared using a Teflon dounce-homogenizer in automatic spinner, cleared by centrifugation at 900*g* for 10 min at 4 °C and stored on ice. The supernatant (S1) was removed and the nuclear pellet was re-homogenized in 10% original volume, spun and the

supernatant (S1') was removed and pooled with the S1. In some experiments, the nuclear pellet was also resuspended and analyzed. S1 was spun at 10,000*g* for 15 min in order to yield S2 and P2 fractions. P2 fraction was resuspended in 80% volume and respun, then washed with 2 volumes of HB. The S2 fraction was also respun and supernatant removed to a fresh tube. The P2 fraction was resuspended in 50% volume and protein concentrations were determined for S1, P2, and S2 fractions by BCA (Pierce). Equal amounts of total protein were resolved on 10% isocratic SDS-PAGE gels and transferred to nitrocellulose for immunoblotting as described in Chapter Two.

In addition to the antibodies described above, antibodies to pThr69 RIIβ (1:15,000, see below) and total RIIβ (1:20,000, BD Transduction), αPKAcat (1:5000, BD Transduction), AKAP150 (1:500, Santa Cruz, C-20), PSD-95 (1:100,000, Cell Signaling), GAPDH (1:50,000, Sigma) were also used. The proteolytic fragment p25 was detected with the antibody to p35 (1:250, Santa Cruz, C-19). .

Striatal neuron culture and immunocytochemistry

Embryonic striatal neurons (E18/19) were cultured from Long Evans rats (Charles River Labs) as previously described (Ventimiglia and Lindsay, 1998) with modifications. Striatal neurons were cultured and provided by C. Dewey and C. Cowan (UT Southwestern Medical Center). The striatal tissues were digested

with papain (10 unit/ml; Worthington) for 4 min at 37 °C before dissociation with a plastic 5 ml pipet. The dissociated neurons were plated at 100,000/well (24 well plate; Corning) on PDL- and laminin (Invitrogen)-coated 12 mm glass coverslips (Bellco) in DMEM supplemented with 10% (v/v) fetal bovine serum, penicillin (50 μg/ml)-streptomycin (50 units/ml) and L-glutamine (4 mM) and incubated at 37 °C in5% CO_2 for 24 h in a humidified incubator. After 24 h, the medium was changed to Neurobasal, B27 supplement (2% (v/v)), penicillin-streptomycin (1X) and L-glutamine (4 mM). After 14 days *in vitro* (DIV), glass coverslips containing cells were washed in PBS, fixed in 4% PFA, and washed three times in PBS before block in 3% NGS/0.3% Triton X-100 in PBS for 1 h. Primary antibodies to Cdk5 (1:100, Santa Cruz, C-8) and RIIβ (1:500, BD Transduction) were diluted in blocking buffer and incubated with coverslips overnight at 4 °C. Three washes were conducted in 0.1% Triton X-100, followed by incubation in secondary antibodies diluted in 0.1% Triton X-100 in PBS. Three washes were conducted in PBS prior to mounting on slides in aquamount. Immunofluorescence imaging was conducted using confocal microscopy.

RIIβ subcloning and site-directed mutagenesis

Recombinant RIIβ was generated by subcloning rat RIIβ cDNA (provided by G.S. McKnight, University of Washington) into a modified pET-16b/28a hybrid bacterial expression vector based on pET-16b and incorporating the

multiple cloning region of pET-28a (Novagen) with a C-terminal histidine purification tag. RIIβ subcloning and mutagenesis was conducted by J.W. Kansy (UT Southwestern Medical Center). The pET-16b/28a-RIIβ vector served as the template for site-directed mutagenesis using PCR. Mutants containing single or multiple amino acid substitutions were generated using the QuickChange kit (Stratagene) and following the manufacturer's recommendations for mutagenic primer design. Mutations were confirmed by DNA sequencing along both strands, using primers specific for the T7 promoter and T7 terminator.

Purification of RIIβ

Chemically competent BL21 (DE3) *E. coli* cells were transformed with pET expression vectors encoding wild-type or mutant rat RIIβ. RIIβ protein expression and purification were conducted with the help of J.W. Kansy and S. Thakar (UT Southwestern Medical Center). Cells were grown in suspension cultures at 37 °C in LB media (1 L) until the OD_{600} reached 0.6-0.8 at which point 0.1 mg/ml isopropyl-β-D-thiogalactopyranoside (IPTG) was added. Cultures were grown either for two hours at 37 °C or overnight at RT at which point cells were harvested by centrifugation at 3000g 30 min 4 °C and washed with TBS. Pellets from 10,000*g* 15 min 4 °C spin were stored at –80 °C prior to lysis. Lysis was performed by freeze-thawing harvested samples and French press in 50 mM

NaH_2PO_4 buffer, pH 8.0, containing 300 mM NaCl and protease inhibitors. Crude lysates were cleared by centrifugation at 10,000*g* for 30 min 4 °C. Cleared lysates were incubated with a nickel-nitrilotriacetic acid-agarose resin (Qiagen) for one hour at 4 °C, followed by 5 washes in lysis buffer. Bound protein was eluted with a continuous gradient of 0–1.0 M imidazole in wash buffer. All forms of RIIβ eluted at approximately the same imidazole concentration (~100 mM). Samples were loaded into dialysis cassettes and dialyzed overnight in 10 mM Tris-HCl, pH 7.5, 1 mM DTT, through three changes of buffer (4 L each). Protein fractions were stored at –80°C following analysis for purity by SDS-PAGE and coomassie brilliant blue staining (CBB), yielding >80% purity of the final protein in peak fractions.

In vitro protein phosphorylation reactions

All *in vitro* protein phosphorylation reactions were performed at 30 °C in a final volume of at least 30 µl containing 10 µM substrate (unless otherwise specified), 100 µM ATP, and 0.2 mCi/ml [γ-^{32}P]ATP. The Cdk5 reaction solution included 30 mM MOPS, pH 7.2, and 5 mM $MgCl_2$. PKA reactions were conducted in 50 mM HEPES, pH 7.4, 1 mM EGTA, 10 mM magnesium acetate, and 0.03 mg/ml BSA. Time course reactions were performed by removing 10-µl aliquots from the reaction solution at various time points and adding an equal

volume of 5X SDS protein sample buffer to stop the reaction. Initial reaction rates were determined from the results of experiments performed in duplicate under empirically defined steady-state conditions. In all cases, stoichiometries and enzyme activities were assessed by SDS-PAGE and PhosphorImager analysis for [^{32}P]phosphate incorporation. To calculate reaction stoichiometries, radiolabeled products and radioactive reaction standards were quantified by densitometry using ImageQuant software (Amersham Biosciences).

In some studies, preparative phosphorylation of RIIβ by Cdk5 was followed by analysis in a subsequent PKA activity assay. For these experiments, phospho-RIIβ was not repurified from *in vitro* protein phosphorylation reaction mixtures. Rather, RIIβ was phosphorylated with Cdk5 for 60 min at 30 °C and frozen prior to subsequent dilution and use in PKA reactions. Reactions conducted with Cdk5 for these studies achieved final stoichiometries of 0.60 mol/mol. In some experiments, we tested the activity of PKA-RIIβ holoenzyme. In these reactions, the PKAcat (40 nM) holoenzyme was formed with recombinant RIIβ (0–160 nM) at 4 °C for 10 min. All reactions were conducted in a final concentration of 0.3 mg/ml BSA with recombinant 6xHis-tagged DARPP-32 (Bibb et al., 1999) (expressed and purified by C. Nguyen, UT Southwestern Medical Center) as substrate. PKA enzyme was first diluted with BSA buffer, followed by 1:1 dilution with RIIβ. This mixture was allowed to sit

at 4 for 10 min, at which point the enzyme was added to the reaction master stock and allowed to sit at 4 °Cc for 5 min. The reaction was then warmed at 30 °C for 60 sec and the ATP start solution was added. After 10 min, the reaction was stopped by removing 10 μl aliquots and adding PSB to stop the reaction.

In one experiment, the activation of PKAcat (10 nM) activity with cAMP (0–25 μM) was assessed in the presence of RIIβ (100 nM). In these experiments, PKA holoenzyme was formed as described above. PKA activity was determined in reactions with recombinant 6xHis-tagged inhibitor-1 (expressed and purified by C. Nguyen, UT Southwestern Medical Center) as substrate. Enzyme was added to the reaction mixture, allowed to sit for 8 min at 30 °C, and combined with ATP start solution. Reaction was stopped after 6 min with PSB.

Identification of Thr69 as site of Cdk5 dependent phosphorylation of RIIβ by tandem mass spectrometry

Phosphorylation of recombinant RIIβ and site identification was conducted using similar approaches to those previously described (Hayashi et al., 2006; Sahin et al., 2006). Preparation of phosphorylated RIIβ for site identification was conducted by S. Thakar (UT Southwestern Medical Center). Briefly, RIIβ from *in vitro* protein phosphorylation reaction mixtures with Cdk5 was subjected to SDS-PAGE and in-gel iodoacetamide acylation followed by

digestion with trypsin. Nano-liquid chromatography tandem mass spectrometry (nano-LC/MS/MS) was conducted on trypic digests directly. Dried digest mixtures were redissolved in trifluoroacetic acid (0.1% TFA) and loaded onto a ZipTip with C_{18} resin (Millipore) for purification. After being washed with 0.1% TFA three times, peptides were eluted directly into a nanoelectrospray needle (Proxeon Biosystems). MS analysis was performed on a QSTAR Pulsar I quadrupole time-of-flight tandem mass spectrometer (Applied Biosystems/MDS SCIEX) equipped with a nanoelectrospray ion source (MDS Proteomics, Odense, Denmark). For precursor ion scanning, the instrument was set in negative ion mode to detect the PO_3^- fragment ion at m/z –79. After data acquisition, the instrument was switched to positive ion mode, and the phosphopeptide sequence and site of phosphorylation were determined by nanoelectrospray-QSTAR Pulsar I quadrupole time-of-flight MS/MS. In the MS/MS scan mode, the precursor ion was selected in the quadrupole (Q1) and fragmented in the collision cell (q2), using argon as the collision gas. The protein sequences derived from MS/MS were used to search NCBI nonredundant mouse or mammalian protein databases for confirmation using computer software.

Generation of phosphorylation state-specific antibodies to Thr69 RIIβ

Polyclonal phosphorylation state-specific antibodies for phospho-Thr69 RIIβ were generated and affinity-purified as previously described (Czernik et al.,

1997a), using synthetic phosphopeptides encompassing the amino acid sequence surrounding Thr69 of rat RIIβ. Slight modifications were made to the protocol. Briefly, female, New Zealand White rabbits were immunized with RIIβ phosphopeptides encompassing phospho-Thr69. Antisera was collected from crude blood by centrifugation at 1,500*g* for 15min at 4 °C. Prior to purification, 10 mM NaF was added to the serum prior to loading on the phosphopeptide affinity column. Phosphorylation state-specific antibodies were purified from the resulting antisera using a SulfoLink resin (Pierce) conjugated to the corresponding phosphopeptide antigens. Column was washed with buffers containing 250 mM NaCl. Antibodies were eluted with 100 mM glycine, pH 2.5, quenched with 1.5 M Tris, pH 9.0, dialyzed into 10 mM MOPS, pH 7.5, 154 mM NaCl, stored at –20 °C. Purified antibodies were evaluated for specificity by immunoblot analysis of dephospho- and phospho- RIIβ standards (50 ng). Phospho-RIIβ was generated by preparative phosphorylation of RIIβ at Thr69 using active Cdk5/p25. As before, these reactions achieved a final stoichiometry of ~0.60 mol/mol at Thr69.

Transfection of HEK293T cells with wild-type and phosphomutant RIIβ

The RIIβ cDNA was subcloned into the pCMV-Tag vector (Stratagene) for eukaryotic expression. RIIβ subcloning and transfections were conducted with the help of E. Castro-Rivera and J.W. Kansy (UT Southwestern Medical

Center). HEK293T cells (provided by E. Nestler, UT Southwestern Medical Center), were cultured in Dulbecco's modified Eagle's medium containing 5% fetal bovine serum and 10% horse serum in 12-well plates. After 24 h, the culture medium was changed, and cells were transfected with 8 μg of DNA using LipofectAMINE in Optimem at 37 °C in a humidified 5% CO_2 incubator according to manufacturer's instructions (1:4 ratio of DNA:LipofectAMINE). Transfected cells were cultured for an additional 40–48 h before being harvested for analysis. Cells were collected in PBS and centrifuged and washed prior to lysis.

In vitro RIIβ binding to AKAP Ht31 peptide

All *in vitro* binding assays were conducted in TBS at 4 °C. The sequence of the Ht31 peptide was: DLIEEAASRIVDAVIEQVKAAGAY; the sequence of the Ht31P peptide was: DLIEEAASRPVDAVIEQVKAAGAY. Neutravidin-agarose gel (Pierce) was equilibrated in TBS, saturated with biotinylated Ht31 or Ht31P peptide for 1 h at 4 °C followed by extensive washing in cold TBS. Limiting amounts of RIIβ (2.5 nM) from preparative phosphorylation reactions were mixed with resin in 1 ml volume for 1h. Resin was pelleted at 2500*g* for 2 min, followed by extensive washing in TBS-T. Bound RIIβ was eluted from resin with 30ul 2xPSB. Samples were boiled, pelleted at 2500*g* for 2 min and resolved by SDS-PAGE. Samples were transferred to nitrocellulose and probed for total

RIIβ. Immunoblotting and quantitation were performed as described in Chapter Two.

Calpain-mediated cleavage of RIIβ

All *in vitro* calpain cleavage reactions were performed at 30 °C in a final volume of at least 60 μl containing substrate (0.05 mg/ml) in 40 mM HEPES, 1 mM CaCl, 5 mM DTT, pH 7.2. Calpain cleavage reactions were conducted by O. Adeyo (UT Southwestern Medical Center). Reactions were initiated by the addition of calpain 1 (0.08 units/ml, Sigma catalog # C6108). In separate experiments, 0.16 units/ml calpain 1 was used. Time course reactions were performed by removing 2.0-μl aliquots from the reaction solution at various time points and adding a volume of 10 μl of 2.5XSDS protein sample buffer to stop the reaction. Samples were resolved by SDS-PAGE, transferred to nitrocellulose, and probed for total RIIβ. Immunoblotting and quantitation were performed as described in Chapter Two.

Statistical analysis

Data were analyzed using statistical methods described in Chapters Two and Three. Data are reported as mean ± *SEM* for each measure. Each sample size is indicated. A value of $p \leq 0.05$ was considered statistically significant.

Results

Effect of forebrain loss of Cdk5 by CaMKII-Cre on cocaine-induced behavioral sensitization

In order to investigate the effect of loss of Cdk5 in the adult forebrain on locomotor responses to cocaine, we utilized transgenic CaMKII-Cre conditional Cdk5 knock-out mice as described in Chapter Two. Adult, fCdk5 mice, with or without CaMKII-Cre transgene were assessed for behavioral sensitization to repeated cocaine exposure (**Figure 4.1**). Following habituation to saline injections in the locomotor chambers, mice were injected with 15 mg/kg cocaine for 5 consecutive days and locomotor responses were recorded for 60 min (**Figure 4.1*A***). There was a main effect of treatment day on locomotor responses in the first 30 min after saline injection and 5 days of cocaine ($F(5,60) = 8.8$; $p < 0.0001$, two-way RM ANOVA) with both genotypes exhibiting progressive increases in locomotor activity over subsequent challenge days. These effects were observed on day 3 for both control mice (245.5 ± 77.8 vs. 41.5 ± 9.3 for saline) and Cdk5 cKO mice (512.0 ± 101.0 vs. 59.0 ± 9.8 for saline). Subsequent treatment days showed robust increased locomotor responses in both genotypes (**Figure 4.1*B***). Notably, there was a trend for increased stereotypic movements after 3 d of cocaine exposure in Cdk5 cKO mice (240.0 ± 41.2) compared to controls (137.2 ± 45.3; Student's *t*-test, $p = 0.1$). Two-way ANOVA revealed a trend for main effect of genotype ($F(1,60) = 2.6$; $p = 0.1$) and no interaction

between genotype and treatment day for locomotor responses ($F(5,60) = 1.6$; $p = 0.2$). However, there was a significant difference in the overall level of behavioral sensitization to repeated cocaine exposure. The level of locomotor responses achieved by Cdk5 cKO mice over the final three days of cocaine challenge was nearly twice that of control mice (522.1 ± 75.9 vs. 275.8 ± 38.1 for controls, $p = 0.01$; **Figure 4.1*C***). These data suggest that forebrain loss of Cdk5 results in enhanced behavioral sensitization to repeated cocaine exposure.

We repeated this experiment, where control and Cdk5 cKO mice were assessed for cocaine-induced locomotor sensitization to 20 mg/kg cocaine dose (**Figure 4.2**). As before, following habituation to saline injections, mice were injected with 20 mg/kg cocaine for 5 consecutive days and locomotor responses were recorded for 60 min (**Figure 4.2*A***). Again, there was a main effect of treatment day on locomotor responses in the first 30 min after saline injection and 5 days of 20 mg/kg cocaine ($F(5,105) = 36.9$; $p < 0.0001$, two-way RM ANOVA) with both genotypes exhibiting progressive increases in locomotor activity over subsequent challenge days. These effects were observed on day 2 for both control mice (692.1 ± 172.6 vs. 84.8 ± 21.8 for saline) and Cdk5 cKO mice (751.0 ± 213.7 vs. 85.8 ± 14.3 for saline). Subsequent treatment days showed robust increased locomotor responses in both genotypes (**Figure 4.2*B***). Notably, no differences in stereotypic movements after cocaine exposure were observed between control and Cdk5 cKO mice. Statistical analyses revealed no main effect

of genotype ($F(5,105) = 0.8$; $p = 0.4$) and no interaction between genotype and treatment day for locomotor responses ($F(5,105) = 0.9$; $p = 0.5$). There was a trend for an increase in the overall level of behavioral sensitization to repeated cocaine exposure achieved by Cdk5 cKO mice over the final three days of cocaine challenge (1416.8 ± 130.9 vs. 1097.3 ± 108.3 for controls, $p = 0.07$; **Figure 4.2*C***). As before, these data indicate that loss of Cdk5 enhances locomotor responses to repeated cocaine exposure.

Although only a trend, these data are in agreement with previous reports that inhibition of Cdk5 activity in the adult brain enhances the degree of behavioral sensitization to repeated cocaine exposure (Taylor et al., 2007). Notably, this trend is distinct from our previous data indicating that selective loss of Cdk5 in postsynaptic neurons of the NAc results in a leftward shift in the behavioral responses to repeated cocaine exposure, with no effect on the maximal response levels (see Chapter Two). These disparities may point to distinct roles for Cdk5 in the network response to repeated cocaine exposure, whereby Cdk5 activity in the postsynaptic compartment regulates sensitivity, and Cdk5 activity in the presynaptic compartment only (or combined pre-and postsynaptic compartments) regulates absolute level of responses to repeated cocaine. Further investigation will undoubtedly provide insight to these putative roles for Cdk5 in the various synaptic compartments.

Behavioral responses to D1-PKA signaling are altered in Cdk5 cKO mice

Dopamine receptor activation converges on cAMP dependent protein kinase (PKA) signal transduction machinery in the reward pathway. Since loss of Cdk5 in the adult animal was associated with elevated response to cocaine exposure, we investigated the behavioral responses of conditional Cdk5 knock-out mice to dopaminergic drugs exposure (**Figure 4.3**). Control and Cdk5 cKO mice were habituated to the locomotor activity chambers prior to injection with dopaminergic agents. In order to assess the response to D1-like receptor activation, animals were challenged with the D1 agonist SKF81297. No difference in locomotor or stereotypic responses were observed between control and Cdk5 cKO mice in the 60 min session prior to the first injection (data not shown). Injection of saline led to a transient increase in activity that was not different between control and Cdk5 cKO mice (**Figure 4.3*A***). However, the response to 1.0 mg/kg SKF81297 exposure was enhanced in Cdk5 cKO mice compared to controls (622.5 ± 60.6 vs. 366.8 ± 54.0 for controls, Student's *t*-test, $p = 0.01$). These data indicate that the behavioral output of the dopamine-D1 receptor signaling in the Cdk5 cKO mice was enhanced. Notably, no such difference was observed in locomotor response to a higher dose (3.0 mg/kg) of SKF81297 (**Figure 4.3*A***). This treatment led to a robust enhancement of locomotor counts in both control (798.8 ± 141.6) and Cdk5 cKO mice (909.1 ± 64.0). These findings suggest that there may be an altered sensitivity to the

locomotor-activating effects of dopamine D1 receptor signaling in Cdk5 cKO mice.

The treatment of mice with dopamine D2 receptor selective agonists are known to suppress locomotor responses. Therefore, we evaluated the effect of the D2 agonist quinpirole on the suppression of novelty-induced locomotor responses in control and Cdk5 cKO mice. For this experiment, animals were not habituated to locomotor activity chambers, and were exposed to the activity chambers for 10 min to observe novelty-induced locomotor activity. The locomotor activity or both control and Cdk5 cKO mice was high in the first exposure to the locomotor chambers (**Figure 4.3*B***). Following injection to 0.1 mg/kg quinpirole, animals were replaced in the locomotor activity chambers. There was a dramatic reduction in the locomotor responses of all mice to quinpirole exposure. Notably, the locomotor suppression was greater in control mice (72.3 ± 11.1) compared to Cdk5 cKO mice compared to controls (132.0 ± 27.5, Student's t-test, $p = 0.05$). This result was further evidenced in response to a higher dose of 0.3 mg/kg quinpirole (55.7 ± 22.1 for controls vs. 213.3 ± 44.9 for cKO, $p < 0.01$, **Figure 4.3*B***). These data indicate that loss of Cdk5 results in less responsiveness to dopamine D2-mediated signal transduction to suppress locomotor responses. In the Cdk5 cKO mice, D2 signaling is not as effective in the modulation of locomotor responses. Taken together, these data suggest that Cdk5 is an important modulator of the behavioral responses to dopaminergic signaling.

Biochemical responses to dopamine signaling are not altered in Cdk5 knock-out animals

We investigated the ability of dopaminergic agents to activate the PKA signaling machinery in striatal slices from control and Cdk5 cKO mice. In order to evaluate the ability of dopaminergic activation of this pathway in the absence of Cdk5, striatal slices from conditional knock-out mice were treated with D1 and D2 specific agonists, either separately or in conjunction. The treatment of slices with SKF81297 (1 μM, 5 min) from both control and Cdk5 cKO taken from the dorsal striatum caused a robust increase in PKA-mediated phosphorylation of Ser845 GluR1 in (**Figure 4.4*A***). Notably, there was an increase in the basal level of pSer845 GluR1 in Cdk5 cKO samples (162.1 ± 22.9% of littermate control, $p < 0.05$). The increase in PKA-mediated phosphorylation of Ser845 GluR1 was not altered in Cdk5 cKO mice. The treatment with quinpirole (1 μM, 5 min) caused no change in the level of pSer845 GluR1 in either genotype (**Figure 4.4*A***). The combination of SKF and quinpirole was in distinguishable from treatment with SKF alone on phosphorylation of GluR1 in either genotype. These data indicated that loss of Cdk5 does not alter dopamine signaling through D1 or D2 receptors in the regulation of PKA-mediated phosphorylation of GluR1. Also, treatment with D2 agonist does not alter the phosphorylation of Ser845 GluR1 by the D1 agonist, consistent with previous reports (Snyder et al., 2000).

These experiments were repeated for striatal slices taken from the nucleus accumbens of control and Cdk5 cKO mice. Unlike in the dorsal striatum, there was no effect in the basal level of pSer845 GluR1 in nucleus accumbens from control and Cdk5 cKO mice. Again, treatment with SKF81297 (1 μM, 5 min) induced robust phosphorylation of GluR1 in both genotypes, while quinpirole was without effect (**Figure 4.4*A***). However, co-application of quinpirole reduced SKF-induced increase in GluR1 phosphorylation in both genotypes (**Figure 4.4*A***). These results indicate that loss of Cdk5 does not alter dopamine signaling to GluR1 phosphorylation. However, these data provide new insight into the distinct effect of co-application of D1 and D2 receptor agonists in dorsal striatum versus nucleus accumbens. Co-application of D1 and D2 yielded different results in slices from the dorsal striatum versus ventral striatum. In the dorsal striatum, the addition of D2 did not affect the D1-mediated increase in pSer845 GluR1 in whether control or Cdk5 cKO slices. However, D2 significantly reduced the D1-mediated increase in pSer845 GluR1 in slices from the nucleus accumbens. These data indicate that the efficacy of D1 and D2 like dopamine receptors act in distinct combinatorial pathways in the various striatal nuclei. However, loss of Cdk5 did not alter the responses observed to any of the dopaminergic treatments conducted.

In order to determine whether cocaine exposure alters PKA-mediated signaling in striatal tissue, Cdk5 and cKO mice were administered cocaine (15

mg/kg for 1, 3, 10 consecutive days) and pSer845 GluR1 was assessed. In these experiments, animals were exposed to cocaine under similar conditions as in the behavioral sensitization experiment (see above). The administration of cocaine caused a robust increase in pSer845 GluR1 levels in the dorsal striatum of control mice 30 min after the last injection of a 10 d exposure regimen (Numbers compared to saline (**Figure 4.4*B***). No difference was seen in the level GluR1 phosphorylation after 1 or 3 days of cocaine in control mice. Notably, there was no effect of cocaine on pSer845 GluR1 levels in Cdk5 cKO dorsal striatum samples at any time point (**Figure 4.4*B***). However, there was a marked increase in the level of pSer845 GluR1 after one exposure to cocaine in samples from nucleus accumbens in Cdk5 cKO mice (1.6 ± 0.2 for Coc1 vs. 1.0 ± 0.02 for saline, $p < 0.05$) that was not present in control mice (1.2 ± 0.1 for Coc1 vs. 1.0 ± 0.1 for saline in controls, **Figure 4.4*B***). Neither genotype showed any significant effect of repeated cocaine exposure on GluR1 phosphorylation in nucleus accumbens samples. These data indicate that repeated cocaine alters the level of pSer845 GluR1 in the dorsal striatum, but not nucleus accumbens of wild-type mice. Furthermore, the regulation of chronic cocaine exposure on phosho-GluR1 levels in dorsal striatum is absent in Cdk5 cKO mice. Interestingly, acute cocaine exposure caused an increase in pSer845 GluR1 in nucleus accumbens from Cdk5 cKO mice. These findings may be functionally related to the behavioral responses to dopaminergics in Cdk5 cKO mice.

Cdk5 inhibition activates PKA signaling in striatal tissue

Cdk5 has been shown to regulate PKA through the phosphorylation of Thr75 DARPP-32 in striatal tissue (Bibb et al., 1999). To determine if Cdk5 phosphorylation of DARPP-32 was the sole mechanism by which Cdk5 regulates PKA, we assessed the effect of Cdk5 inhibition on PKA activity in striatal slices of Thr75Ala DARPP-32 (T75A-D32) mutant mice (Svenningsson et al., 2003). Treatment of wild-type slices with roscovitine caused a dose-dependent increase in phosphorylation of Ser845 GluR1 and Thr34 DARPP-32 (**Figure 4.5*A,C***). Surprisingly, roscovitine treatment caused the same effect on Ser845 GluR1 phosphorylation T75A-D32 mice (**Figure 4.5*B,C***). These data indicate that the effect of Cdk5 inhibition on the activation of PKA-mediated phosphorylation of target synaptic substrates is not dependent only on Cdk5 phosphorylation of Thr75 DARPP-32. However, there was a significant increase in the effect of 50 μM roscovitine on Thr34 DARPP-32 phosphorylation in Thr75A-D32 slices (**Figure 4.5*D***). Roscovitine treatment also caused a dose-dependent decrease in Thr75 DARPP-32 levels in wild-type slices (**Figure 4.5*A***). As expected, there were no detectable levels of phospho-Thr75 DARPP-32 in slices from Thr75A D32 mice. These data may indicate that the loss of intramolecular regulation of phosphorylation of DARPP-32 may be important to determining its ability to serve as a substrate for PKA. Indeed, there were significantly reduced basal

levels of Thr34 DARPP-32 in T75A-D32 mice compared to controls (49.9 ± 7.0% compared to controls 100 ± 20.6%, p = 0.05, Student's *t*-test). Nonetheless, these data indicate that the relationship between Cdk5 inhibition and the activation of PKA signaling may not be mediated exclusively by the PKA-D32-PP1 pathway.

RIIβ and Cdk5 are colocalized in striatal neurons

Cdk5 regulates PKA through the phosphorylation of DARPP-32 (Bibb 1999). Since regulation of PKA activity has been implicated in cocaine reward and instrumental responding for reward (Lynch and Taylor, 2005), we searched for candidate Cdk5 substrates within the PKA signaling pathway that may explain the mechanism by which conditional loss of Cdk5 exerts its effects on cocaine reward and behavior. PKA exists as a R_2C_2 tetramer. PKA-RIIβ is the principle form of PKA within neurons, particularly within striatal and cortical tissue (Ventra et al., 1996). In order to investigate the localization of Cdk5 and RIIβ in striatal neurons, we conducted immunocytochemistry on striatal neurons. After 14 DIV, rat striatal neurons were stained for Cdk5 and RIIβ to assess the distribution of each (**Figure 4.6*A***). Cdk5 localized to cytosolic, nuclear, and perinuclear regions of the mature striatal neurons. RIIβ labeled the processes and perinuclear regions of the neurons robustly, while there was a markedly decreased labeling of RIIβ in the nucleus. The overlay of Cdk5 and RIIβ staining

demonstrates pronounced colocalization throughout the processes of the dendrites as well as the perinuclear area (**Figure 4.6*A***). These data indicate that Cdk5 and RIIβ are found in the same compartments of striatal neurons.

In order to further investigate the localization of Cdk5 and RIIβ, we conducted subcellular fractionation experiments in striatal samples from the dorsal striatum and nucleus accumbens of wild-type mice. Membrane pellet (P2) and soluble (S2) fractions were immunoblotted for various proteins (**Figure 4.6*B***). While there was modest enrichment in P2 levels of AKAP150 compared to the soluble fraction, there was robust distinction in the distribution of synaptic marker, PSD-95 (**Figure 4.6*B***). These data provide evidence for effective fractionation in the striatal lysates. RIIβ is distributed evenly between P2 and S2 fractions, with a slight enrichment in soluble levels in nucleus accumbens compared to the insoluble fraction. Likewise, the catalytic subunit of PKA is also distributed in both compartments, with some enrichment in the soluble fraction. Cdk5 is almost exclusively detected in the soluble fraction of both dorsal striatum and nucleus accumbens. These data indicate that Cdk5 and RIIβ are colocalized in the soluble fraction of striatal lysates.

Cdk5 phosphorylates PKA regulatory subunit IIβ

In order to explore the direct regulation of the PKA holoenzyme by Cdk5, we tested PKA catalytic and regulatory subunits as substrates for Cdk5 *in vitro*.

While PKA catalytic subunit was not a substrate for Cdk5 (data not shown), the regulatory subunit RIIβ did serve as an efficient substrate *in vitro* (**Figure 4.7*A***). The phosphorylation of RIIβ by Cdk5/p25 yielded time-dependent incorporation of ^{32}P, reaching a final stoichiometry of approximately 0.60 mol/mol at 90 min. Subsequent reactions with RIIβ and Cdk5/p25 conducted for up to 3 h *in vitro* failed to reach final stoichiometry greater than 60-70%. Incubation of RIIβ with Cdk5/p25 did lead to a time-dependent mobility shift of RIIβ. Notably, phosphorylation of RIIβ resulted in altered migration in SDS-PAGE, whereby all the incorporated ^{32}P was present in the slower-migrating form of the protein (**Figure 4.7*A***). No such mobility shift was observed if RIIβ was incubated with Cdk5/p25 in the absence of ATP (data not shown). Although the RIIβ primary amino acid sequence contains three candidate proline-directed serine/threonine residues for Cdk5-dependent phosphorylation, there is only with the correct consensus sequence ([S/T]PX[K,H,R]) at Thr69. In order to determine the site of phosphorylation, mass spectrometry was conducted on tryptic digests of preparatively phosphorylated RIIβ material in the absence of ^{32}P-ATP. LC tandem mass spectrometry analysis yielded one phosphopeptide encompassing amino acids 57-72 of the primary RIIβ sequence, suggesting Thr69 as the site of phosphorylation (**Figure 4.7*B***). The presence of the dephospho-peptide precursor ion at 702.3 m/z in the sample allowed the identification of the y-ions for the

phosphopeptide. The phosphopeptide at 742.3 m/z corresponded to the incorporation of one phosphate moiety into the precursor peptide. We confirmed Thr69 as the sole site of Cdk5 dependent phosphorylation using site-directed mutagenesis. The use of a Thr69Ala (T69A) phosphomutant RIIβ protein was not a substrate for Cdk5 *in vitro* (**Figure 4.7*C***), while wild-type RIIβ in parallel reactions was phosphorylated very efficiently. As further confirmation, the Thr69Ala phosphomutant did not display the mobility shift seen in wild-type RIIβ following incubation with Cdk5, suggesting that Cdk5 dependent phosphorylation of RIIβ at Thr69 is responsible for the electrophoretic mobility shift seen in SDS-PAGE. Furthermore, phosphomimetic mutation of Thr69 to Glu or Asp (T69D and T69E, respectively) displayed a similar, retarded electrophoretic mobility shift relative to wild-type RIIβ (data not shown). These data indicate that the PKA regulatory subunit RIIβ is efficiently phosphorylated at Thr69 by Cdk5/p25 *in vitro*. Taken with the previous findings, these data implicate a role for Cdk5-dependent phosphorylation of RIIβ in the function or PKA-RIIβ.

Generation of phosphorylation state-specific antisera to Thr69 RIIβ

The use of specific antibodies to phosphorylation-sites have been widely utilized to study the *in vivo* relevance of phosphorylation sites identified *in vitro*. In order to study Cdk5 phosphorylation of RIIβ in brain tissue, we raised

phosphorylation specific antisera against Thr69 RIIβ (**Figure 4.8**). The site of Cdk5 dependent phosphorylation of RIIβ is situated between the well-characterized N-terminal dimerization/docking domain and the C-terminal tandem cAMP binding cassettes (**Figure 4.8*A***). We generated antibodies selective for pThr69 RIIβ, in order to study this modification in intact brain tissue. Rabbits were immunized with synthetic phopshopeptides mimicking the local region surrounding Thr69 of RIIβ and state-specific antisera was purified by affinity chromatography. The resulting antisera was used to detect preparatively phosphorylated RIIβ from *in vitro* reactions with Cdk5. This antisera displayed striking selectivity for the phosphorylated form of RIIβ (**Figure 4.8*B***). Furthermore, the antisera was highly selective for RIIβ, as there was complete loss of detection from striatal samples from RIIβ knock-out mice (**Figure 4.8*C***). Taken together, these data demonstrate the successful generation of phosphorylation state specific antisera to pThr69 RIIβ. The antibodies detected pThr69 RIIβ in various brain regions from wild-type mice (**Figure 4.8*D***). These data indicate that RIIβ is phosphorylated at Thr69 in intact brain tissue. Notably, striatal lysates from Cdk5 cKO mice demonstrated a robust reduction in levels of pThr69 RIIβ compared to controls (55.1 ± 5.1% compared to controls 100 ± 12.5%, $p < 0.05$, Student's *t*-test, **Figure 4.8*E***). Indeed, conditional loss of Cdk5 in the striatum has also been shown to alter the phosphorylation of other Cdk5

targets in this tissue (see Chapter Two). Furthermore, the level of pThr69 RIIβ is highest in striatal tissue, matching closely to the absolute expression level of RIIβ in this tissue (**Figure 4.8F**). Taken together, these that Cdk5 phosphorylates Thr69 of RIIβ in the brain.

Phosphorylation of RIIβ is stable to inhibition of Cdk5 in striatal tissue

The use of pharmacological inhibitors to regulate Cdk5 has been widely employed. To determine if Cdk5 phosphorylation of RIIβ, we assessed the effect of Cdk5 inhibition by Indolinone A (IndoA) on pThr69 RIIβ levels in striatal slices. Treatment of wild-type slices with IndoA (0–5000 nM, 60 min) caused a dose-dependent decrease in pThr75 DARPP-32, but no alteration in pThr69 RIIβ level (**Figure 4.9*A***). Notably, treatment of slices with the inactive analog Indolinone B (IndoB, 5000 nM, 60 min) caused no change in pThr75 DARPP-32 levels. In time course experiments, the application of IndoA (5000 nM) caused a time-dependent decrease in pThr75 DARPP-32, but was without effect on Thr69 RIIβ levels (**Figure 4.9*B***). These data indicate that acute inhibition of Cdk5 activity is not sufficient to alter Cdk5 dependent phosphorylation of RIIβ in striatal tissue.

Recent studies have implicated novel pathways by which NMDA regulates Cdk5 signaling (Nguyen et al., 2007). In order to test this possibility,

striatal slices were treated with NMDA (25 or 50 μM, 5 min) to exam in the level of pThr69 RIIβ. NMDA treatment did not alter RIIβ phosphorylation, but caused a dose-dependent decrease in pThr75 DARPP-32 as expected (**Figure 4.9*C***). These data indicate that NMDA-mediated regulation of Cdk5 signaling does not regulate the level of pThr69 RIIβ in striatal cells.

RIIβ is phosphorylated in transfected HEK293T cells and pThr69 RIIβ is soluble

In order to study the localization of Cdk5 dependent phosphorylation of RIIβ *in vivo*, HEK293T cells were transfected with expression plasmids containing RIIβ. Notably, Cdk5 is expressed and activity has been reported in HEK293 cells (Li et al., 2000). Transfection of both wild-type RIIβ and the T69A phosphomutant plasmids led to robust overexpression of RIIβ over endogenous levels in mock transfected HEK293T cell lysates (**Figure 4.11*A***). There was virtually no detection of endogenous pThr69 RIIβ in mock transfected HEK293T cell lysates (**Figure 4.11*A***). Phosphorylation of RIIβ at Thr69 could be detected in lysates from cells transfected with the wild-type RIIβ plasmid, but not so with transfection of the Thr69Ala mutant RIIβ (**Figure 4.11*A***). These data indicate that Cdk5 is able to phosphorylate RIIβ in cells and further confirms the specificity of Thr69 as the site of phosphorylation. These data also indicate that endogenous Cdk5 activity towards RIIβ in HEK293T may be tightly regulated

and difficult to observe. For this reason, wild-type RIIβ was transfected into HEK293T cells in order to determine the localization of pThr69 RIIβ.

HEK293T cell lysates from transfected cells were subjected to differential centrifugation to separate the lysate in subcellular fractions (**Figure 4.11*B***). The use of GAPDH confirmed the generation of membrane (P2) and soluble (S2) fractions, as it was almost exclusively present in the soluble fraction. The detection of pThr69 RIIβ was restricted to the soluble (S2) fraction in transfected lysates, while total RIIβ was detected at comparable levels in all fractions tested from cells transfected with the wild-type RIIβ plasmid (**Figure 4.11*B***). These data indicate that Cdk5-dependent phosphorylation of RIIβ in HEK293T cells is associated with the soluble, cytosolic cellular compartments.

In order to study the distribution of pThr69 RIIβ in neurons, striatal lysates from the nucleus accumbens were fractionated and analyzed using similar approaches. As with the HEK293T cell lysates, subcellular fractionation of striatal lysates from mice indicated that Thr69 RIIβ was also more prevalent in the soluble fraction compared to the pellet (**Figure 4.11*C***). As before, RIIβ was detected in both pellet and soluble fractions, as was the catalytic subunit of PKA. As with RIIβ, catalytic PKA is more enriched in the soluble fraction of these preparations from striatal lysates. These data indicate that Cdk5 dependent phosphorylation of RIIβ is localized in the soluble fraction of cellular lysates.

These findings may have important functional consequences in the regulation of cAMP-PKA signaling by Cdk5.

Evaluation of functional effect of phosphorylation of T69 RIIβ on PKA

RIIβ complexes into heterotetrameric R_2C_2 structures with catalytic PKA in cells. PKA regulatory subunits mediate inhibition of catalytic subunits, cAMP binding, and subcellular localization through interaction with anchoring proteins. To investigate the function of pThr69 RIIβ, we conducted *in vitro* biochemical reactions to assess PKA inhibition and cAMP responsiveness (**Figure 4.12**). RIIβ is known to serve as a competitive inhibitor of PKA activity *in vitro*. Steady-state PKA enzymatic activity towards a control substrate was assessed in the presence of various amounts of RIIβ. As expected, incubation of catalytic PKA with RIIβ led to a dose-dependent decrease in PKA activity (**Figure 4.12*A***). RIIβ preparatively phosphorylated at Thr69 with Cdk5/p25 also caused a dose-dependent decrease in catalytic PKA activity indistinguishable from that of dephospho-RIIβ. These data indicate that pThr69 has no effect on RIIβ binding to catalytic PKA or inhibition of its activity. In order to study the responsiveness of RIIβ to cAMP, catalytic PKA-RIIβ holoenzyme was formed *in vitro* and assessed for activity in the presence of various amounts of cAMP (**Figure 4.12*B***). The addition of cAMP to PKA-RIIβ led to dose-dependent increase in PKA

activity, due to the release of catalytic PKA from the PKA-RIIβ complex. Use of the phosphomimetic T69D RIIβ in the holoenzyme preparation resulted in an identical cAMP activation curve to that of dephospho-RIIβ. These data reproduce the previously reported k_{act} of cAMP for the PKA-RIIβ holoenzyme of ~350 μM (Cummings et al., 1996). These data indicate that the Cdk5-dependent phosphorylation of RIIβ has no effect on the activation of the PKA-RIIβ complex by cAMP.

AKAPs regulate cAMP signaling through the coordination and scaffolding of various proteins in the PKA pathway. The use of Ht31, a peptide modeled after an AKAP RII-binding motif, has allowed the functional significance of RII-AKAP interactions to be tested in neurons (Cantrell et al., 1999). We utilized this peptide to determine if Cdk5-dependent phosphorylation of Thr69 RIIβ had any effect on the ability for the molecule to bind to the AKAP motif. The use of a biotinylated-Ht31 peptide allowed the molecule to be immobilized on agarose-resin. The resulting beads were incubated with excess RIIβ, either mock or preparatively phosphorylated with Cdk5, and washed. The use of a mutant peptide sequence, Ht31P, allowed the background binding of RIIβ to the resin to be discerned. There was notable binding of the RIIβ to the agarose-resin alone (data not shown); however, the binding of RIIβ to the resin was increased in the presence of the Ht31 peptide, but decreased in the presence of the Ht31P peptide

(**Figure 4.13**). The binding of pThr69 RIIβ to the active Ht31 peptide was double that of dephospho RIIβ. This is in contrast to no significant difference in the binding of pThr69 to Ht31P compared to dephospho RIIβ binding to the inactive Ht31P peptide. These data indicate that Cdk5-dependent phosphorylation of RIIβ may increase the association of RIIβ with AKAP complexes. Taken together with the subcellular fractionation data, these findings may indicate a selective targeting of pThr69 RIIβ to soluble AKAP complexes within striatal neurons. These data may have important implications in the regulation of the spatiotemporal aspects of cAMP-PKA signaling.

Phosphorylation of Thr69 RIIβ enhances calpain-dependent cleavage in vitro

RIIβ is known to be subject to cleavage by μ-calpain *in vitro* (Alexa et al., 1996). To assess the role for Cdk5-dependent phosphorylation of Thr69 of RIIβ, *in vitro* calpain cleavage assays were conducted in the presence of wild-type RIIβ phosphorylated or mock phosphorylated with Cdk5/p25 (**Figure 4.13**). Incubation of RIIβ with Cdk5 led to the anticipated shift in mobility and final stoichiometry of ~60%. Cleavage of RIIβ by calpain *in vitro* proceeded in a time-dependent manner, reaching nearly 80% complete 15 min (data not shown). This cleavage of RIIβ was significantly enhanced towards the preparatively phosphorylated material. The rate of the RIIβ degradation was nearly twice as

fast in the cleavage of pThr69 RIIβ compared to dephospho RIIβ (**Figure 4.13**). We have previously reported that Cdk5 mediates the activation of calpain-mediated degradation of synaptic proteins (Hawasli et al., 2007). In order to rule out a possible contribution of Cdk5 to the reaction, we conducted parallel experiments in which Cdk5 was added to the reaction in the absence of ATP or excluded altogether. The presence of Cdk5 in the calpain cleavage reaction under these experimental conditions did not affect the rate of RIIβ degradation by calpain. The facilitated degradation of pThr69 RIIβ was evidenced by the fact that RIIβ incubated with Cdk5 in the absence of ATP showed indistinguishable cleavage rate as RIIβ alone. Furthermore, the use of phosphomimetic mutants at the Thr69 site (T69D) also displayed enhanced cleavage by calpain compared to WT-RIIβ (data not shown). These data may indicate that T69D is an appropriate phosphomimetic for the functional consequences of Cdk5-dependent phosphorylation of Thr69 of RIIβ. Furthermore, these data indicate that Cdk5-dependent phosphorylation of RIIβ enhances calpain-mediated cleavage of the protein. These findings may be important for the regulation of the turnover of the PKA signaling machinery activated by cAMP.

Evaluation of regulation of pThr69and total RIIβ levels calpain activation in striatal slices

To assess the relevance of phosphorylation of RIIβ to cleavage *in vivo*, we treated striatal slices from wild-type mice with NMDA to activate endogenous calpain. Pretreatment of striatal slices with the calpain inhibitor calpeptin (20 μM, 30 min) caused no effect on pThr69 RIIβ or total RIIβ levels (**Figure 4.14**). The incubation of slices with NMDA (100 μM, 30 min) induced excitotoxic activation of calpain, as evidenced by the robust increase in the generation of the proteolytic cleavage fragment p25 (**Figure 4.14**). However, there was no discernible change in the level of pThr69 RIIβ or total RIIβ levels. Finally, the calpain-dependence of the effect of NMDA on p25 generation was confirmed by the pretreatment and co-application of calpeptin with NMDA. The NMDA-induced generation of p25 was completed blocked by calpeptin (**Figure 4.14**). Notably, this treatment did not alter RIIβ level or phosphorylation. These results indicate that NMDA-induced activation of calpain in striatal slices does not regulate RIIβ degradation. These findings are in conflict with the observations made *in vitro*. However, there are numerous reasons why the regulation observed *in vitro* is obscured *in vivo*, including calpain abundance, subcellular localization of RIIβ and calpain, Ca^{2+} level, etc. Future investigations will provide insight into the physiological relevance of the enhanced calpain cleavage of pThr69 RIIβ.

Electrophysiological responses to dopamine are altered in Cdk5 cKO mice

Dopamine receptors govern the signaling of PKA in striatal neurons and contribute to the state of excitability of these normally hyperpolarized cells. We previously reported that conditional loss of Cdk5 from striatal neurons led to enhance excitability of NAc neurons (see Chapter Two). In the current study, we utilized similar approaches to discern the effect of dopamine receptor activation on excitability of striatal neurons from Cdk5 cKO mice. Whole-cell current clamp recordings of MSNs in NAc slices from control and CaMKII Cdk5 cKO mice were performed. Current injections were adjusted to elicit equal numbers of spikes in both genotypes under baseline conditions. As shown in **Figure 4.15*A***, the addition of dopamine (100 μM) to the slices led to a dramatic increase in firing rate in NAc slices from control animals (62.5 ± 5.4% compared to baseline in controls, n = 5). However, the effect of dopamine on excitability was significantly attenuated in cells from Cdk5 cKO mice (18.4 ± 3.2% compared to baseline, n = 7). These data indicate that the actions of dopamine on striatal excitability are altered in the cells deficient in Cdk5. In order to further investigate the mechanism of these alterations, we utilized specific dopamine D1 and D2 receptor agonists. The addition of the D1 agonist SKF81297 (20uM) reliably induced an increase in spike number in control slices (40.4 ± 5.4% increase from baseline, n = 6) but had a significantly reduced effect on the firing

rate of MSNs from Cdk5 cKO (17.8 ± 1.4% increase, n = 5, **Figure 4.15*B***). The addition of the D2 agonist quinpirole (20uM) had almost no effect on spike number in either NAc MSNs from control mice (7.8 ± 4.5% increase from baseline, n = 4) or Cdk5 cKO mice (4.8 ± 4.8%, n = 3). These data indicate that the dopamine-dependent modulation of neuronal excitability is mediated by dopamine D1-like receptors in the NAc. Furthermore, this effect of dopamine is disrupted in Cdk5 cKO mice. These findings may be functionally related to the behavioral alterations observed in responses to dopaminergics in Cdk5 cKO mice.

Discussion

Conditional loss of Cdk5 in mice led to dysregulation of PKA signaling in striatal tissue. Basal PKA-dependent phosphorylation of Ser845 of GluR1 subunit of the AMPA receptor was elevated in these animals. Furthermore, the ability of dopamine to enhance striatal neuron excitability was significantly decreased in Cdk5 cKO cells. These data suggest that Cdk5 serves as a crucial component of normal signal transduction from D1-like receptors to cellular targets. Finally, behavioral responses to D1 and D2 specific agonists were altered in Cdk5 cKO mice compared to controls. The administration of D1 agonist induced a significantly enhanced locomotor response in Cdk5 cKO mice. Given the profound effects Cdk5 loss had on these various parameters, we sought to

identify new targets in the PKA signaling pathway that may be important in Cdk5-mediated modulation of dopamine signaling in the striatum.

We found that Cdk5 regulates PKA signaling by DARPP-32 independent mechanisms. We identified PKA regulatory subunit RIIβ as a direct substrate for Cdk5-dependent phosphorylation. We have provided direct physical identification of Thr69 as the site of Cdk5-dependent phosphorylation of RIIβ. Phosphorylation state-specific antisera to pThr69 RIIβ was raised to investigate this modification in brain tissue. The functional role for Cdk5-dependent phosphorylation may be to enhance calpain-mediated cleavage of RIIβ, as evidenced from *in vitro* calpain activity assays. No effect of pThr69 RIIβ was found for cAMP binding, or PKA inhibition. A previous report suggested that phosphorylation of PKA regulatory subunit RIIβ by cyclin B/p34^{cdc2} occurs at Thr69 (Keryer et al., 1993). Cdk5 and cdc2 have the same consensus phosphorylation sequence ([S/T]PX[K,H,R]). As cdc2 is not active in postmitotic neurons, it is likely that Cdk5 is the predominant kinase that regulates phosphorylation of this site *in vivo* in neurons. Previous work implicated phosphorylation of Thr69 RIIβ to enhance RIIβ-binding to the AKAP, MAP2 (Keryer et al., 1993). In the present study, we find that phosphorylation by Cdk5 leads to enhanced association with an AKAP derived peptide sequence *in vitro*.

Further analysis will reveal the relevance of these findings towards cellular function and protein complex formation or stability.

Dopamine receptor activation converges on cAMP dependent protein kinase (PKA) signal transduction. Dopamine signaling in the reward pathway, including the striatum, is a key means of cAMP signal generation in this circuit. We studied the abundance of pThr69 RIIβ in brain regions in order to investigate the potential role for this phosphorylation in the regulation of cAMP signaling. In order to compare the abundance of pThr69 RIIβ phosphorylation *in vivo*, brain tissue lysates were examined to estimate the relative level of phosphorylation in the tissue (**Figure 4.8*F*).** It is important to note that the absolute level of RIIβ differs across these tissues as well. It appears as though the striatum is the most highly-enriched tissue for RIIβ and contains the highest stoichiometry of phosphorylation of pThr69 RIIβ.

Striatal slices from Cdk5 knock-out mice also showed enhanced levels of phosphorylation of the PKA site, pSer845, of the GluR1 subunit (**Figure 4.4*A***). These data may indicate that the reduction of pThr69 RIIβ may be functionally linked to the steady-state PKA-dependent phosphorylation of synaptic substrates. Indeed, we have shown that inhibition of Cdk5 with roscovitine causes a dramatic increase in the PKA-mediated phosphorylation of pSer845 GluR1. However, the level of pThr69 is resistant to regulation by inhibition of Cdk5 activity in striatal

slices (**Figure 4.9**). These findings from Cdk5 knock-out and pharmacological inhibition studies may appear to be in conflict. However, it may be possible that the regulation of phosphorylation of RIIβ by Cdk5 occurs over a longer time course, such that acute inhibition is not adequate to alter the basal state of pThr69 RIIβ levels. Notably, long-standing loss of Cdk5 activity in the conditional knock-out model produces a dramatic reduction in the level of pThr69 RIIβ, consistent with the observation that Cdk5 targets this site *in vivo*. Overall, the findings presented in this chapter demonstrate that conditional knockout of Cdk5 has robust effects on behavior, physiology, and dopamine signaling. How phosphorylation of RIIβ regulates these changes has yet to be determined, but promises to be a rich area for future investigation.

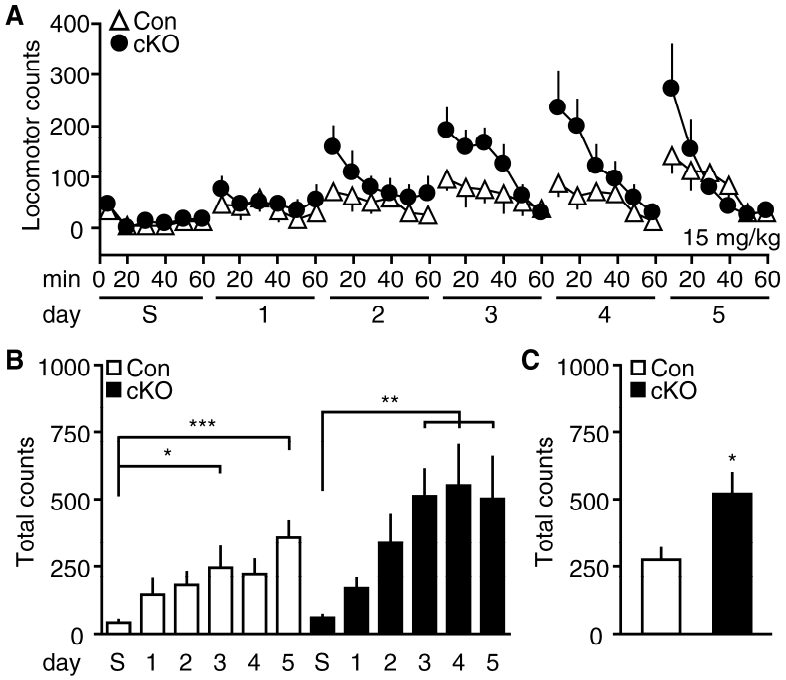

Figure 4.1. Effect of Cdk5 cKO on behavioral sensitization to repeated 15 mg/kg cocaine exposure. **A**, Locomotor activity in response to saline injection (S), followed by repeated 15 mg/kg cocaine injection over 5 consecutive days (1–5). Mean locomotor counts (± *SEM*) in 10 min bins for 60 min immediately following injection for each day are shown for control (Con) vs. Cdk5 cKO groups. **B**, Locomotor data for the first 30 min following injection are summarized in histograms (*$p < 0.05$, **$p < 0.01$, ***$p < 0.0001$ compared to saline, post hoc Tukey, n = 6–8 per group). **C**, Mean locomotor counts to final 3 days of 15 mg/kg cocaine (3–5) in control (Con) and Cdk5 cKO mice (*$p < 0.05$ compared to saline, Student's *t*-test, n = 6–8 per group).

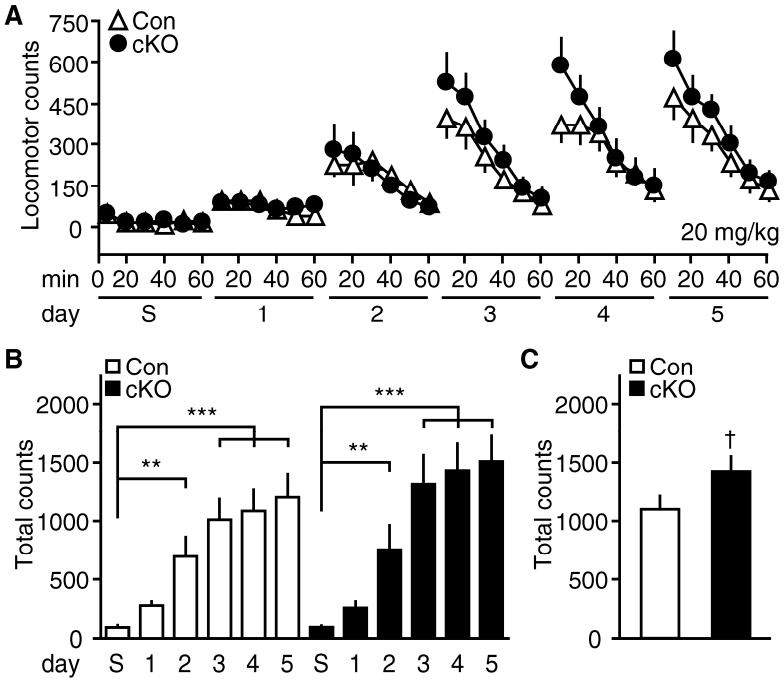

Figure 4.2. Effect of Cd5k cKO on behavioral sensitization to repeated 20 mg/kg cocaine exposure. **A**, Locomotor activity in response to saline injection (S), followed by repeated 20 mg/kg cocaine injection over 5 consecutive days (1–5). Mean locomotor counts (± *SEM*) in 10 min bins for 60 min immediately following injection for each day are shown for control (Con) vs. Cdk5 cKO groups. **B**, Locomotor data for the first 30 min following injection are summarized in histograms (**$p < 0.01$, ***$p < 0.0001$ compared to saline, post hoc Tukey, n = 11–12 per group). **C**, Mean locomotor counts to final 3 days of 20 mg/kg cocaine (3–5) in control (Con) and Cdk5 cKO mice (†$p = 0.07$ compared to saline, Student's *t*-test, n = 11–12 per group).

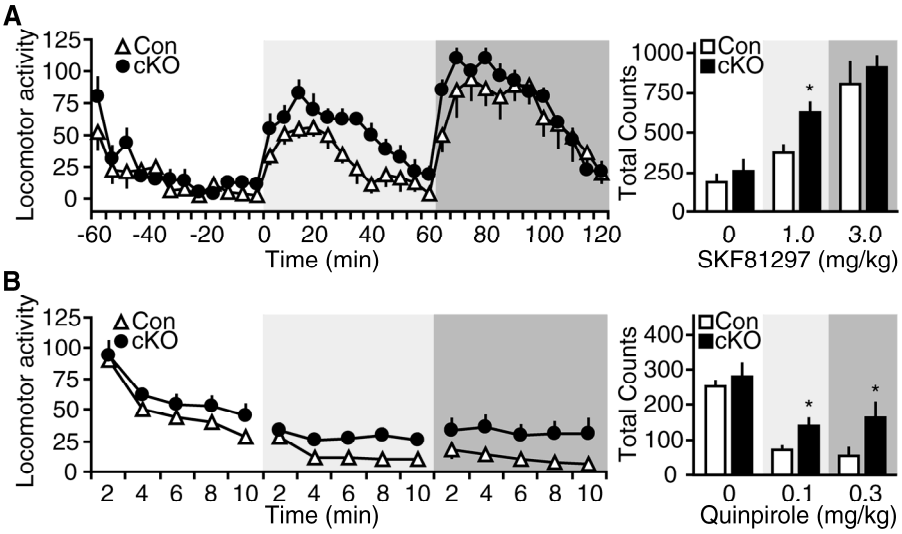

Figure 4.3. Behavioral responses of Cdk5 cKO mice to dopaminergic drug exposure. **A**, Locomotor activity of control and Cdk5 cKO mice following saline (white background), 1.0 mg/kg SKF81297 (light grey background), and 3.0 mg/kg SKF81297 (dark grey background). Cumulative counts for each 60 min session are shown in bar graph at right (*$p < 0.05$, Student's *t*-test, n = 6 per group). **B**, Locomotor activity in Cdk5 cKO mice following administration of quinpirole. The graph depicts mean locomotor counts in 2 min bins 30 min after exposure to saline (white background), 0.1 mg/kg quinpirole (light grey background), or 0.3 mg/kg (dark grey background). The total locomotor counts for each 10 min session are displayed in bar graph at right (*$p < 0.05$, Student's *t*-test, n = 5–7 per group).

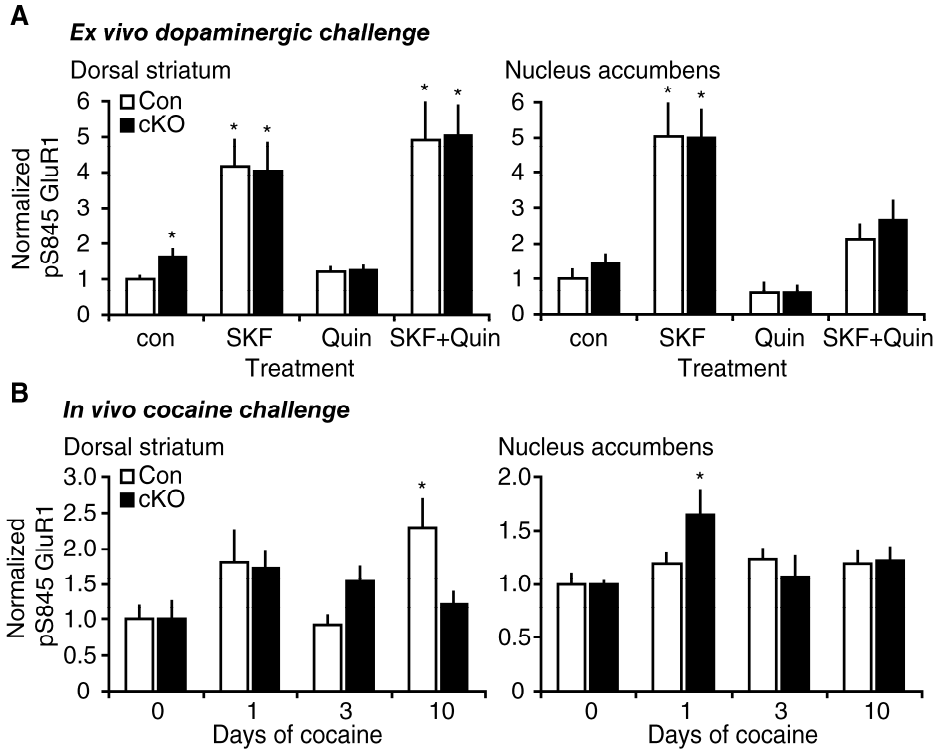

Figure 4.4. Effect of Cdk5 cKO on dopaminergic modulation of PKA signaling in striatal tissue. **A**, Quantitation of PKA targets in striatal slices in response to dopaminergic agents. Left graph depicts levels of pSer845 GluR1 in response to buffer (con), SKF81297 (1 μM, SKF), quinpirole (1 μM, Quin), or SKF and Quin in combination (SKF+Quin) for 5 min. Graph at right depicts the level of pSer845 GluR1 in nucleus accumbens slices in response to treatment as before. Data are presented as normalized mean (± *SEM*) for each treatment condition (*$p < 0.05$ compared to buffer control, Student's *t*-test, n = 4–8 per group). **B**, Quantitation of pSer845 levels in striatal tissue after cocaine exposure. Graph depicts normalized pSer845 GluR1 levels in dorsal striatum samples from control (Con) and Cdk5 cKO mice, 30 min after the administration of 15 mg/kg cocaine for the indicated number of days. Graph at right depicts pSer845 GluR1 levels in nucleus accumbens samples in treatments as before. Data are presented as normalized mean (± *SEM*) for each treatment condition (*$p < 0.05$ compared to saline, Student's *t*-test n = 3–6 per group).

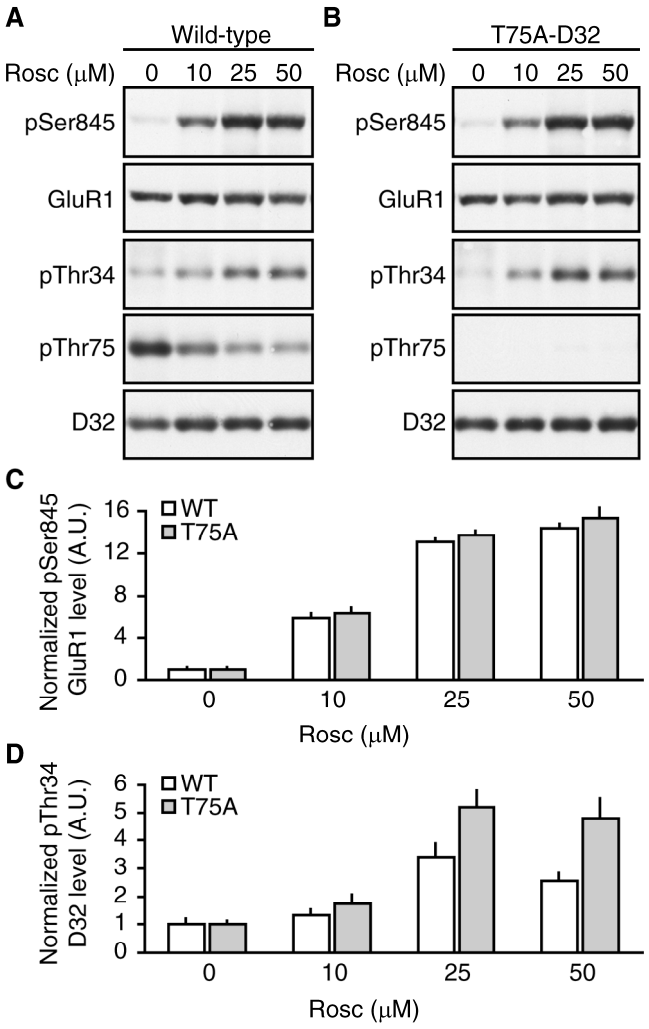

Figure 4.5. Cdk5 inhibition regulates PKA activity in T75A-DARPP-32 phosphomutant mice. **A**, Immunoblot analysis of striatal slices from wild-type (*WT*) mice treated with Cdk5 inhibitor, Roscovitine (*Rosc*), for 60 min. Slices were treated with 0, 10, 25, or 50 μM *Rosc*, as indicated. **B**, Immunoblots of striatal slices from T75A-DARPP-32 phosphomutant mice treated as in **A**. Immunoblots for PKA-dependent phosphorylation of GluR1 (*pSer845*) and D32 (*pThr34*) are indicated. Cdk5-dependent phosphorylation of D32 (*pThr75*) is also shown. The inhibition of Cdk5 resulted in an increase in the level of pSer845 GluR1 and pThr34 D32. **C**, Quantitation of effect of Cdk5 inhibition on pSer845 GluR1 level in *WT* and *T75A* striatal samples. **D**, Quantitation of effect of *Rosc* on pThr34 D32 level as in **C**. Quantitative immunoblots indicated a dose-dependent decrease in Cdk5-dependent phosphorylation of pThr75 D32 in *WT*

slices in response to *Rosc*, as well as a lack of pThr75 D32 signal in *T75A* phosphomutant mice. Data are presented as mean ± *SEM*.

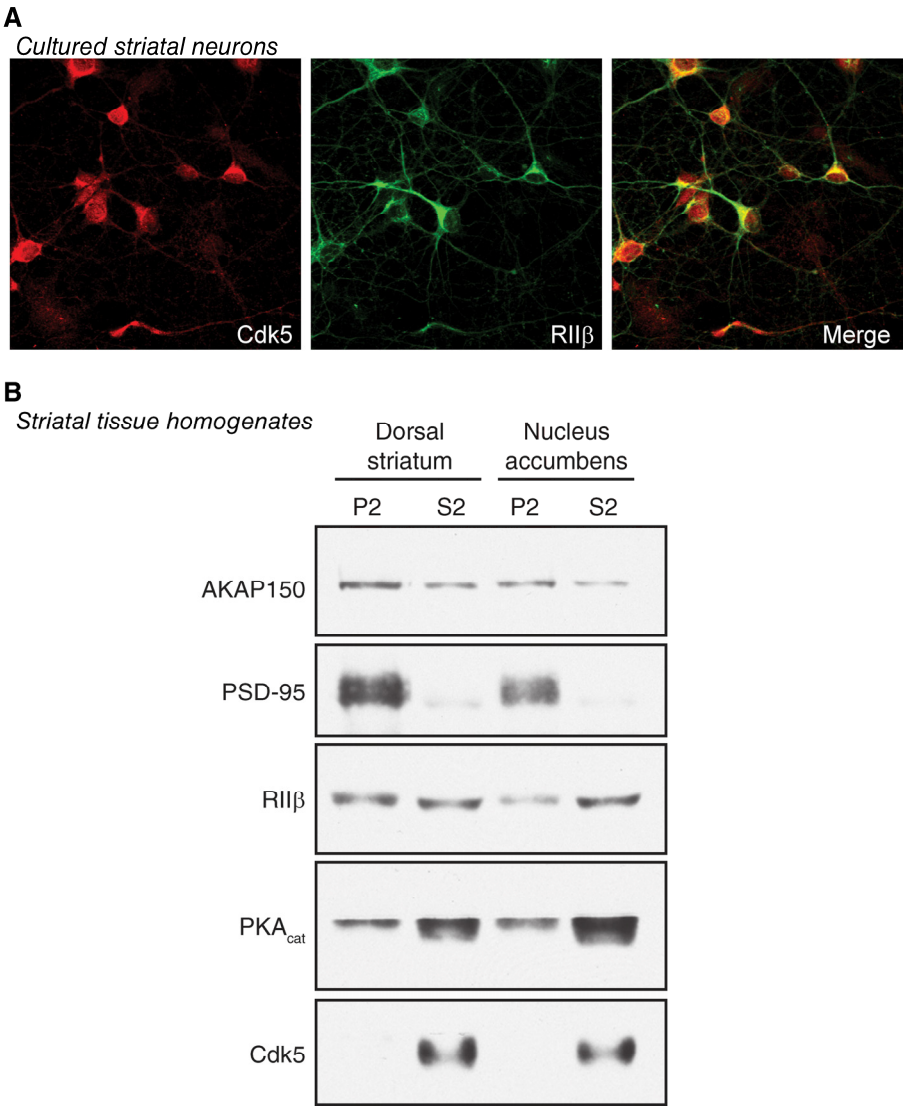

Figure 4.6. Colocalization and fractionation of Cdk5 and RIIβ in cells. **A**, Immunocytochemistry for Cdk5 and RIIβ in 14 DIV rat striatal cultures. Cdk5 (red) and RIIβ (green) are overlayed in image at right (merge) to show colocalization (yellow). **B**, Subcellular fractionation of striatal lysates. Tissue samples from dorsal striatum (left) and nucleus accumbens (right) were subjected to subcellular fractionation, yielding pellet (P2) and soluble (S2) fractions for each. Immunoblots for AKAP150, PSD-95, RIIβ, PKA cat, and Cdk5 are shown.

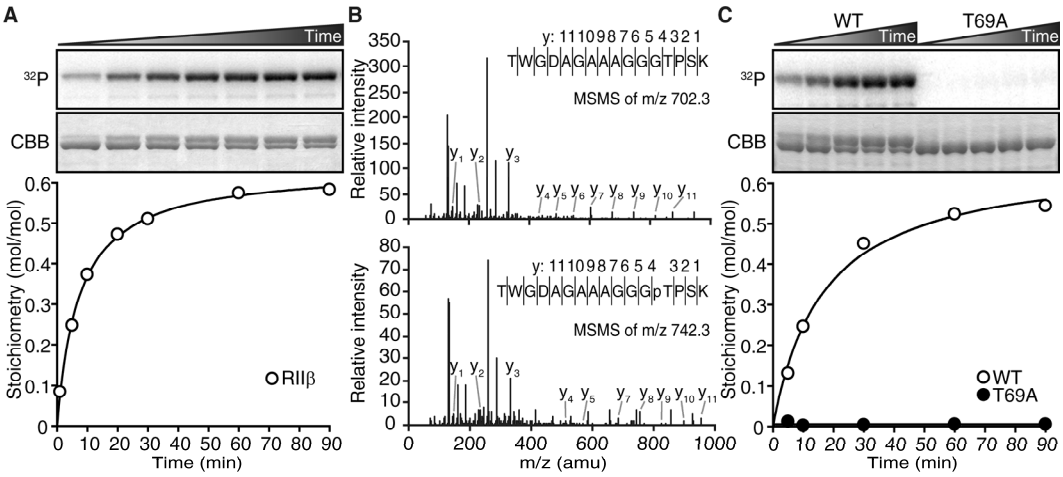

Figure 4.7. Cdk5 phosphorylates PKA Regulatory II β subunit at Thr69. A, Evaluation of RIIβ as substrate for Cdk5-dependent phosphorylation. The panels show time course of *in vitro* phosphorylation of RIIβ by Cdk5/p25. Time-dependent incorporation of ^{32}P (top panel) and CBB-stained (bottom panel) RIIβ are depicted. **B**, Physical identification of site of Cdk5-dependent phosphorylation of RIIβ by MS/MS analysis. Spectra indicate the identity of peptides produced by tryptic digests of RIIβ phosphorylated with Cdk5. The presence of a single charged peptide (TWGDAGAAAGGGTPSK) containing the site of phosphorylation at position 69 of the RIIβ sequence. The phosphopeptide denotes the position of the phospho-threonine as pT. The peptide sequences in both panels depict the y-ion series as a vertical line in the peptide sequence and corresponding site of y-ion generation (*i.e.* y_1, y_2, etc.). **C**, Confirmation of Thr69 as the site of Cdk5-dependent phosphorylation of RIIβ. The panels show time course of *in vitro* phosphorylation (as in *A*) of wild-type (*WT*) RIIβ and site-directed Thr69→Ala (*T69A*) RIIβ. Top panel depicts Cdk5-dependent incorporation of ^{32}P into *WT* RIIβ and not *T69A* RIIβ mutant. Graphs depicts stoichiometry of reaction at indicated times. Data are representative of experiments conducted in triplicate. Representative gels of coomassie brilliant blue (*CBB*) stains and autoradiograms are depicted.

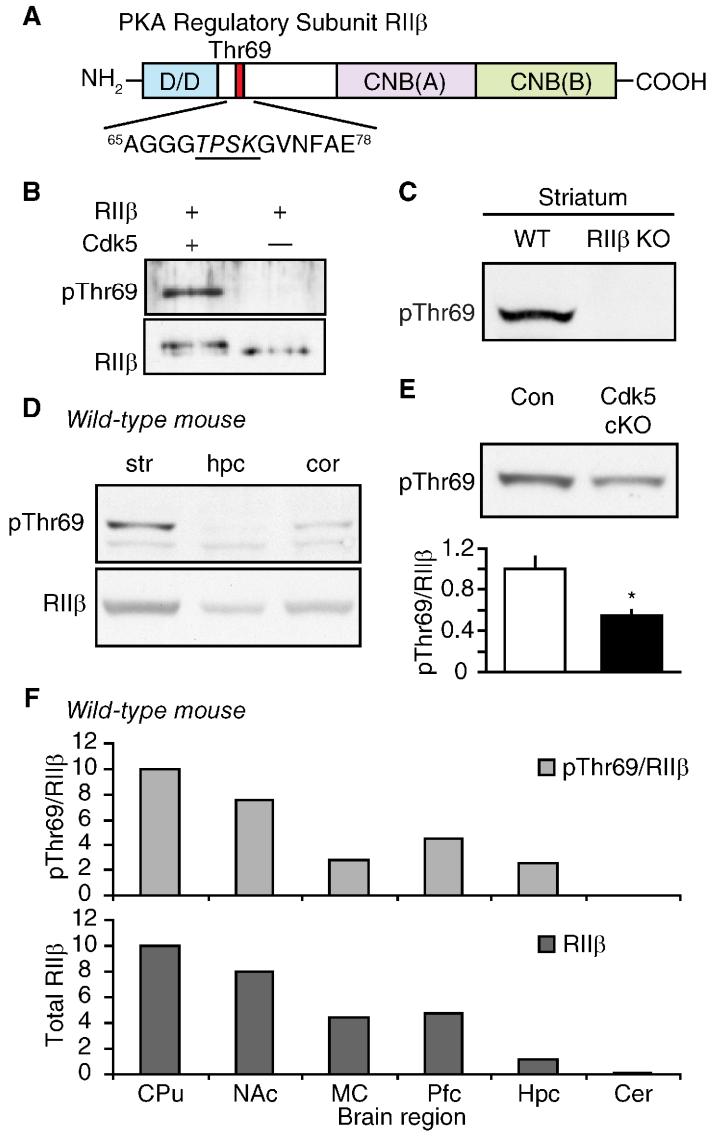

Figure 4.8. Generation and characterization of phosphorylation state-specific antisera to pThr69 RIIβ. **A**, Diagram depicting location of Thr69 in primary structure of RIIβ. The RIIβ dimerization docking and domain (*D/D*) and tandem cyclic nucleotide-binding domains (*CNB(A)* & *CNB(B)*) are indicated. The amino acid sequencing around Thr69 is shown, depicting Cdk5 consensus phosphorylation site (*TPSK*) and phosphopeptide encompassing Thr69 used to generate phosphorylation state-specific antibodies. **B**, Immunoblot analysis of recombinant RIIβ phosphorylated or mock phosphorylated with Cdk5 using antisera for phospho-Thr69 (pThr69) and total RIIβ (RIIβ). **C**, Immunoblot

analysis of pThr69 RIIβ in striatal samples from wild-type and RIIβ KO mice. **D**, Immunoblots showing the distribution of pThr69 and total RIIβ in brain regions from wild-type mice (*str*, striatum; *hpc*, hippocampus; *cor*, cerebral motor cortex). **E**, Immunoblot analysis of pThr69 RIIβ in striatal samples from control and Cdk5 cKO mice. Quantitation of pThr69 RIIβ level (± *SEM*) are shown in bar graph (*$p < 0.05$, Student's *t*-test, n = 4–6 per group). **F**, Analysis of distribution of pThr69 and total RIIβ in adult mouse brain regions. Quantitative levels of pThr69 and total RIIβ from caudatoputamen (CPu), nucleus accumbens (NAc), motor cortex (MC), prefrontal cortex (Pfc), hippocampus (hpc), and cerebellum (cer). Values are plotted as arbitrary units for each brain region.

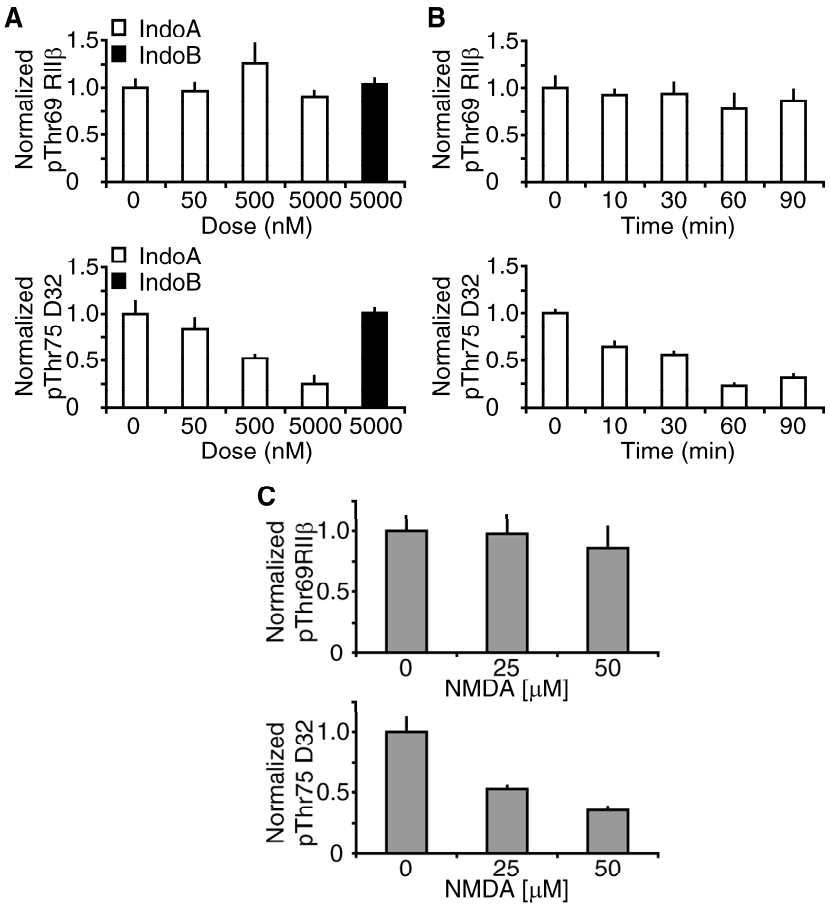

Figure 4.9. Effect of Cdk5 inhibition or NMDA treatment on striatal levels of pThr69 RIIβ and pThr75 D32. **A**, Dose response to Indolinone A (IndoA) in striatal slices from wild-type mice. Quantitation of pThr69 RIIβ levels (top) in response to IndoA (0–5000 nM, white bars) or IndoB (5000 nM, black bar) for 60 min. Quantitation of pThr75 D32 levels (bottom) in response to IndoA (0–5000 nM) or IndoB (5000 nM) for 60 min as above. **B**, Time course for IndoA treatment of striatal slices. Top graph depicts pThr69 RIIβ level in response to IndoA (5000 nM) for time indicated on abscissa. Bottom graph shows pThr75 D32 levels in response to IndoA (5000 nM) treatment. **C**, Dose response to NMDA treatment of striatal slices. Quantitation of pThr69 RIIβ levels in response to NMDA (0–50 mM) for 5 min is shown in top graph. Bottom graph depicts pThr75 D32 levels in response to NMDA treatment as above.

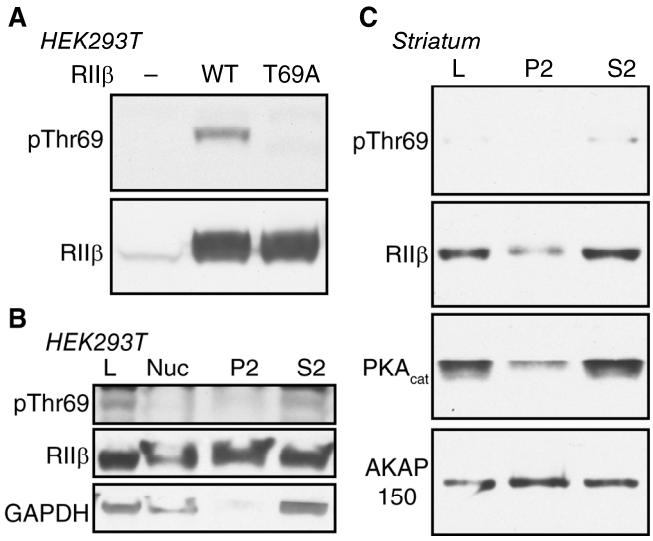

Figure 4.10. Phosphorylation and subcellular distribution of RIIβ in HEK293T cells and striatal samples. **A**, Immunoblot analysis of HEK293T cells transfected with RIIβ (WT), T69A phosphomutant RIIβ (T69A) or mock (−). Top immunoblot shows pThr69 RIIβ level in transfected HEK293T cells. Bottom panel shows total RIIβ levels. **B**, Subcellular fractionation of RIIβ-transfected HEK293T cells. Immunoblot shows detection of pThr69 RIIβ in crude lysate (L), nuclear pellet (Nuc), and membrane pellet (P2) and soluble (S2) fractions. Middle immunoblot depicts the detection of total RIIβ. Bottom panel depicts GAPDH levels in fractions as above. **C**, Subcellular fractionation of striatal tissue. Tissue samples from dorsal striatum were subjected to subcellular fractionation, yielding crude lysate (L), and pellet (P2) and soluble (S2) fractions. Immunoblots for pThr69 RIIβ, RIIβ, PKA cat, and AKAP150 are shown.

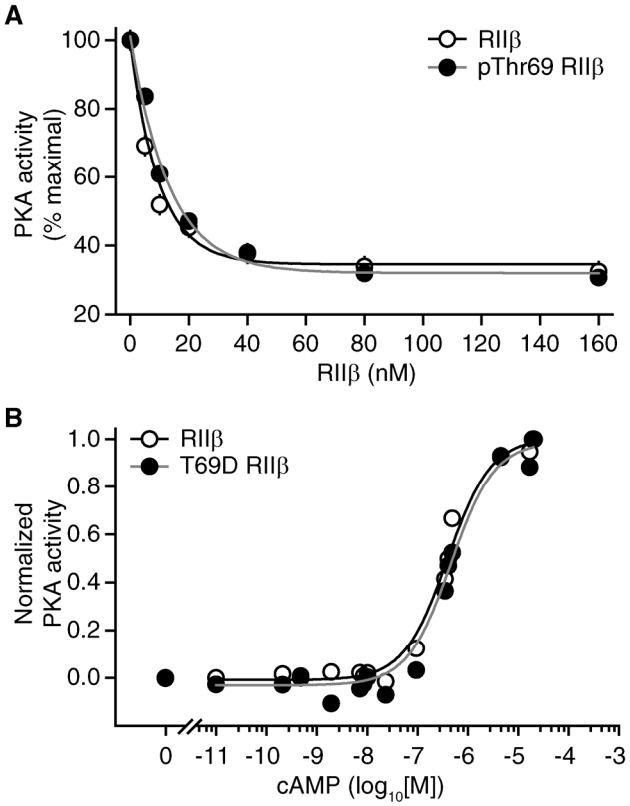

Figure 4.11. Functional analysis of pThr69 RIIβ on PKA inhibition and cAMP responsiveness. **A**, Analysis of RIIβ-mediated inhibition of PKAcat activity *in vitro*. Graph depicts activity of PKA (40 nM) in presence of various amounts of RIIβ (0–160 nM). Data represent normalized values (± *SEM*) for each condition. **B**, Analysis of cAMP binding by PKA-RIIβ holoenzyme. Graph depicts cAMP response curve for PKA holoenzyme formed with wild-type RIIβ (RIIβ) and T69D phosphomimetic RIIβ (T69D RIIβ). Data are presented as normalized values from 0 (no cAMP) to 1.0 (25 μM cAMP).

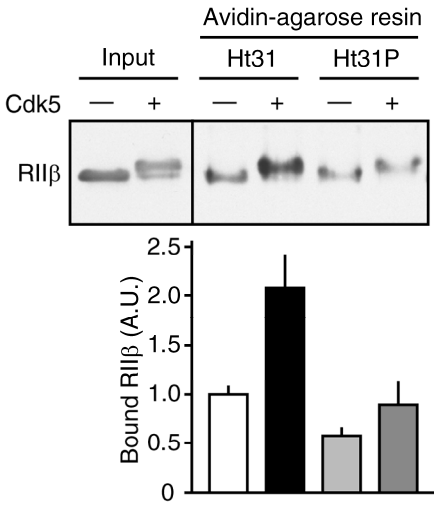

Figure 4.12. Effect of phosphorylation of Thr69 RIIβ on AKAP binding by RIIβ *in vitro*. Quantitation of steady-state binding of RIIβ to synthetic AKAP peptide Ht31 *in vitro*. Immunoblot depicts starting material (input, left) from mock (−) and Cdk5 preparatively phosphorylated RIIβ (+). Immunoblot also shows detection of RIIβ bound to Ht31-conjugated resin or Ht31P-conjugated resin. Graph shows quantitation of normalized bound RIIβ (± *SEM*) for each condition.

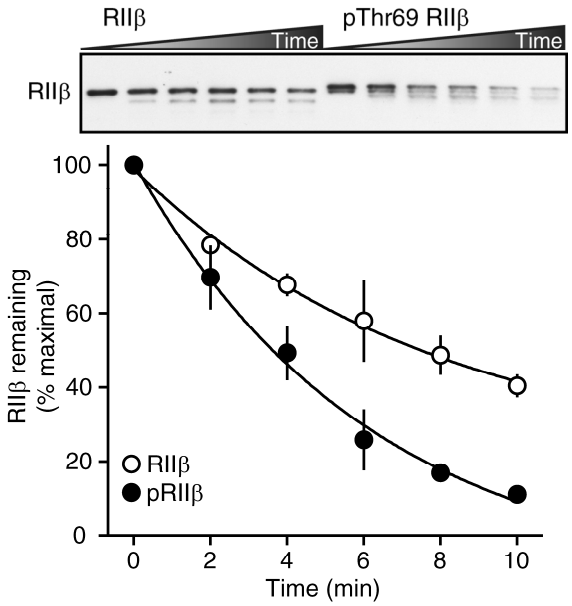

Figure 4.13. Effect of phosphorylation of Thr69 on cleavage of RIIβ by calpain. Time course of calpain-mediated cleavage of RIIβ *in vitro*. Top panel depicts immunoblot detection of RIIβ from cleavage reactions with mock phosphorylated RIIβ (RIIβ) or Cdk5 preparatively phosphorylated RIIβ (pThr69 RIIβ). Bottom graph represents degradation of RIIβ by calpain. Data are represented as % RIIβ remaining (± *SEM*) over time indicated on abscissa.

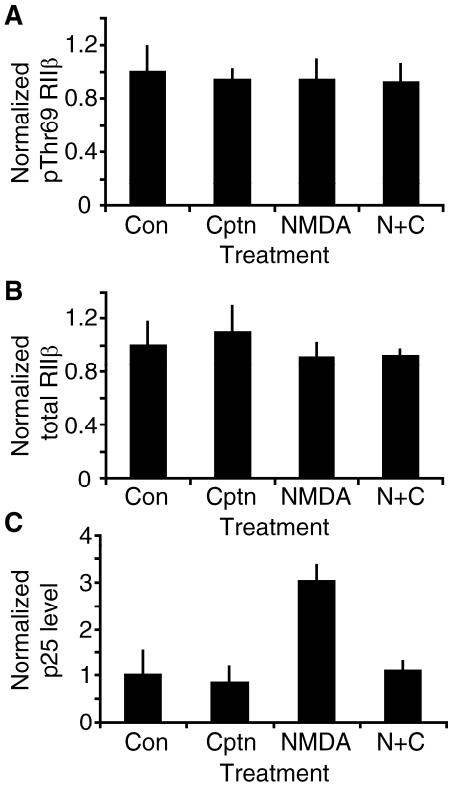

Figure 4.14. Effect of NMDA-mediated activation of calpain in striatal slices on pThr69 RIIβ levels. **A**, Quantitation of pThr69 RIIβ in response to treatment with calpeptin (20 μM, Cptn), NMDA (100 μM, NMDA), or both calpeptin and NMDA (N+C) for 30 min. **B**, Level of total RIIβ following striatal slice treatment with agents as in **A**. **C**, Quantitation of calpain-mediated generation of p25 in striatal slices. Graph depicts level of p25 detected in striatal slices treated with agents as in **A**. Data represent normalized mean (± *SEM*) for each treatment (n = 4 per treatment).

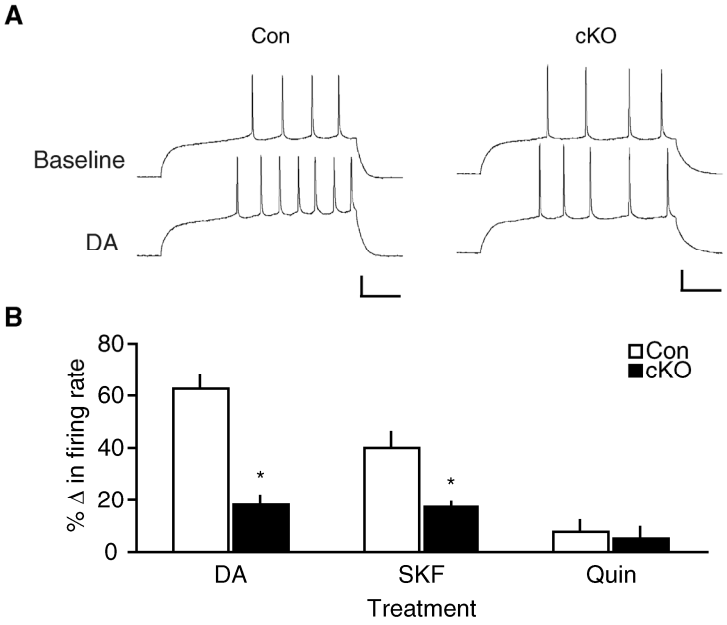

Figure 4.15. Effect of Cdk5 cKO on dopamine-dependent modulation of striatal neuron excitability. **A**, Effect of dopamine (DA; 100 μM) on NAc firing rate from control (Con) and cKO mice. Representative traces of action potential firing evoked by a depolarizing current step from control and cKO mice before (Baseline) or after dopamine (DA) application. Scale bars: 20 mV, 100 ms. **B**, Bar graphs showing the percentage change of NAc neuron firing rate (mean ± *SEM*) by dopaminergic agents, including dopamine (DA; 100 μM), SKP81297 (SKF; 20 μM), and quinpirole (Quin; 20 μM) in control and cKO mice (*$p < 0.05$, compared to control, Student's *t*-test, n = 3–7 per group).

CHAPTER FIVE

REGULATION OF cAMP SIGNALING NETWORKS BY CDK5, PKA, AND ERK

Summary

cAMP degradation is mediated exclusively by phosphodiesterases (PDEs). PDEs are encoded by 4 subfamilies and produce numerous splice variant isoforms. The complexity in the numbers of these enzymes is further complicated by a vast array of subcellular localization and activity modification pathways. "Long" forms of the PDE4 family members have been shown to be phosphorylated and activated by PKA. ERK-dependent phosphorylation of PDE has been demonstrated to regulate steady-state inhibition of enzymatic activity. We investigated the effect Cd5k inhibition by pharmacological and knock-out methods on PDE activity in striatal samples. Inhibition of Cdk5 led to a dose-dependent decrease in PDE activity. Also, conditional Cdk5 knock-out resulted in decreased PDE activity in the striatum. These data indicate that Cdk5 regulates PDE activity in striatal tissue

To date, phosphorylation state-specific antisera have not been generated to study the state of phosphorylation of PDE4 isoforms in tissue. We successfully raised phosphorylation state-specific antisera to both the PKA (Ser53 PDE4D3) and ERK (Ser573 PDE4D3) sites on PDE4 and screened these antibodies against

recombinant protein and brain tissue lysates. Furthermore, we utilized subfamily specific antisera to investigate the relative expression level of the four PDE4 sub-family members in various brain tissues. These reagents and studies provide useful tools and insight in the investigation of PDE activity and the regulation of PDE in various brain regions, including the reward pathway and the striatum.

Although cocaine administration causes a significant increase in the level of PKA-mediated phosphorylation of PDE4 in the nucleus accumbens in wild-type animals, this regulation was absent in Cdk5 cKO mice. These findings suggest a link between Cdk5 and PKA and ERK pathways in the regulation of PDE activity in the context of chronic psychostimulant exposure. In a separate but related study, we sought to confirm the site of Cdk5-dependent phosphorylation of MEK1. We found that Cdk5 phosphorylates MEK1 at Thr292, rather than the previously reported Thr286. This finding was confirmed by the use of phosphorylation state-specific antibodies towards recombinant protein. These findings provide novel reagents and insight into the biochemical mechanisms by which Cdk5 may regulate dopamine mediated signal transduction and drug addiction.

Introduction

cAMP is a ubiquitous second messenger that is employed in a vast number of cellular functions (Houslay and Milligan, 1997). The cAMP signaling pathway is initiated by the conversion of ATP to cAMP by adenylyl cyclases. While the generation of cAMP is of wide interest and the source of much of the literature regarding the signaling of G-protein coupled receptors (GPCRs) signaling through Gαs, it is also important to consider the turnover of cAMP. The only known degradation pathway for cAMP involves enzymatic hydrolysis of cAMP to AMP by cyclic nucleotide phosphodiesterases (PDEs). PDEs are encoded by a large multigene family of enzymes that are able to hydrolyze cAMP *in vitro*. Fortunately, the use of selective PDE inhibitors has demonstrated the specificity and importance of the cAMP-specific phosphodiesterase family PDE4 in numerous physiological responses. Thus, PDE4 may serve as the most relevant target with which to regulate cAMP signaling in the cell.

Despite the identification of the PDE4 family members, relatively little has been discerned regarding the complex regulatory mechanisms that control the large number of PDE4 isoforms. There are four genes encoding PDE4 enzymes (PDE4A, PDE4B, PDE4C, and PDE4D). Each gene is subject to mRNA splicing and alternative promoters to produce numerous splice variant isoforms. Each PDE4 sub-family isoform contains a shared core region consisting of a catalytic and C-terminal domain. In addition, various isoforms are distinguished by the

presence of a unique N-terminal domain. Furthermore, various isoforms are further classified as either "long" or "short" based on the presence or absence, respectively, of two highly conserved sequences that are unique to the PDE4 enzyme family. These sequences are located immediately adjacent to the catalytic domain, and are referred to as upstream conserved region 1 (UCR1) and upstream conserved region 2. Accordingly, "long" isoforms contain both UCRs, "short" isoforms contain only UCR2, and "super-short" isoforms contain a truncated UCR2 (Houslay, 2001). Since all PDE4 gene families encode "long" isoforms, and many studies have implicated the UCRs as catalytic modulatory domains for PDE activity.

Interestingly, elevated cAMP levels have been shown to enhance PDE4 activity (Houslay, 2001). Long-standing elevations in cAMP lead to an increase in mRNA level and protein expression for various PDE4 isoforms, perhaps as a compensatory mechanism to adapt to increased levels of cAMP. Furthermore, there have been studies implicating more rapid, direct cAMP-driven pathways by which PDE4 activity may be modified. Specifically, PDE4 isoforms may be activated through direct phosphorylation by cAMP dependent protein kinase (PKA). PKA phosphorylates PDE4D3 at Ser54 in the UCR1 domain to mediate its activation of the molecule (Hoffmann et al., 1998). Interestingly, the Arg-Arg-Glu-Ser-Phe PKA phosphorylation consensus site that is present in PDE4D3 is also found in the UCR1 of the "long" isoforms of all four PDE4 sub-families

(Sette and Conti, 1996). Very detailed studies have demonstrated that the UCR1 of the "long" isoforms of the four PDE4 sub-families are subject to phosphorylation and activation by PKA (MacKenzie et al., 2002).

Furthermore, PDE4 isoforms are localized to specific subcellular sites by virtue of anchoring domains in the protein (Houslay, 2001). Thus, it may be that PKA activation of PDE4 may lead to changes in steady-state levels of cAMP and PKA activity in subcellular microdomains. Indeed, there are increasing number of studies indicating the role for PDE and other proteins, including A-kinase anchoring proteins (AKAPs) in controlling cAMP gradients within cells and the importance of these proteins in cAMP signaling (Colledge and Scott, 1999). Interestingly, while all PDE4 families were able to be activated, only PDE4D3 of the isoforms tested was able to alter mobility in SDS-PAGE following phosphorylation. This difference, as well as the greater activation of the molecule relative to other PDE4s following phosphorylation may be attributed to the additional site of PKA-mediated phosphorylation in the unique N-terminal region of PDE4D3 (MacKenzie et al., 2002). Indeed, there is evidence that the N-terminal regions of the four sub-families can confer functional differences in the activity of these enzymes (Shakur et al., 1993; Huston et al., 1997).

Here, we investigate the regulation of PDE activity in striatal tissue following pharmacological inhibition or conditional knock-out of Cdk5. Our findings indicate that Cdk5 regulates PDE activity in this tissue. Through the use

of novel phosphorylation state-specific antibodies, we found that PKA-mediated activation of PDE4 is lost in CaMKII Ck5 cKO tissue. These findings compliment ongoing collaborative efforts in the labortatory to characterize the role of direct, Cdk5-dependent phosphorylation of PDE4 in the striatum. Meanwhile, we also investigated the potential cross-talk from ERK signaling to PKA signaling through PDE. We identified a novel site of Cdk5-dependent phosphorylation of MEK1. These findings will liekly expand the insight into the regulation of dopamine neurotransmission by Cdk5 to new aspects of PKA and ERK signaling pathways.

Experimental Procedures

Drugs and reagents

All drugs and reagents were from Sigma, except where indicated. Unactive rabbit MEK1 and active ERK were from Upstate (Lake Placid, NY).

Protein phosphorylation reactions and site identification

In vitro kinase assays were conducted as described in Chapter Three. In the case of MEK1, the material was phosphorylated by Cdk5 at a final substrate concentration of 1.41 μM. Stoichiometry of the final material was ~0.80 mol/mol and the sample was submitted for site identification as described in Chapter Four.

Immunoblotting

Immunoblots were conducted as described in Chapter Two and Three. Primary antibodies to PDE4A, PDE4B, PDE4C, and PDE4D (1:10,000) were provided by M.D. Houslay (University of Glasgow, Glasgow, Scotland). Also, antibodies to pSer53 PDE4 (1:20,000, see below) and pSer573 PDE4 (1:20,000, see below), pThr286 MEK1 (1:1000, Cell Signaling), pThr292 MEK1 (1:1000, Phosphosolutions) and total MEK1 (1:1000, Santa Cruz, H-8) were utilized.

Expression and purification of MBP-PDE4

Plasmids containing MBP-PDE4B1 and MBP-PDE4D isoforms were provided by M.D. Houslay (University of Glasgow). MBP-PDE4B1 was expressed in *E.coli* (BL21) as described in Chapter Four. Supernatant from cell lysates were incubated with Amylose resin (New England Biolabs) and 0.05% NP-40 are added to the supernatant and the supernatant is rotated for 2 hour at 4°C. The resin was washed with washing buffer (50 mM Tris-HCl, pH 8.0, 10 mM NaCl, 10 mM β-mercaptoethanol and 0.05% NP-40). Finally MBP-PDE4B1 was eluted with elution buffer (50 mM Tris-HCl, pH 8.0 and 10 mM Maltose) and dialyzed with dialysis buffer (50 mM Tris-HCl pH 7.5, 100 mM NaCl and 5% glycerol). Protein fractions were stored at –80 °C following analysis for purity by SDS-PAGE and Coomassie Brilliant Blue staining. The primary PDE4 products

were observed at ~100 kDa, with both higher and lower molecular weight species detected. The higher bands likely represented impurities, whereas the lower bands likely corresponded to degradation products.

In vitro phosphorylation reactions

Kinase assays were conducted as described in described in Chapter Four.

Generation of phosphorylation state specific antibodies

Rabbit polyclonal phosphorylation state-specific antibodies for phospho-Ser53 PDE4 and phospho-Ser573 PDE4 were generated and affinity-purified according to methodology described in Chapter Four (Czernik et al., 1997a, b) with slight modification. Antisera (1:200) were used against phospho- and dephospho- protein standards (50 ng), as well as brain tissue homogenates from wild-type mice. In the case of the Ser 54-PDE4 antibody, such blots proved inconclusive due to the mobility of PDE in the SDS-PAGE. Therefore, dot blots were performed in order to assess phospho-specificity, as previously described (Czernik et al., 1997a).

Acute slice preparation and slice pharmacology

Striatal slices were prepared from C57BL/6 adult male mice or CaMKII Cdk5 cKO mice and littermate controls as described in Chapter Four. In some

experiments, we utilized tamoxifen Cdk5 CKO mice 2-4 weeks after induction of knock-out by 15 daily intraperitoneal injections of 66.7 mg/kg hydroxytamoxifen as described in Chapter Three.

PDE activity assay

Phosphodiesterase activity was assayed in striatal tissue using a two-step radioenzymatic assay as described (Keravis et al., 2005) with slight modification. PDE activity assays were performed by K. Hayashi (UT Southwestern Medical Center). Striatal tissue from control and CaMKII Cdk5 cKO mice were dissected and homogenized in lysis buffer containing 20 mM Tris-HCl, pH 7.5 and 1 mM DTT, and protease inhibitor cocktail. Assays were performed with 2 µg of homogenate (40 µl) in 50 µl of cAMP mixture (2 µM cAMP and [2, 8-^{3}H]-cAMP (Amersham)) with or without 10 µl of inhibitor (theophilline or rolipram), and incubated for 10 min at 30°C. The assay was stopped by the addition of stop buffer containing 100 mM Tris-HCl, pH 7.5, 50 mM EDTA, and 30 mM theophiline and samples were boiled for 3 min. Snake Venom (Sigma) was added to the sample for the nucleotidase reaction (convert 5'-AMP to adenosine) and samples are incubated for 20 min at 30 °C. The reaction was stopped by adding SV-stop buffer containing 15 mM EDTA and 0.1 mM adenosine, adjusted to pH 6.5. QAE sephadex formate anion-exchange column is added to the sample and the samples were rotated for 30 min at 4 °C and centrifuged. Bound [2, 8-^{3}H]-

adenosine on the column was eluted with 0.02 M ammonium formate and transferred to a vial containing scintillation fluid. The amount of [2, 8-^{3}H]-adenosine is counted by a scintillation counter and PDE activity is reported as pmol product/min/mg tissue.

Statistical analysis

Data analysis was conducted as described in previous Chapters.

Results

Effect of Cdk5 inhibition on PDE activity in striatal slices

An important regulatory of cAMP signaling in striatal tissue is PDE. In order to investigate PDE as a point of regulation by Cdk5, we conducted PDE activity assays in lysates from striatal samples treated with Cdk5 inhibitor roscovitine. Roscovitine treatment caused a dose dependent decrease in PDE activity in striatal slices (**Figure 5.1*A***). Furthermore, the addition of exogenous Cdk5/p25 to the striatal lysates resulted in increased PDE activity compared to control levels (457 pmol/min/mg vs. 393 pmol/min/mg in control). These data indicate the Cdk5 suppresses PDE activity in striatal lysates. Interestingly, inhibition of the ERK signaling pathway caused a similar increase in PDE activity as that of Cdk5 addition (**Figure 5.1*A***). In order to further investigate the

possibility that Cdk5 regulates PDE activity, we conducted PDE activity assays in lysates from CaMKII-Cre Cdk5 cKO mice. In these samples, PDE activity was significantly reduced compared to littermate controls (**Figure 5.1*B***). Together, these findings provide compelling evidence that Cdk5 regulates PDE activity in the striatum, via direct or indirect mechanisms.

Evaluation of cAMP specific PDE4 expression in adult mouse brain

In order to investigate the expression of PDE4 family members, we conducted immunoblots of various brain regions from adult C57BL/6 mice. Notably, our findings indicate that the long isoforms of PDE4B and PDE4D were more abundant in brain tissue than the shorter isoforms. PDE4B1 and especially PDE4D3 were enriched in the striatal regions tested (**Figure 5.2**). Also, PDE4A (~70 kDa) was expressed at relatively high levels in most brain regions. A short form of PDE4C (~ 55 kDa) was particularly enriched in nucleus accumbens and thalamus samples. These data indicate that various PDE4 family members are expressed throughout the adult brain, with particular abundance of the long isoforms of PDE4B and PDE4D.

Generation of phosphorylation state-specific antisera to PKA and ERK sites of PDE4

Regulation of PDE activity by protein phosphorylation has been widely implicated in the control of cAMP-PKA signaling. The use of specific antibodies to phosphorylation-sites has been widely utilized to study the *in vivo* relevance of phosphorylation sites. In order to investigate these signaling pathways in intact brain tissue, we generated novel phosphorylation state-specific antibodies to the activating, PKA site (Ser53) and inhibitory, ERK site (Ser573) of long forms of PDE4. The structure of PDE4 family members is depicted in **Figure 5.3*A***. The N-terminal region of PDE4B is alternatively spliced, giving rise to the long isoforms detected in various brain regions, including PDE4B1 (see **Figure 5.2**). The activating PKA site lies within the upstream conserved region 1 (UCR1) which is found in all long isoforms of PDE4B (note its absence in PDE4B2, which lacks the UCR1). The inhibitory ERK phosphorylation site lies as the extreme C-terminus of the catalytic domain (**Figure 5.3*A***). The use of PDE4B1 allowed for the investigation of PKA-dependent phosphorylation *in vitro*. Indeed, PKA caused a time-dependent increase in the incorporation of 32P into PDE4B1 (**Figure 5.3*B***). We generated antibodies to pSer53 PDE4 to study this phosphorylation event in tissue. Rabbits were immunized with synthetic phosphopeptides mimicking the local region surrounding Ser53 of PDE4D3 and state-specific antisera was purified by affinity chromatography. The resulting antisera were used to detect phosphopeptides in dot blots (**Figure 5.3*C***). This antisera displayed striking selectivity for the phosphorylated peptides of PDE4D3.

Virtually no detection of the dephospho-peptide could be appreciated. Furthermore, in striatal slice treated with forskolin (10 μM, 10 min), there was robust increase in the detection of pSer53 PDE4 (**Figure 5.3*C***). Together, these data indicate that we successfully raised phosphorylation state-specific antisera to the PKA-dependent phosphorylation site of PDE4.

Likewise, the use of a truncated form of PDE4D2 (containing the conserved catalytic domain) allowed us to investigate the ability of ERK to phosphorylate PDE4. As expected, ERK caused a robust phosphorylation of PDE4D2 *in vitro* (**Figure 5.3*B***). We raised phosphorylation state-specific antisera to the ERK site of PDE4. The site of ERK-dependent phosphorylation of PDE4 is situated in the C-terminal catalytic domain (**Figure 5.3*A***). We generated antibodies selective for pSer573 PDE4D3 in order to study this modification in intact brain tissue. Rabbits were immunized with synthetic phopshopeptides mimicking the local region surrounding Ser573 PDE4D3 and state-specific antisera were purified by affinity chromatography. The resulting antisera were used to detect preparatively phosphorylated PDE4D2 from *in vitro* reactions with ERK (**Figure 5.3*C***). This antisera displayed striking selectivity for the phosphorylated form of PDE4D2 (**Figure 5.3*C***). Furthermore, the antisera detected pSer573 levels in lysates from striatal slices. Furthermore, treatment of striatal slices with the MEK inhibitor, U0126 (50 μM, 60 min) caused a reduction in the level of pSer573 detected (**Figure 5.4*C***). Taken together, these data

demonstrate the successful generation of phosphorylation state specific antisera to ERK-mediated phosphorylation of PDE4. Notably, the antisera described here were raised to specific motifs of the PDE4D3 protein sequence. However, the high homology amongst the UCR1 and catalytic domain of PDE4 family members makes it likely that the antisera will detect multiple PDE4 subfamily members. The use of the molecular weight standards and total antibodies will make the identification of specific isoform and family members more precise. Nonetheless, these reagents are of great utility in the study of the regulation of PDE in the brain.

Effect of chronic cocaine on pSer53 PDE4 level in Cdk5 cKO mice

In order to determine whether cocaine exposure alters PKA-mediated phosphorylation of PDE in striatal tissue, Cdk5 and cKO mice were administered cocaine (15 mg/kg for 1, 3, 10 consecutive days) and pSer53 PDE4 was assessed. In these experiments, animals were exposed to cocaine under the conditions described for the behavioral sensitization experiment (see Chapter Four). The administration of cocaine caused a robust increase in pSer53 PDE4 levels in the nucleus accumbens of control mice 30 min after the last injection of a 10 d exposure regimen (1.9 ± 0.3 compared to saline1.0 ± 0.1, $p < 0.05$,**Figure 5.4**). No difference was seen in the level PDE4 phosphorylation after 1 or 3 days of cocaine in control mice. Notably, there was no effect of cocaine on pSer53 PDE4

levels in CaMKII Cdk5 cKO samples at any time point (**Figure 5.4**). These data indicate that repeated cocaine alters the level of pSer53 PDE4 in the nucleus accumbens of wild-type mice. Furthermore, the regulation of chronic cocaine exposure on phospho-Ser53 PDE4 levels in nucleus accumbens is absent in Cdk5 cKO mice. Interestingly, in related studies conducted in the Bibb laboratory, PDE4 has been shown to be directly phosphorylated by Cdk5 and this event appears to be necessary for PKA-mediated phosphorylation and activation of PDE (K. Hayashi, unpublished observation). These data are in agreement with the observed lack of PKA phosphorylation of PDE4 in Cdk5 cKO tissue. These findings may be functionally related to the behavioral responses to dopaminergics and chronic cocaine observed in Cdk5 cKO mice (see Chapter Two and Four).

Evaluation of PKA-ERK crosstalk in striatal slices from Tamoxifen Cdk5 CKO mice

The ERK signaling pathway has been implicated as an important downstream effector of dopamine signaling in the striatum. Cdk5 regulates ERK signaling through the phosphorylation of MEK1 (Sharma et al., 2002). Therefore, we investigated the effect of ERK inhibition on PKA signaling in acute striatal slices (**Figure 5.5**). Treatment of slices with the MEK inhibitor, U0126 (50 μM, 60 min) induced a robust increase in PKA-mediated phosphorylation of Thr34 DARPP-32 (3.2 ± 0.3 vs. 1.0 ± 0.2 basal, $p < 0.01$, **Figure 5.5*A***). Furthermore,

regulation of pSer845 GluR1 showed a trend for elevation in response to U0126 in control slices (2.4 ± 0.4 vs. 1.0 ± 0.4 basal , $p = 0.06$). Conversely, this effect was absent in striatal slices from tamoxifen-inducible Cdk5 CKO mice (**Figure 5.5**). As reported in Chapter Three, we observed an increase in the basal state of PKA-mediated phosphorylation of GluR1 in Cdk5 CKO samples (2.4 ± 0.1 for cKO vs. 1.0 ± 0.4 for control, $p < 0.05$). However, the effect on basal levels of pThr34 DARPP-32 was not reproduced with this small sample size (n = 3 per group). In the case of DARPP-32 phosphorylation, U0126 treatment appeared to cause a decrease in pThr34 levels in Cdk5 CKO mice, although the data did not reach statistical significance (1.6 ± 0.4 for baseline vs. 0.7 ± 0.1 for U0126, $p = 0.1$). Treatment with U0126 was completely without effect on pSer845 GluR1 levels in slices from Cdk5 CKO^{HT} mice (2.4 ± 0.1 vs. 2.3 ± 0.5 for U0126, **Figure 5.5*B***). These data suggest that the cross-talk between ERK and PKA signaling pathways are disrupted in Cdk5 cKO mice. Furthermore, these findings suggest that the Cdk5-dependent inhibition of the ERK signaling pathway may be an important target for the regulation of PKA signaling.

Identification and confirmation of Thr292 as the site of Cdk5-dependent phosphorylation of MEK1

The ERK signaling pathway has been implicated as an important downstream effector of dopamine signaling in the striatum. In order to explore

the direct regulation of the ERK pathway by Cdk5, we tested MEK1 as a substrate for Cdk5 *in vitro*. MEK1 served as an efficient substrate *in vitro* (**Figure 5.6*A***). The phosphorylation of MEK1 by Cdk5/p25 yielded time-dependent incorporation of ^{32}P, reaching a final stoichiometry of approximately 0.65 mol/mol at 120 min. In subsequent reactions with MEK1 and Cdk5/p25 conducted for 3 h *in vitro*, final reaction stoichiometry reached 80%. Previous reports have implicated Thr286 as the site of Cdk5-dependent phosphorylation of MEK (Sharma et al., 2002; Takahashi et al., 2005). In order to determine the site of phosphorylation, mass spectrometry was conducted on chymotrypsin digests of preparatively phosphorylated MEK1 material in the absence of ^{32}P-ATP. LC tandem mass spectrometry analysis yielded one phosphopeptide encompassing amino acids 276-297 of the primary MEK1 sequence, suggesting that either Thr286 or Thr292 could be the site of phosphorylation (data not shown). However, the mass spectrometry analysis only detected a single phosphorylation on this peptide. Furthermore, another peptide was detected which was not phosphorylated, comprised of amino acids 270-291. Thus, the single site of phosphorylation must exist between residues 292 and 297. Thr 292 is the sole Ser/Thr in this region, and in amidst a Cdk5 consensus phosphorylation sequence (TPGR) at Thr292. Thus, these data provide compelling evidence that Cdk5-dpednent phosphorylation of MEK1 occurs at Thr 292.

In order to confirm this finding, we conducted immunoblot analysis of samples from reactions in which MEK1 was phosphorylated by Cdk5/p25 (**Figure 5.6*B***). In these experiments, we detect time-dependent increase in the level of pThr292 signal in the MEK1 product. There is a striking lack of signal in the immunoblot for pThr286 in the same samples (**Figure 5.6*B***). Immunoblot analysis with a pan-specific antibody for MEK1 shows equal loading of samples over the entire time course reaction. These data confirm the phosphorylation of MEK1 by Cdk5 to be at Thr292. These data will undoubtedly clarify the regulation of ERK signaling by Cdk5 and the possible interplay between ERK and PKA signaling pathways in the striatum.

Discussion

Crosstalk between ERK and cAMP signaling pathways has been appreciated most clearly in regards to cellular proliferation (Dumaz and Marais, 2005). However, recent work has implicated ERK signaling as a principle target of psychostimulant action. Here, we generated novel reagents for the investigation of PDE activity in intact brain tissue.

The use of phosphorylation state-specific antisera for PKA-phosphorylated "long" PDE4 isoforms was previously attempted, but with little success. The early antisera proved useless in the detection of pPDE4 from tissue

samples, likely owing to the long peptide sequence used for antibody generation (M.D. Houslay, personal communication). Thus, it would appear that the successful generation of antisera that could maintain selectivity and specificity for the pPDE4 isoforms in tissue lysates is of great utility to the study of these enzymes *in vivo*. These types of reagents make specific investigation into the possibility that PDE4 isoforms form distinct complexes with other AKAPs in or to carry out distinct functional roles. Furthermore, they would allow the investigation of sub-family specific PDE4 inhibitors on the activation of PDE4 *in vivo*.

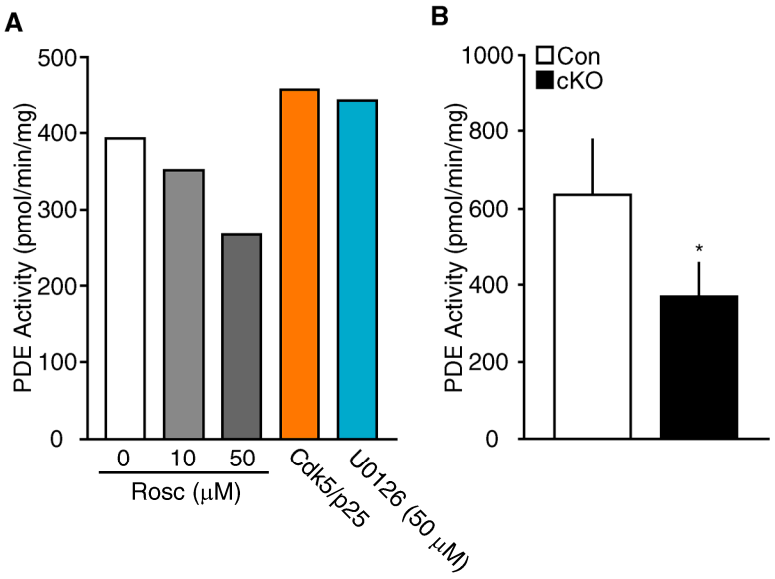

Figure 5.1. PDE activity in response to modulation of Cdk5 or ERK activity. **A**, PDE activity in striatal slices treated with Roscovitine (Rosc, 0–50 μM), recombinant active Cdk5 (orange bar), or U0126 (50 μM, blue bar). **B**, PDE activity in striatal lysates from control and CaMKII-Cre Cdk5 cKO mice. Data represent mean PDE activity (pmol/min/mg) ± *SEM*($p < 0.05$ compared to controls, Student's *t*-test, n = 6–10 per group).

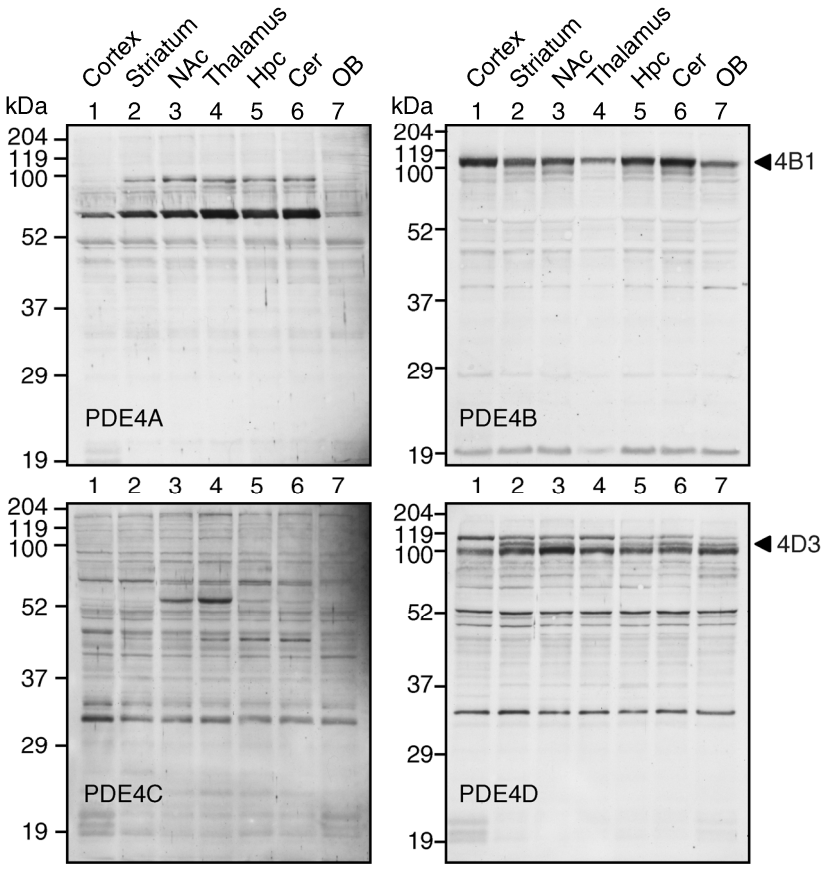

Figure 5.2. Evaluation of expression profile of PDE4 subfamily members in adult mouse brain. Representative immunoblots of acutely dissected brain regions for PDE4A, 4B, 4C, and 4D expression. Lysates from cortex (1), striatum (2), nucleus accumbens (NAc, 3), thalamus (4), hippocampus (Hpc, 5), cerebellum (Cer, 6), and olfactory bulb (OB, 7) were utilized. Molecular weight markers are indicated for each blot. Immunoblots represent detection of PDE4 family members with subfamily-specific antisera noted in lower left corner of each blot. Arrowheads indicate location of long isoforms of PDE4B (PDE4B1) and PDE4D (PDE4D3).

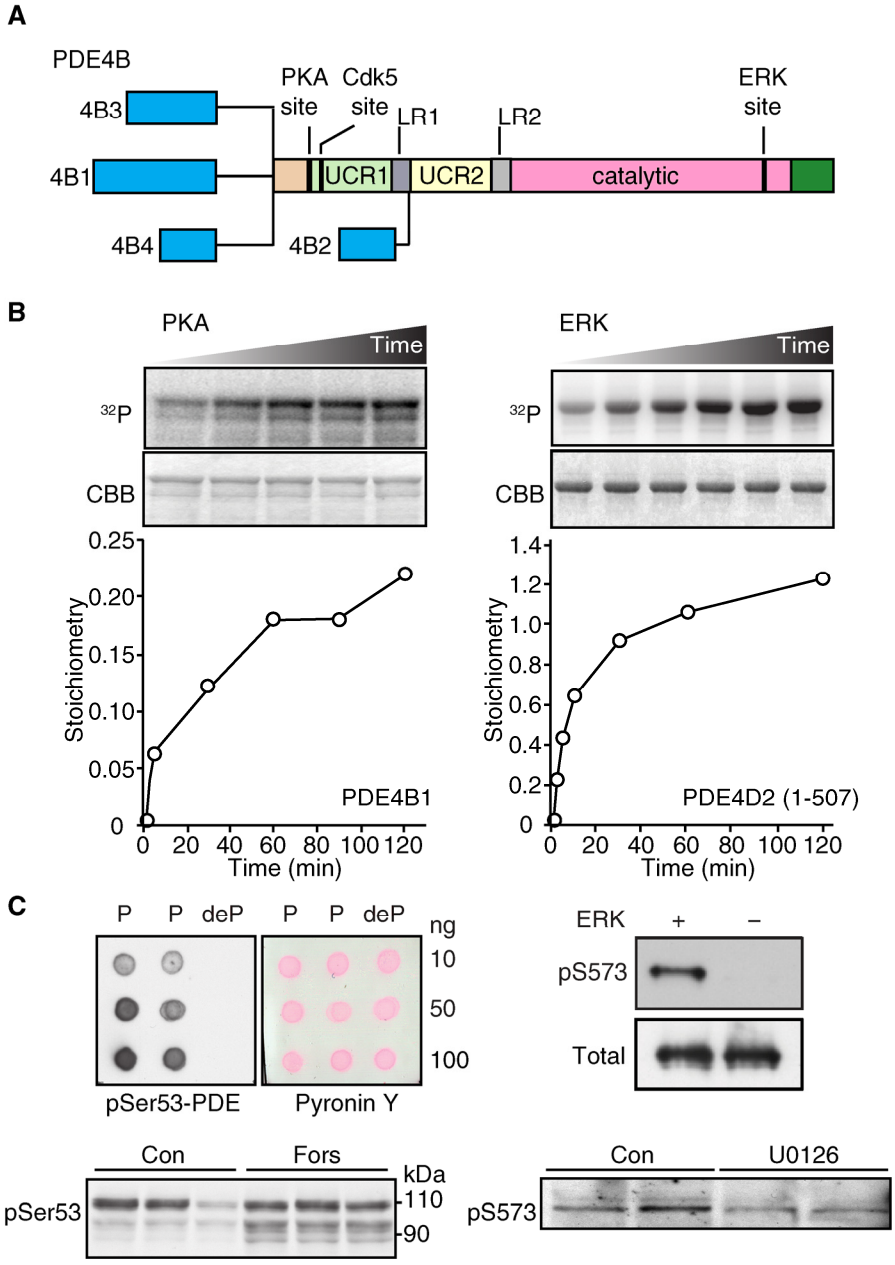

Figure 5.3. Generation of phosphorylation state-specific antibodies to PDE4. A, Diagram depicting structure of PDE4B. Location of PKA, Cdk5, and ERK phosphorylation sites are indicated. Note alternatively spliced N-termini (blue boxes), UCR1 and UCR2, and catalytic domain (pink). Linker regions (LR) are also indicated. **B**, Phosphorylation of PDE4 by PKA and ERK *in vitro*. **C**, Screening of pSer53 (PKA) and pSer573 (ERK) antisera to PDE4. Dot blot

analysis for pSer53 PDE and screen of in vitro material for pSer573 are shown. Immunoblots of striatal slices treated with forskolin (10 μM, 10 min) or U0126 (50 μM, 60 min) are also shown.

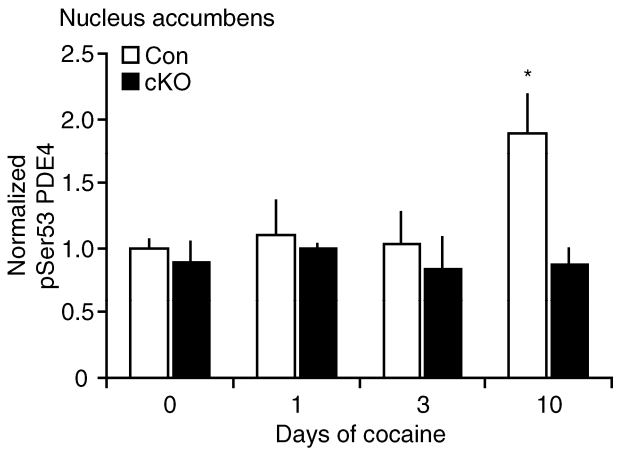

Figure 5.4. Regulation of pSer53 PDE4 in response to chronic cocaine in Cdk5 cKO mice. Quantitative of PKA-dependent phosphorylation of PDE4 in nucleus accumbens tissue after cocaine exposure. Graph depicts normalized pSer53 PDE4 levels in nucleus accumbens samples from control (Con) and Cdk5 cKO mice, 30 min after the administration of 15 mg/kg cocaine for the indicated number of days. Data are presented as normalized mean (± *SEM*) for each treatment condition (*$p < 0.05$ compared to saline, Student's *t*-test n = 3–6 per group).

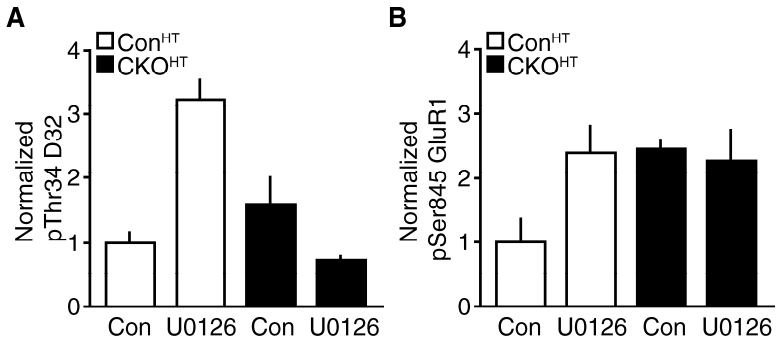

Figure 5.5. Evaluation of effect of ERK inhibition on PKA signaling in Tamoxifen Cdk5 CKO mice. **A**, Quantitation of pThr34 DARPP-32 levels in striatal slices from cont Con^{HT} and Cdk5 CKO^{HT} mice in response to treatment with U0126 (50 μM, 60 min). **B**, Quantitation of pSer845 GluR1 levels in response to U0126 as in **A** (n = 3 per group).

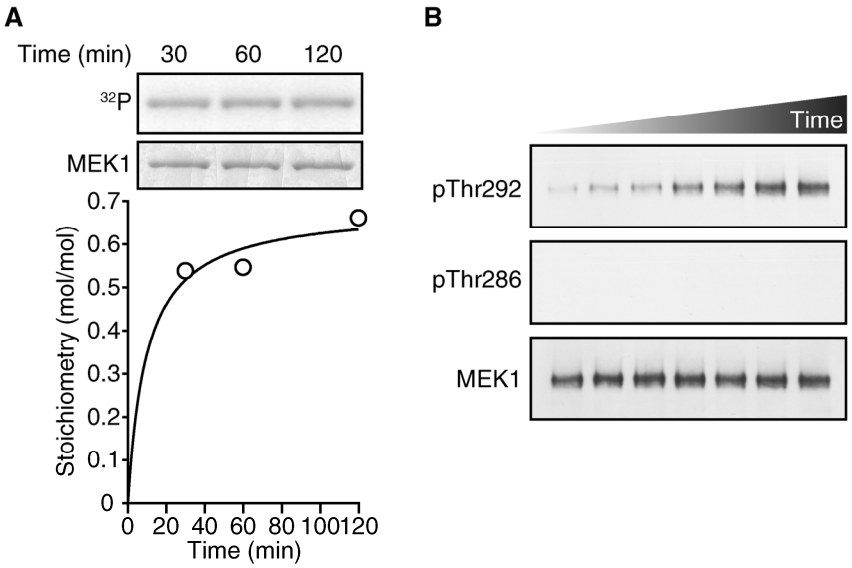

Figure 5.6. Evaluation of MEK1 as a substrate for Cdk5 *in vitro*. A, Evaluation of MEK1 as substrate for Cdk5-dependent phosphorylation. The panels show time course of *in vitro* phosphorylation of RIIβ by Cdk5/p25. Time-dependent incorporation of ^{32}P (top panel) and CBB-stained (bottom panel) MEK1 are depicted. Graph depicts stoichiometry of reaction at indicated times. **B**, Confirmation of Thr292 as the site of Cdk5-dependent phosphorylation of MEK1. The panels show time course of *in vitro* phosphorylation (time course 0–180 min) of MEK1. Top panel depicts immunoblot of reaction samples with phosphorylation state-specific antibody to pThr292 MEK1. Middle panel shows immunoblot using pThr286 MEK1 antibody. Bottom panel depicts detection with total MEK1 antibody.

CHAPTER SIX

GENERAL DISCUSSION

Regulation of synaptic efficacy and neuronal plasticity are largely regarded as the mechanisms by which learning and memory are achieved in the brain. Plasticity in the neural circuitry of the brain contributes to the execution of various behaviors. Thus, it is therefore likely that the regulatory mechanisms controlling neuronal plasticity and synaptic function, underlie alterations in behavioral profiles. Previous studies from the Bibb laboratory have demonstrated a role for Cdk5 in the regulation of dopamine signaling and behavioral responses to rewarding stimuli (Bibb et al., 2001; Taylor et al., 2007). Cdk5 is enriched in both the pre- and post-synaptic compartments and is believed to be involved in mediating neuronal plasticity (Dhavan and Tsai, 2001; Bibb, 2003). Thus, Cdk5 may act through presynaptic or postsynaptic mechanisms to achieve these functions.

The perinatal lethality and congenital defects associated with constitutive knock-out mice (Nikolic et al., 1996; Ohshima et al., 1996; Kwon and Tsai, 1998; Ko et al., 2001) have hampered the use of behavioral paradigms to study Cdk5 function. Therefore, previous studies have relied heavily on pharmacological approaches to modulate Cdk5 activity. These studies should be interpreted carefully, as the pharmacological agents employed have limited selectivity for

Cdk5 and have off-target effects as well (Yan et al., 2002). Nonetheless, these studies have provided the foundation for the current work that has sought to confirm and extend the notion that Cdk5 regulates dopamine signaling and behavioral responses to drugs of abuse. Here, we employed an approach that allows for temporal and spatial control of Cdk5 activity in the brain in order to clarify the role of this kinase in various behaviors. Our recent studies have employed conditional knock-out technology to implicate loss of Cdk5 in the regulation of NMDAR function and hippocampal-dependent learning and memory (Hawasli et al., 2007). This approach has uncovered novel insight into the regulation of behaviors by Cdk5 and is far superior to previous approaches.

Regulation of biochemical signaling cascades is an important mechanism of controlling the response to chronic psychomotor drugs of abuse. Taken together, the studies presented here indicate that the acute and chronic cellular effects of cocaine and dopamine neurotransmission are regulated by signal transduction pathways involving Cdk5. The background for the majority of the studies conducted in the present work relied on the use of pharmacological inhibitors that inhibit Cdk5 *in vitro* and *in vivo*. The use of conditional knock-out technology made it possible to provide a clearer understanding of the role of Cdk5 in the homeostasis that counteracts dopamine signaling. We report the development of novel animal models in which conditional Cdk5 knockout is achieved in spatially restricted regions of the adult nervous system, allowing for

the investigation of the effects of loss of Cdk5 on the psychoactive properties of cocaine and motivation for reward. It also provides a better model for the search for novel targets of Cdk5 signaling. Loss of Cdk5 in the adult brain enhanced the psychoactive responses to cocaine exposure and reduced the threshold for behavioral sensitization and conditioned place preference for cocaine. This enhanced sensitization was also observed in a model system in which Cdk5 loss was restricted specifically to NAc neurons. Using rAAV delivery to the nucleus accumbens, we are able to discern the effect of Cdk5 loss specifically within the post-synaptic compartment of striatal nucleus accumbens neurons on reward behavior. Furthermore, mice lacking Cdk5 throughout the forebrain displayed increased incentive motivation for reward, and tamoxifen Cdk5 CKO mice show enhanced performance on motor tasks, including wire maneuver and rotarod. Tamoxifen inducible CKO mice also displayed antidepressant-like phenotypes compared to controls. These data are consistent with the notion that Cdk5 negatively regulates signaling pathways involved in and the modulation of motor function and reward-related behavior. These data contribute to the growing literature implicating the importance of Cdk5 in signaling downstream of dopamine receptors.

A well characterized physiological trait of striatal neurons is that they fire multiple times (spike) in response to stimulation via current injection. Conditional knockout of Cdk5 increased the intrinsic excitability of striatal

neurons, revealing the importance of Cdk5 in controlling electrophysiological properties of medium spiny neurons, perhaps by altering dopamine signaling. Further investigation revealed that dopamine-dependent modulation of NAc firing was altered in Cdk5 cKO mice. These data suggest that Cdk5 negatively regulates the behavioral effects of reward through alterations in neuronal excitability and dopamine signaling within the mesolimbic reward pathway. Previous studies have shown *in vivo* chronic cocaine exposure produces increases in the intrinsic excitability of neurons within the reward circuitry (Dong et al., 2006). Furthermore, inhibition of Cdk5 has been shown to elevate the basal state or phosphorylation of the GluR1 subunit of AMPA receptors (Bibb et al., 2001) and potentiate voltage gated Ca^{2+} channel conductance (Bibb et al., 1999). Recent reports have shown the necessity of dopamine-D1 receptor signaling in the modulation of depotentiation at corticostriatal synapses (Centonze et al., 2006). In these studies, bath application of Cdk5 inhibitors mimicked the effect of activation of dopamine D1 receptor-PKA signaling in the blockade of LFS-induced depotentiation. These findings support the idea that Cdk5 activity may be able to regulate synaptic plasticity within the striatum through regulation of dopamine-D1/PKA signaling. Indeed, the current study and past work has shown that Cdk5 inhibitors are effective activators of PKA signaling (Kansy et al., 2004). While the decrease in pThr75 DARPP-32 phosphorylation and

disinhibition of PKA is an attractive explanation, it is likely that Cdk5 regulates dopamine D1-PKA signaling.thorugh numerous other pathways.

Our findings suggest that Cdk5 is involved in the suppression of the psychoactive behavioral properties of cocaine as well as the incentive motivation for appetitive reward. PKA activity, specifically within the nucleus accumbens, has been implicated in the control of reward-related incentive motivation (Lynch and Taylor, 2005). As discussed, disinhibition of PKA/DARPP-32/PP-1 signaling within the nucleus accumbens in Cdk5 cKO mice is an attractive mechanism for the observed findings. However, recent studies have shown that Cdk5 also phosphorylates WAVE1 and regulates actin cytoskeletal remodeling pathways (Kim et al., 2006). This pathway provides a possible mechanism for the role of Cdk5 in cocaine-mediated morphological alterations (Norrholm et al., 2003) which are integral components to the behavioral aspects of drug exposure. Furthermore, this work highlights other aspects of the cross-talk between Cdk5 and PKA signaling pathways, as WAVE1 is also functions as a cAMP kinase anchoring protein (AKAP) to regulate subcellular PKA localization. The subcellular localization of PKA is dependent upon interaction of regulatory subunit RII with specific A-kinase anchoring proteins (AKAPs). These interactions are crucial for the proper spatial regulation of PKA signaling.

In order to investigate possible biochemical mechanisms for Cdk5 modulation of dopamine signaling, we identified a novel Cdk5 phosphorylation

site on the PKA regulatory subunit IIβ (RIIβ) and raised phosphorylation state-specific antisera to the site. We recently implicated Cdk5 in the regulation of calpain-mediated cleavage of key neural substrates (Hawasli et al., 2007). In order to investigate this novel regulatory mechanism, we assessed the ability of pThr69 RIIβ for calpain-mediated cleavage. We found that phospho-RIIβ served as a better substrate than dephospho-RIIβ. Investigation of the regulation of pThr69 revealed that this site is a stable Cdk5-dependent phosphorylation, in contrast to Cdk5-depdendent phosphorylation sites on inhibitor-1 and DARPP-32. Treatment of acute striatal slices with Cdk5 inhibitors, or other agents did not affect pThr69 RIIβ levels. These studies uncovered a potential new regulatory mechanism for by which Cdk5 controls PKA signaling. This new target may provide insight previously unknown aspects of regulation of PKA signaling by Cdk5.

Previous studies have implicated the phosphorylation of PDE4 as an important modulator of PKA signaling. We found evidence that PDE activity was reduced in the striatum of Cdk5 cKO mice. These data indicate that Cdk5 is involved, either directly or indirectly, in the regulation of PDE activity. In order to investigate this regulation, we generated novel phosphorylation state-specific antisera to the PKA (Ser53) and ERK (Ser573) targeted sites of PDE4B1. In related studies, Cdk5 was found to directly phosphorylate PDE4. Thus, Cdk5 may function in the regulation of PKA signaling through phosphorylation of

DARPP-32, RIIβ, and regulation of PDE activity in the striatum. In related studies, phosphorylation state-specific antisera were generated to both the PKA- and ERK- dependent phosphorylation sites of cAMP-specific phosphodiesterase 4 (PDE4). These reagents compliment other studies involving the Cdk5-dependent phosphorylation of PDE4 recently discovered by the Bibb laboratory. Furthermore, these reagents allow for the analysis of the regulation and crosstalk between PKA and ERK, as well as the involvement of Cdk5 in this pathway. Finally, the site of Cdk5-dependent phosphorylation of MEK1 was identified and confirmed as Thr292, rather than the previously reported Thr286. These data provide the foundation for investigation into novel mechanisms by which Cdk5 may regulate intracellular signaling pathways important in the control of motivation, motor function, reward-related behavior, and emotional state.

In conclusion, we utilized the conditional Cdk5 knock-out mouse models to investigate motor and emotionally-motivated behaviors. We found that loss of Cdk5 throughout the adult forebrain produced elevated locomotor activity and potentiated responses to cocaine exposure, and enhanced motor-learning. These changes were accompanied by enhanced cocaine conditioned place preference and enhanced learning and memory. Loss of Cdk5 in targeted regions of the reward circuitry resulted in enhanced responses to cocaine as well, but no effect on basal locomotor activity. Furthermore, loss of Cdk5 in restricted populations of cells in the adult brain produced increased cocaine responses and enhanced

motivation for reinforcement. These findings were accompanied by elevated striatal neuron excitability in medium spiny neurons of the nucleus accumbens. Taken together with the biochemical data, hese findings suggest that Cdk5 acts in the regulation of various signaling pathways that are important for dopamine-signaling and responses to drugs of abuse. These data provide the foundation for investigation into novel mechanisms by which Cdk5 may regulate intracellular signaling pathways important in the control of motivation, motor function, reward-related behavior, and emotional state.

BIBLIOGRAPHY

Alexa A, Tompa P, Baki A, Vereb G, Friedrich P (1996) Mutual protection of microtubule-associated protein 2 (MAP2) and cyclic AMP-dependent protein kinase II against mu-calpain. J Neurosci Res 44:438-445.

Andersen PH, Gingrich JA, Bates MD, Dearry A, Falardeau P, Senogles SE, Caron MG (1990) Dopamine receptor subtypes: beyond the D1/D2 classification. Trends Pharmacol Sci 11:231-236.

Barot SK, Ferguson SM, Neumaier JF (2007) 5-HT(1B) receptors in nucleus accumbens efferents enhance both rewarding and aversive effects of cocaine. Eur J Neurosci 25:3125-3131.

Barrot M, Olivier JD, Perrotti LI, DiLeone RJ, Berton O, Eisch AJ, Impey S, Storm DR, Neve RL, Yin JC, Zachariou V, Nestler EJ (2002) CREB activity in the nucleus accumbens shell controls gating of behavioral responses to emotional stimuli. Proc Natl Acad Sci U S A 99:11435-11440.

Benavides DR, Bibb JA (2004) Role of Cdk5 in drug abuse and plasticity. Ann N Y Acad Sci 1025:335-344.

Bertolucci-D'Angio M, Serrano A, Scatton B (1990) Differential effects of forced locomotion, tail-pinch, immobilization, and methyl-beta-carboline carboxylate on extracellular 3,4-dihydroxyphenylacetic acid levels in the rat striatum, nucleus accumbens, and prefrontal cortex: an in vivo voltammetric study. J Neurochem 55:1208-1215.

Berton O, McClung CA, Dileone RJ, Krishnan V, Renthal W, Russo SJ, Graham D, Tsankova NM, Bolanos CA, Rios M, Monteggia LM, Self DW, Nestler EJ (2006) Essential role of BDNF in the mesolimbic dopamine pathway in social defeat stress. Science 311:864-868.

Bibb JA (2003) Role of Cdk5 in neuronal signaling, plasticity, and drug abuse. Neurosignals 12:191-199.

Bibb JA, Chen J, Taylor JR, Svenningsson P, Nishi A, Snyder GL, Yan Z, Sagawa ZK, Ouimet CC, Nairn AC, Nestler EJ, Greengard P (2001) Effects of chronic exposure to cocaine are regulated by the neuronal protein Cdk5. Nature 410:376-380.

Bibb JA, Snyder GL, Nishi A, Yan Z, Meijer L, Fienberg AA, Tsai LH, Kwon YT, Girault JA, Czernik AJ, Huganir RL, Hemmings HC, Jr., Nairn AC, Greengard P (1999) Phosphorylation of DARPP-32 by Cdk5 modulates dopamine signalling in neurons. Nature 402:669-671.

Burger C, Gorbatyuk OS, Velardo MJ, Peden CS, Williams P, Zolotukhin S, Reier PJ, Mandel RJ, Muzyczka N (2004) Recombinant AAV viral vectors pseudotyped with viral capsids from serotypes 1, 2, and 5 display differential efficiency and cell tropism after delivery to different regions of the central nervous system. Mol Ther 10:302-317.

Cai XH, Tomizawa K, Tang D, Lu YF, Moriwaki A, Tokuda M, Nagahata S, Hatase O, Matsui H (1997) Changes in the expression of novel Cdk5 activator messenger RNA (p39nck5ai mRNA) during rat brain development. Neurosci Res 28:355-360.

Campbell DG, Hardie DG, Vulliet PR (1986) Identification of four phosphorylation sites in the N-terminal region of tyrosine hydroxylase. J Biol Chem 261:10489-10492.

Cantrell AR, Tibbs VC, Westenbroek RE, Scheuer T, Catterall WA (1999) Dopaminergic modulation of voltage-gated Na+ current in rat hippocampal neurons requires anchoring of cAMP-dependent protein kinase. J Neurosci 19:RC21.

Carr DW, Stofko-Hahn RE, Fraser ID, Cone RD, Scott JD (1992) Localization of the cAMP-dependent protein kinase to the postsynaptic densities by A-kinase anchoring proteins. Characterization of AKAP 79. J Biol Chem 267:16816-16823.

Centonze D, Costa C, Rossi S, Prosperetti C, Pisani A, Usiello A, Bernardi G, Mercuri NB, Calabresi P (2006) Chronic cocaine prevents depotentiation at corticostriatal synapses. Biol Psychiatry 60:436-443.

Chen J, Kelz MB, Hope BT, Nakabeppu Y, Nestler EJ (1997) Chronic Fos-related antigens: stable variants of deltaFosB induced in brain by chronic treatments. J Neurosci 17:4933-4941.

Chen J, Kelz MB, Zeng G, Sakai N, Steffen C, Shockett PE, Picciotto MR, Duman RS, Nestler EJ (1998) Transgenic animals with inducible, targeted gene expression in brain. Mol Pharmacol 54:495-503.

Chen PC, Chen JC (2005) Enhanced Cdk5 activity and p35 translocation in the ventral striatum of acute and chronic methamphetamine-treated rats. Neuropsychopharmacology 30:538-549.

Chergui K, Svenningsson P, Greengard P (2004) Cyclin-dependent kinase 5 regulates dopaminergic and glutamatergic transmission in the striatum. Proc Natl Acad Sci U S A 101:2191-2196.

Colledge M, Scott JD (1999) AKAPs: from structure to function. Trends Cell Biol 9:216-221.

Cruz JC, Tseng HC, Goldman JA, Shih H, Tsai LH (2003) Aberrant Cdk5 activation by p25 triggers pathological events leading to neurodegeneration and neurofibrillary tangles. Neuron 40:471-483.

Cummings DE, Brandon EP, Planas JV, Motamed K, Idzerda RL, McKnight GS (1996) Genetically lean mice result from targeted disruption of the RII beta subunit of protein kinase A. Nature 382:622-626.

Czernik AJ, Mathers J, Mische SM (1997a) Phosphorylation State-specific Antibodies. In: Regulatory Protein Modification: Techniques and Protocols (Hemmings HC, Jr., ed), pp 219–250. Totowa, NJ: Humana Press Inc.

Czernik AJ, Mathers J, Mische SM (1997b) Phosphorylation state-specific antibodies. In: Regulatory protein modification: techniques and protocols (Hemmings HC, Jr., ed), pp 219-250. Totowa, N.J.: Humana Press.

Dalmau J, Gultekin SH, Voltz R, Hoard R, DesChamps T, Balmaceda C, Batchelor T, Gerstner E, Eichen J, Frennier J, Posner JB, Rosenfeld MR (1999) Ma1, a novel neuron- and testis-specific protein, is recognized by the serum of patients with paraneoplastic neurological disorders. Brain 122:27-39.

Desdouits F, Siciliano JC, Greengard P, Girault JA (1995) Dopamine- and cAMP-regulated phosphoprotein DARPP-32: phosphorylation of Ser-137 by casein kinase I inhibits dephosphorylation of Thr-34 by calcineurin. Proc Natl Acad Sci U S A 92:2682-2685.

Devys D, Lutz Y, Rouyer N, Bellocq J-P, Mandel J-L (1993) The FMR-1 protein is cytoplasmic, most abundant in neurons and appears normal in carriers of a fragile X premutation. Nat Genet 4:335-340.

Dhavan R, Tsai LH (2001) A decade of CDK5. Nat Rev Mol Cell Biol 2:749-759.

Di Chiara G, Morelli M, Consolo S (1994) Modulatory functions of neurotransmitters in the striatum: ACh/dopamine/NMDA interactions. Trends Neurosci 17:228-233.

Dong Y, Green T, Saal D, Marie H, Neve R, Nestler EJ, Malenka RC (2006) CREB modulates excitability of nucleus accumbens neurons. Nat Neurosci 9:475-477.

Dumaz N, Marais R (2005) Integrating signals between cAMP and the RAS/RAF/MEK/ERK signalling pathways. Based on the anniversary prize of the Gesellschaft fur Biochemie und Molekularbiologie Lecture delivered on 5 July 2003 at the Special FEBS Meeting in Brussels. Febs J 272:3491-3504.

Emerich DF, McDermott P, Krueger P, Banks M, Zhao J, Marszalkowski J, Frydel B, Winn SR, Sanberg PR (1993) Locomotion of aged rats: relationship to neurochemical but not morphological changes in nigrostriatal dopaminergic neurons. Brain Res Bull 32:477-486.

Evans GJO, Cousin MA (2007) Activity-dependent control of slow synaptic vesicle endocytosis by cyclin-dependent kinase 5. J Neurosci 27:401-411.

Feil R, Wagner J, Metzger D, Chambon P (1997) Regulation of Cre recombinase activity by mutated estrogen receptor ligand-binding domains. Biochem Biophys Res Commun 237:752-757.

Fischer A, Sananbenesi F, Pang PT, Lu B, Tsai LH (2005) Opposing roles of transient and prolonged expression of p25 in synaptic plasticity and hippocampus-dependent memory. Neuron 48:825-838.

Fitzpatrick PF (1999) Tetrahydropterin-dependent amino acid hydroxylases. Annu Rev Biochem 68:355-381.

Girault JA, Hemmings HC, Jr., Williams KR, Nairn AC, Greengard P (1989) Phosphorylation of DARPP-32, a dopamine- and cAMP-regulated phosphoprotein, by casein kinase II. J Biol Chem 264:21748-21759.

Gold SJ, Ni YG, Dohlman HG, Nestler EJ (1997) Regulators of G-protein signaling (RGS) proteins: region-specific expression of nine subtypes in rat brain. J Neurosci 17:8024-8037.

Goto S, Matsukado Y, Mihara Y, Inoue N, Miyamoto E (1986) The distribution of calcineurin in rat brain by light and electron microscopic immunohistochemistry and enzyme-immunoassay. Brain Res 397:161-172.

Gray N, Detivaud L, Doerig C, Meijer L (1999) ATP-site directed inhibitors of cyclin-dependent kinases. Curr Med Chem 6:859-875.

Green TA, Alibhai IN, Hommel JD, DiLeone RJ, Kumar A, Theobald DE, Neve RL, Nestler EJ (2006) Induction of inducible cAMP early repressor expression in nucleus accumbens by stress or amphetamine increases behavioral responses to emotional stimuli. J Neurosci 26:8235-8242.

Greengard P, Allen PB, Nairn AC (1999) Beyond the dopamine receptor: the DARPP-32/protein phosphatase-1 cascade. Neuron 23:435-447.

Hall FS, Sora I, Drgonova J, Li XF, Goeb M, Uhl GR (2004) Molecular mechanisms underlying the rewarding effects of cocaine. Ann N Y Acad Sci 1025:47-56.

Halpain S, Girault JA, Greengard P (1990) Activation of NMDA receptors induces dephosphorylation of DARPP-32 in rat striatal slices. Nature 343:369-372.

Han JR, Gu W, Hecht NB (1995) Testis-brain RNA-binding protein, a testicular translational regulatory RNA-binding protein, is present in the brain and binds to the 3' untranslated regions of transported brain mRNAs. Biol Reprod 53:707-717.

Hawasli AH, Bibb JA (2007) Alternative roles for Cdk5 in learning and synaptic plasticity. Biotechnol J.

Hawasli AH, Benavides DR, Nguyen C, Kansy JW, Hayashi K, Chambon P, Greengard P, Powell CM, Cooper DC, Bibb JA (2007) Cyclin-dependent kinase 5 governs learning and synaptic plasticity via control of NMDAR degradation. Nat Neurosci 10:880-886.

Hayashi K, Pan Y, Shu H, Ohshima T, Kansy JW, White CL, 3rd, Tamminga CA, Sobel A, Curmi PA, Mikoshiba K, Bibb JA (2006) Phosphorylation of the tubulin-binding protein, stathmin, by Cdk5 and MAP kinases in the brain. J Neurochem 99:237-250.

Hellmich MR, Pant HC, Wada E, Battey JF (1992) Neuronal cdc2-like kinase: a cdc2-related protein kinase with predominantly neuronal expression. Proc Natl Acad Sci U S A 89:10867-10871.

Hemmings HC, Jr., Greengard P, Tung HY, Cohen P (1984a) DARPP-32, a dopamine-regulated neuronal phosphoprotein, is a potent inhibitor of protein phosphatase-1. Nature 310:503-505.

Hemmings HC, Jr., Williams KR, Konigsberg WH, Greengard P (1984b) DARPP-32, a dopamine- and adenosine 3':5'-monophosphate-regulated neuronal phosphoprotein. I. Amino acid sequence around the phosphorylated threonine. J Biol Chem 259:14486-14490.

Hernandez-Lopez S, Bargas J, Surmeier DJ, Reyes A, Galarraga E (1997) D1 receptor activation enhances evoked discharge in neostriatal medium spiny neurons by modulating an L-type Ca2+ conductance. J Neurosci 17:3334-3342.

Hirooka K, Tomizawa K, Matsui H, Tokuda M, Itano T, Hasegawa E, Wang JH, Hatase O (1996) Developmental alteration of the expression and kinase activity of cyclin-dependent kinase 5 (Cdk5)/p35nck5a in the rat retina. J Neurochem 67:2478-2483.

Hoffmann R, Wilkinson IR, McCallum JF, Engels P, Houslay MD (1998) cAMP-specific phosphodiesterase HSPDE4D3 mutants which mimic activation and changes in rolipram inhibition triggered by protein kinase A phosphorylation of Ser-54: generation of a molecular model. Biochem J 333 (Pt 1):139-149.

Holland HC, Weldon E (1968) A note on a new technique of recording ambulation in the open field test and its validation. Acta Psychol (Amst) 28:293-300.

Hommel JD, Sears RM, Georgescu D, Simmons DL, DiLeone RJ (2003) Local gene knockdown in the brain using viral-mediated RNA interference. Nat Med 9:1539-1544.

Hope BT, Nye HE, Kelz MB, Self DW, Iadarola MJ, Nakabeppu Y, Duman RS, Nestler EJ (1994) Induction of a long-lasting AP-1 complex composed of altered Fos-like proteins in brain by chronic cocaine and other chronic treatments. Neuron 13:1235-1244.

Houslay MD (2001) PDE4 cAMP-specific phosphodiesterases. Prog Nucleic Acid Res Mol Biol 69:249-315.

Houslay MD, Milligan G (1997) Tailoring cAMP-signalling responses through isoform multiplicity. Trends Biochem Sci 22:217-224.

Howland RH (1996) Induction of mania with serotonin reuptake inhibitors. J Clin Psychopharmacol 16:425-427.

Huston E, Lumb S, Russell A, Catterall C, Ross AH, Steele MR, Bolger GB, Perry MJ, Owens RJ, Houslay MD (1997) Molecular cloning and transient expression in COS7 cells of a novel human PDE4B cAMP-specific phosphodiesterase, HSPDE4B3. Biochem J 328 (Pt 2):549-558.

Hyman SE, Malenka RC (2001) Addiction and the brain: the neurobiology of compulsion and its persistence. Nat Rev Neurosci 2:695-703.

Isbister GK, Buckley NA (2005) The pathophysiology of serotonin toxicity in animals and humans: implications for diagnosis and treatment. Clin Neuropharmacol 28:205-214.

Ishizuka T, Ino H, Sawa K, Suzuki N, Tatibana M (1995) Promoter region of the mouse cyclin-dependent kinase 5-encoding gene. Gene 166:267-271.

Kansy JW, Katsovich L, McIver KS, Pick J, Zabriskie JB, Lombroso PJ, Leckman JF, Bibb JA (2006) Identification of pyruvate kinase as an antigen associated with Tourette syndrome. J Neuroimmunol 181:165-176.

Kansy JW, Daubner SC, Nishi A, Sotogaku N, Lloyd MD, Nguyen C, Lu L, Haycock JW, Hope BT, Fitzpatrick PF, Bibb JA (2004) Identification of tyrosine hydroxylase as a physiological substrate for Cdk5. J Neurochem 91:374-384.

Karler R, Calder LD, Thai LH, Bedingfield JB (1995) The dopaminergic, glutamatergic, GABAergic bases for the action of amphetamine and cocaine. Brain Res 671:100-104.

Kavaliers M, Ossenkopp KP (1986) Stress-induced opioid analgesia and activity in mice: inhibitory influences of exposure to magnetic fields. Psychopharmacology (Berl) 89:440-443.

Kelley AE, Berridge KC (2002) The neuroscience of natural rewards: relevance to addictive drugs. J Neurosci 22:3306-3311.

Keravis T, Thaseldar-Roumié R, Lugnier C (2005) Assessment of Phosphodiesterase Isozyme Contribution in Cell and Tissue Extracts. In: Phosphodiesterase Methods and Protocols (Lugnier C, ed), pp 63-74. Totowa, NJ: Humana Press.

Keryer G, Luo Z, Cavadore JC, Erlichman J, Bornens M (1993) Phosphorylation of the regulatory subunit of type II beta cAMP-dependent protein kinase by cyclin B/p34cdc2 kinase impairs its binding to microtubule-associated protein 2. Proc Natl Acad Sci U S A 90:5418-5422.

Keryer G, Yassenko M, Labbe JC, Castro A, Lohmann SM, Evain-Brion D, Tasken K (1998) Mitosis-specific phosphorylation and subcellular redistribution of the RIIalpha regulatory subunit of cAMP-dependent protein kinase. J Biol Chem 273:34594-34602.

Kim Y, Sung JY, Ceglia I, Lee KW, Ahn JH, Halford JM, Kim AM, Kwak SP, Park JB, Ho Ryu S, Schenck A, Bardoni B, Scott JD, Nairn AC, Greengard P (2006) Phosphorylation of WAVE1 regulates actin polymerization and dendritic spine morphology. Nature 442:814-817.

Ko J, Humbert S, Bronson RT, Takahashi S, Kulkarni AB, Li E, Tsai LH (2001) p35 and p39 are essential for cyclin-dependent kinase 5 function during neurodevelopment. J Neurosci 21:6758-6771.

Kumar A, Choi KH, Renthal W, Tsankova NM, Theobald DE, Truong HT, Russo SJ, Laplant Q, Sasaki TS, Whistler KN, Neve RL, Self DW, Nestler EJ (2005) Chromatin remodeling is a key mechanism underlying cocaine-induced plasticity in striatum. Neuron 48:303-314.

Kwon YT, Tsai LH (1998) A novel disruption of cortical development in p35(-/-) mice distinct from reeler. J Comp Neurol 395:510-522.

Lee SY, Wenk MR, Kim Y, Nairn AC, De Camilli P (2004) Regulation of synaptojanin 1 by cyclin-dependent kinase 5 at synapses. Proc Natl Acad Sci U S A 101:546-551.

Lew J, Huang QQ, Qi Z, Winkfein RJ, Aebersold R, Hunt T, Wang JH (1994) A brain-specific activator of cyclin-dependent kinase 5. Nature 371:423-426.

Li BS, Zhang L, Gu J, Amin ND, Pant HC (2000) Integrin alpha(1) beta(1)-mediated activation of cyclin-dependent kinase 5 activity is involved in neurite outgrowth and human neurofilament protein H Lys-Ser-Pro tail domain phosphorylation. J Neurosci 20:6055-6062.

Lilja L, Yang SN, Webb DL, Juntti-Berggren L, Berggren PO, Bark C (2001) Cyclin-dependent kinase 5 promotes insulin exocytosis. J Biol Chem 276:34199-34205.

Lindskog M, Svenningsson P, Fredholm BB, Greengard P, Fisone G (1999) Activation of dopamine D2 receptors decreases DARPP-32 phosphorylation in striatonigral and striatopallidal projection neurons via different mechanisms. Neuroscience 88:1005-1008.

Liu QS, Pu L, Poo MM (2005) Repeated cocaine exposure in vivo facilitates LTP induction in midbrain dopamine neurons. Nature 437:1027-1031.

Liu X, Gershenfeld HK (2001) Genetic differences in the tail-suspension test and its relationship to imipramine response among 11 inbred strains of mice. Biol Psychiatry 49:575-581.

Luikart BW, Nef S, Virmani T, Lush ME, Liu Y, Kavalali ET, Parada LF (2005) TrkB has a cell-autonomous role in the establishment of hippocampal Schaffer collateral synapses. J Neurosci 25:3774-3786.

Lynch WJ, Taylor JR (2005) Persistent changes in motivation to self-administer cocaine following modulation of cyclic AMP-dependent protein kinase A (PKA) activity in the nucleus accumbens. Eur J Neurosci 22:1214-1220.

MacKenzie SJ, Baillie GS, McPhee I, MacKenzie C, Seamons R, McSorley T, Millen J, Beard MB, van Heeke G, Houslay MD (2002) Long PDE4 cAMP specific phosphodiesterases are activated by protein kinase A-mediated phosphorylation of a single serine residue in Upstream Conserved Region 1 (UCR1). Br J Pharmacol 136:421-433.

Meijer L, Borgne A, Mulner O, Chong JP, Blow JJ, Inagaki N, Inagaki M, Delcros JG, Moulinoux JP (1997) Biochemical and cellular effects of roscovitine, a potent and selective inhibitor of the cyclin-dependent kinases cdc2, cdk2 and cdk5. Eur J Biochem 243:527-536.

Moita MA, Lamprecht R, Nader K, LeDoux JE (2002) A-kinase anchoring proteins in amygdala are involved in auditory fear memory. Nat Neurosci 5:837-838.

Monteggia LM, Luikart B, Barrot M, Theobold D, Malkovska I, Nef S, Parada LF, Nestler EJ (2007) Brain-derived neurotrophic factor conditional knockouts show gender differences in depression-related behaviors. Biol Psychiatry 61:187-197.

Moy LY, Tsai LH (2004) Cyclin-dependent kinase 5 phosphorylates serine 31 of tyrosine hydroxylase and regulates its stability. J Biol Chem 279:54487-54493.

Musa FR, Tokuda M, Kuwata Y, Ogawa T, Tomizawa K, Konishi R, Takenaka I, Hatase O (1998) Expression of cyclin-dependent kinase 5 and associated cyclins in Leydig and Sertoli cells of the testis. J Androl 19:657-666.

Nairn AC, Shenolikar S (1992) The role of protein phosphatases in synaptic transmission, plasticity and neuronal development. Current Opinion in Neurobiology 2:296-301.

Narita M, Shibasaki M, Nagumo Y, Narita M, Yajima Y, Suzuki T (2005) Implication of cyclin-dependent kinase 5 in the development of psychological dependence on and behavioral sensitization to morphine. J Neurochem 93:1463-1468.

Nestler EJ (2001) Molecular basis of long-term plasticity underlying addiction. Nat Rev Neurosci 2:119-128.

Nguyen C, Hosokawa T, Kuroiwa M, Ip NY, Nishi A, Hisanaga S, Bibb JA (2007) Differential regulation of the Cdk5-dependent phosphorylation sites of inhibitor-1 and DARPP-32 by depolarization. J Neurochem 103:1582-1593.

Nguyen MD, Lariviere RC, Julien JP (2001) Deregulation of Cdk5 in a mouse model of ALS: toxicity alleviated by perikaryal neurofilament inclusions. Neuron 30:135-147.

Nikolic M, Dudek H, Kwon YT, Ramos YF, Tsai LH (1996) The cdk5/p35 kinase is essential for neurite outgrowth during neuronal differentiation. Genes Dev 10:816-825.

Nikolic M, Chou MM, Lu W, Mayer BJ, Tsai LH (1998) The p35/Cdk5 kinase is a neuron-specific Rac effector that inhibits Pak1 activity. Nature 395:194-198.

Nishi A, Snyder GL, Greengard P (1997) Bidirectional regulation of DARPP-32 phosphorylation by dopamine. J Neurosci 17:8147-8155.

Nishi A, Bibb JA, Snyder GL, Higashi H, Nairn AC, Greengard P (2000) Amplification of dopaminergic signaling by a positive feedback loop. Proc Natl Acad Sci U S A 97:12840-12845.

Norrholm SD, Bibb JA, Nestler EJ, Ouimet CC, Taylor JR, Greengard P (2003) Cocaine-induced proliferation of dendritic spines in nucleus accumbens is dependent on the activity of cyclin-dependent kinase-5. Neuroscience 116:19-22.

Ohshima T, Ward JM, Huh CG, Longenecker G, Veeranna, Pant HC, Brady RO, Martin LJ, Kulkarni AB (1996) Targeted disruption of the cyclin-dependent kinase 5 gene results in abnormal corticogenesis, neuronal pathology and perinatal death. Proc Natl Acad Sci U S A 93:11173-11178.

Ohshima T, Ogura H, Tomizawa K, Hayashi K, Suzuki H, Saito T, Kamei H, Nishi A, Bibb JA, Hisanaga S, Matsui H, Mikoshiba K (2005) Impairment of hippocampal long-term depression and defective spatial learning and memory in p35 mice. J Neurochem 94:917-925.

Ouimet CC, Greengard P (1990) Distribution of DARPP-32 in the basal ganglia: an electron microscopic study. J Neurocytol 19:39-52.

Ouimet CC, Miller PE, Hemmings HC, Jr., Walaas SI, Greengard P (1984) DARPP-32, a dopamine- and adenosine 3':5'-monophosphate-regulated phosphoprotein enriched in dopamine-innervated brain regions. III. Immunocytochemical localization. J Neurosci 4:111-124.

Patrick GN, Zukerberg L, Nikolic M, de la Monte S, Dikkes P, Tsai LH (1999) Conversion of p35 to p25 deregulates Cdk5 activity and promotes neurodegeneration. Nature 402:615-622.

Porsolt RD, Bertin A, Jalfre M (1977) Behavioral despair in mice: a primary screening test for antidepressants. Arch Int Pharmacodyn Ther 229:327-336.

Robinson TE, Kolb B (1999) Alterations in the morphology of dendrites and dendritic spines in the nucleus accumbens and prefrontal cortex following repeated treatment with amphetamine or cocaine. Eur J Neurosci 11:1598-1604.

Robinson TE, Gorny G, Mitton E, Kolb B (2001) Cocaine self-administration alters the morphology of dendrites and dendritic spines in the nucleus accumbens and neocortex. Synapse 39:257-266.

Rogers DC, Fisher EM, Brown SD, Peters J, Hunter AJ, Martin JE (1997) Behavioral and functional analysis of mouse phenotype: SHIRPA, a proposed protocol for comprehensive phenotype assessment. Mamm Genome 8:711-713.

Sahin B, Shu H, Fernandez J, El-Armouche A, Molkentin JD, Nairn AC, Bibb JA (2006) Phosphorylation of protein phosphatase inhibitor-1 by protein kinase C. J Biol Chem 281:24322-24335.

Sahin B, Kansy JW, Nairn AC, Spychala J, Ealick SE, Fienberg AA, Greene RW, Bibb JA (2004) Molecular characterization of recombinant mouse adenosine kinase and evaluation as a target for protein phosphorylation. Eur J Biochem 271:3547-3555.

Saito T, Onuki R, Fujita Y, Kusakawa G, Ishiguro K, Bibb JA, Kishimoto T, Hisanaga S (2003) Developmental regulation of the proteolysis of the p35 cyclin-dependent kinase 5 activator by phosphorylation. J Neurosci 23:1189-1197.

Self DW (2004) Regulation of drug-taking and -seeking behaviors by neuroadaptations in the mesolimbic dopamine system. Neuropharmacology 47 Suppl 1:242-255.

Sette C, Conti M (1996) Phosphorylation and activation of a cAMP-specific phosphodiesterase by the cAMP-dependent protein kinase. Involvement of serine 54 in the enzyme activation. J Biol Chem 271:16526-16534.

Shakur Y, Pryde JG, Houslay MD (1993) Engineered deletion of the unique N-terminal domain of the cyclic AMP-specific phosphodiesterase RD1 prevents plasma membrane association and the attainment of enhanced thermostability without altering its sensitivity to inhibition by rolipram. Biochem J 292 (Pt 3):677-686.

Sharma P, Veeranna, Sharma M, Amin ND, Sihag RK, Grant P, Ahn N, Kulkarni AB, Pant HC (2002) Phosphorylation of MEK1 by cdk5/p35 down-regulates the mitogen-activated protein kinase pathway. J Biol Chem 277:528-534.

Shevtsova Z, Malik JM, Michel U, Bahr M, Kugler S (2005) Promoters and serotypes: targeting of adeno-associated virus vectors for gene transfer in the rat central nervous system in vitro and in vivo. Exp Physiol 90:53-59.

Sibley DR, Monsma FJ, Jr., McVittie LD, Gerfen CR, Burch RM, Mahan LC (1992) Molecular neurobiology of dopamine receptor subtypes. Neurochem Int 20 Suppl:17S-22S.

Snyder GL, Allen PB, Fienberg AA, Valle CG, Huganir RL, Nairn AC, Greengard P (2000) Regulation of phosphorylation of the GluR1 AMPA receptor in the neostriatum by dopamine and psychostimulants in vivo. J Neurosci 20:4480-4488.

Soriano P (1999) Generalized lacZ expression with the ROSA26 Cre reporter strain. Nat Genet 21:70-71.

Srinivas S, Watanabe T, Lin CS, William CM, Tanabe Y, Jessell TM, Costantini F (2001) Cre reporter strains produced by targeted insertion of EYFP and ECFP into the ROSA26 locus. BMC Dev Biol 1:4.

Strekalova T, Spanagel R, Dolgov O, Bartsch D (2005) Stress-induced hyperlocomotion as a confounding factor in anxiety and depression models in mice. Behav Pharmacol 16:171-180.

Svenningsson P, Nairn AC, Greengard P (2005) DARPP-32 mediates the actions of multiple drugs of abuse. Aaps J 7:E353-360.

Svenningsson P, Lindskog M, Rognoni F, Fredholm BB, Greengard P, Fisone G (1998) Activation of adenosine A2A and dopamine D1 receptors stimulates cyclic AMP-dependent phosphorylation of DARPP-32 in distinct populations of striatal projection neurons. Neuroscience 84:223-228.

Svenningsson P, Tzavara ET, Carruthers R, Rachleff I, Wattler S, Nehls M, McKinzie DL, Fienberg AA, Nomikos GG, Greengard P (2003) Diverse psychotomimetics act through a common signaling pathway. Science 302:1412-1415.

Takahashi S, Ohshima T, Cho A, Sreenath T, Iadarola MJ, Pant HC, Kim Y, Nairn AC, Brady RO, Greengard P, Kulkarni AB (2005) Increased activity of cyclin-dependent kinase 5 leads to attenuation of cocaine-mediated dopamine signaling. Proc Natl Acad Sci U S A 102:1737-1742.

Tan TC, Valova VA, Malladi CS, Graham ME, Berven LA, Jupp OJ, Hansra G, McClure SJ, Sarcevic B, Boadle RA, Larsen MR, Cousin MA, Robinson PJ (2003) Cdk5 is essential for synaptic vesicle endocytosis. Nat Cell Biol 5:701-710.

Taylor JR, Lynch WJ, Sanchez H, Olausson P, Nestler EJ, Bibb JA (2007) Inhibition of Cdk5 in the nucleus accumbens enhances the locomotor-activating and incentive-motivational effects of cocaine. Proc Natl Acad Sci U S A 104:4147-4152.

Tella SR (1995) Effects of monoamine reuptake inhibitors on cocaine self-administration in rats. Pharmacol Biochem Behav 51:687-692.

Thomas MJ, Malenka RC (2003) Synaptic plasticity in the mesolimbic dopamine system. Philos Trans R Soc Lond B Biol Sci 358:815-819.

Tomizawa K, Ohta J, Matsushita M, Moriwaki A, Li ST, Takei K, Matsui H (2002) Cdk5/p35 regulates neurotransmitter release through phosphorylation and downregulation of P/Q-type voltage-dependent calcium channel activity. J Neurosci 22:2590-2597.

Tomizawa K, Sunada S, Lu YF, Oda Y, Kinuta M, Ohshima T, Saito T, Wei FY, Matsushita M, Li ST, Tsutsui K, Hisanaga S, Mikoshiba K, Takei K, Matsui H (2003) Cophosphorylation of amphiphysin I and dynamin I by Cdk5 regulates clathrin-mediated endocytosis of synaptic vesicles. J Cell Biol 163:813-824.

Tsai LH, Takahashi T, Caviness VS, Jr., Harlow E (1993) Activity and expression pattern of cyclin-dependent kinase 5 in the embryonic mouse nervous system. Development 119:1029-1040.

Tsai LH, Delalle I, Caviness VS, Jr., Chae T, Harlow E (1994) p35 is a neural-specific regulatory subunit of cyclin-dependent kinase 5. Nature 371:419-423.

Tsien JZ, Chen DF, Gerber D, Tom C, Mercer EH, Anderson DJ, Mayford M, Kandel ER, Tonegawa S (1996) Subregion- and cell type-restricted gene knockout in mouse brain. Cell 87:1317-1326.

Ungless MA, Whistler JL, Malenka RC, Bonci A (2001) Single cocaine exposure in vivo induces long-term potentiation in dopamine neurons. Nature 411:583-587.

Ventimiglia R, Lindsay RM (1998) Rat Striatal Neurons in Low-Density, Serum-Free Culture In: Culturing Nerve Cells, 2nd Edition (Banker G, Goslin K, eds). London: MIT Press.

Ventra C, Porcellini A, Feliciello A, Gallo A, Paolillo M, Mele E, Avvedimento VE, Schettini G (1996) The differential response of protein kinase A to cyclic AMP in discrete brain areas correlates with the abundance of regulatory subunit II. J Neurochem 66:1752-1761.

Wang H, Pickel VM (2002) Dopamine D2 receptors are present in prefrontal cortical afferents and their targets in patches of the rat caudate-putamen nucleus. J Comp Neurol 442:392-404.

Wang L, Sunahara RK, Krumins A, Perkins G, Crochiere ML, Mackey M, Bell S, Ellisman MH, Taylor SS (2001) Cloning and mitochondrial localization of full-length D-AKAP2, a protein kinase A anchoring protein. Proceedings of the National Academy of Sciences 98:3220-3225.

Wattler S, Kelly M, Nehls M (1999) Construction of gene targeting vectors from lambda KOS genomic libraries. Biotechniques 26:1150-1156, 1158, 1160.

Weber P, Metzger D, Chambon P (2001) Temporally controlled targeted somatic mutagenesis in the mouse brain. Eur J Neurosci 14:1777-1783.

Wedzony K, Markowicz-Kula K, Chocyk A, Fijal K, Mackowiak M (2005) The effect of 'binge' cocaine administration on the expression of cyclin-dependent kinase 5 and its activator p35 in various regions of rat brain. Brain Res 1063:195-200.

Wei F-Y, Nagashima K, Ohshima T, Saheki Y, Lu Y-F, Matsushita M, Yamada Y, Mikoshiba K, Seino Y, Matsui H, Tomizawa K (2005) Cdk5-dependent regulation of glucose-stimulated insulin secretion. Nat Med 11:1104-1108.

Werme M, Messer C, Olson L, Gilden L, Thoren P, Nestler EJ, Brene S (2002) Delta FosB regulates wheel running. J Neurosci 22:8133-8138.

Yamazaki A, Moskvin O, Yamazaki RK (2002) Phosphorylation by cyclin-dependent protein kinase 5 of the regulatory subunit (Pgamma) of retinal cgmp phosphodiesterase (PDE6): its implications in phototransduction. Adv Exp Med Biol 514:131-153.

Yan Z, Chi P, Bibb JA, Ryan TA, Greengard P (2002) Roscovitine: a novel regulator of P/Q-type calcium channels and transmitter release in central neurons. J Physiol 540:761-770.

Zachariou V, Sgambato-Faure V, Sasaki T, Svenningsson P, Berton O, Fienberg AA, Nairn AC, Greengard P, Nestler EJ (2006) Phosphorylation of DARPP-32 at Threonine-34 is required for cocaine action. Neuropsychopharmacology 31:555-562.

Zhang XF, Hu XT, White FJ (1998) Whole-cell plasticity in cocaine withdrawal: reduced sodium currents in nucleus accumbens neurons. J Neurosci 18:488-498.

Zheng M, Leung CL, Liem RK (1998) Region-specific expression of cyclin-dependent kinase 5 (cdk5) and its activators, p35 and p39, in the developing and adult rat central nervous system. J Neurobiol 35:141-159.

Zhong P, Gu Z, Wang X, Jiang H, Feng J, Yan Z (2003) Impaired modulation of GABAergic transmission by muscarinic receptors in a mouse transgenic model of Alzheimer's disease. J Biol Chem 278:26888-26896.

Zolotukhin S, Byrne BJ, Mason E, Zolotukhin I, Potter M, Chesnut K, Summerford C, Samulski RJ, Muzyczka N (1999) Recombinant adeno-associated virus purification using novel methods improves infectious titer and yield. Gene Ther 6:973-985.